MOLECULAR PHYSIOLOGY AND BIOPHYSICS

THE ROLE OF LEPTIN IN MACROPHAGE-DRIVEN AORTIC ROOT LESION FORMATION AND OF MACROPHAGE INFLAMMATORY PROTEIN-1α IN LEUKOCYTE INFILTRATION OF WHITE ADIPOSE TISSUE

BONNIE KAE WASSON SURMI

Dissertation under the direction of Professor Alyssa Herweyer Hasty

Obesity is a strong risk factor for type 2 diabetes and cardiovascular disease partly because of the changes that occur in white adipose tissue (WAT) during weight gain. As obesity progresses, WAT expands, becomes dysfunctional, and increases its secretion of numerous adipokines, including two that will be highlighted in this dissertation, the hormone leptin and the chemokine macrophage inflammatory protein-1α (MIP-1α). Our underlying hypothesis was that elevated secretion of leptin and MIP-1α from WAT during obesity would influence development of obesity-related atherosclerosis, WAT inflammation, and systemic insulin resistance.

To test the role of hematopoietic cell leptin receptor (LepR) in aortic root lesion formation, we conducted three different bone marrow transplantation studies in which bone marrow, with or without LepR, was transplanted into lethally irradiated: 1) low density lipoprotein receptor deficient ($LDLR^{-/-}$) mice with moderate hyperleptinemia due to Western Diet (WD) feeding, 2) WD-fed $LDLR^{-/-}$

mice with pharmacologically induced hyperleptinemia (daily injection of 125 μg leptin), or 3) obese, hyperleptinemic, LepR deficient LDLR$^{-/-}$ (LepR$^{db/db}$;LDLR$^{-/-}$) mice. To test the role of MIP-1α in WAT inflammation, we fed WD to male and female MIP-1α deficient (MIP-1α$^{-/-}$), heterozygous (MIP-1α$^{+/-}$), and MIP-1α sufficient (MIP-1α$^{+/+}$) mice for 16 weeks to induce obesity and examined their WAT. To identify the effects of hyperlipidemia on the metabolic role of MIP-1α, we fed WD to male and female MIP-1α$^{-/-}$;LDLR$^{-/-}$, MIP-1α$^{+/-}$;LDLR$^{-/-}$, and MIP-1α$^{+/+}$;LDLR$^{-/-}$ mice and measured aortic root lesion area and fat mass.

Removal of macrophage LepR did not influence atherosclerotic lesion formation. This suggests that non-hematopoietic cells, rather than macrophages, are potential mediators of leptin's effects on aortic root lesion formation. We also demonstrated that although expression of MIP-1α increases as a consequence of weight gain this chemokine is not critical for the recruitment of monocytes and T-lymphocytes to WAT in mice with diet induced obesity. Furthermore, in the presence of hyperlipidemia, the absence of MIP-1α was not sufficient to attenuate fat mass gain or atherosclerosis during WD feeding. Taken together, these data demonstrate that although MIP-1α may be involved in WAT growth under some circumstances, the metabolic phenotype of MIP-1α$^{-/-}$ mice is similar to that of MIP-1α$^{+/+}$ mice.

Approved: Professor Alyssa H. Hasty

THE ROLE OF LEPTIN IN MACROPHAGE-DRIVEN AORTIC ROOT LESION FORMATION AND OF MACROPHAGE INFLAMMATORY PROTEIN-1α IN LEUKOCYTE INFILTRATION OF WHITE ADIPOSE TISSUE

By

Bonnie Kae Wasson Surmi

Dissertation

Submitted to the Faculty of the

Graduate School of Vanderbilt University

in partial fulfillment of the requirements

for the degree of

DOCTOR OF PHILOSOPHY

in

Molecular Physiology and Biophysics

December, 2009

Nashville, Tennessee

Approved:

Professor Owen P. McGuinness

Professor Richard O'Brien

Professor Larry Swift

Professor Amy Major

Professor Dave Wasserman

In honor of my father, David Wesley Wasson

(December 15, 1942 – September 20, 2004).

Nine years ago you wrote,

“Since you will probably go on to earn a PhD,

on December 13, you’ll be 5.556% finished!”

In admiration of a man who loved the Lord,

praised his wife, and bragged about everyone else.

You declared what I did not yet see.

You showed me the Father.

And to my faithful husband, Benjamin,

with love and gratitude.

ACKNOWLEDGEMENTS

As I reflect on these years at Vanderbilt, many names and faces come to mind. I am grateful for the supportive colleagues who have invested in my life and nurtured me as a scientist. I an especially thankful for the kindness I was shown by administrators, professors, and classmates when my father passed away one month into my graduate career.

My advisor, Dr. Alyssa Hasty, has truly mentored me. She has modeled integrity and humility in her leadership of our lab. With persistence and cheerfulness, she works hard so that each member of our lab is able to succeed and so that together we can uncover some of the mysteries we study. I am thankful for the opportunity to work under her.

I have learned much from my labmates and am thankful for their friendship. They have made this a good place to work, and I have grown as a scientist because of their skills and intelligence.

My committee members have been supportive and encouraging as they test the limits of my knowledge. They have guided me as I follow the unpredictable path that research projects often take.

My family and friends have been an enormous encouragement and strength to me. Many prayers have been offered on my behalf—thank you.

Lastly, I acknowledge the Eternal One, Creator of all that we study: “The earth is the Lord’s, and everything in it, the world, and all who live in it; for He founded it upon the seas and established it upon the waters” (Psalm 24:1-2). It is

a privilege to study what His hands have made as we do the daily work of biomedical research.

Prior publications and financial support

Some of the material in this dissertation is published or is currently in submission. The research in Chapter III was published in *American Journal of Physiology: Endocrinology and Metabolism* (Surmi BK, Atkinson RD, Gruen ML, Coenen KR, Hasty AH. 2008 Mar;294(3):E488-95. Epub 2008 Jan 8). Portions of the Introduction have been published in *Future Lipidology* (Surmi BK and Hasty AH. 2008;3(5):545-556).

Funding for this research has been provided to Dr. Hasty through a Junior Faculty Award from the American Diabetes Association (1-04-JF-20), a Pilot and Feasibility Grant from the Digestive Diseases Research Center (DK058404), and a Career Development Award from the American Diabetes Association (1-07-CD-10). I have been supported by a Molecular Endocrinology Training Grant (NIH T32DK07563) and by a pre-doctoral fellowship from the American Heart Association (0815231E). Insulin and leptin assays were performed in the Analytical Services Core of the Diabetes Research and Training Center (DK20593)/ MMPC (DK59637).

TABLE OF CONTENTS

LIST OF FIGURES

LIST OF TABLES

CHAPTER I

INTRODUCTION

Prevalence of obesity

Obesity (BMI>30 kg/m^2) and overweight (BMI>25 kg/m^2) are both conditions of excess energy storage, the majority of which is stored as triglycerides (TGs) in white adipose tissue (WAT). According to the World Health Organization, 1 billion people worldwide are estimated to be overweight, at least 300 million of whom are obese (109). In the United States, more than 60% of adults are estimated to be overweight or obese (Figure 1.1) (2). Obesity increases the risk for numerous diseases including cardiovascular disease and type 2 diabetes. Being overweight or obese also increases the likelihood of having other cardiovascular risk factors such as hypertension and dyslipidemia (68), and obesity itself is an independent risk factor for cardiovascular disease (CVD) (37, 58, 75). Obese individuals usually have elevated plasma leptin, referred to as hyperleptinemia, which is an additional, independent risk factor for CVD (154). Obesity is also a strong risk factor for type 2 diabetes (1, 10), and the prevalence of both obesity and type 2 diabetes has been increasing steadily over the past few decades (99). The reasons for these associations are only partially understood, and this dissertation will address some of the factors thought to link these conditions with obesity.

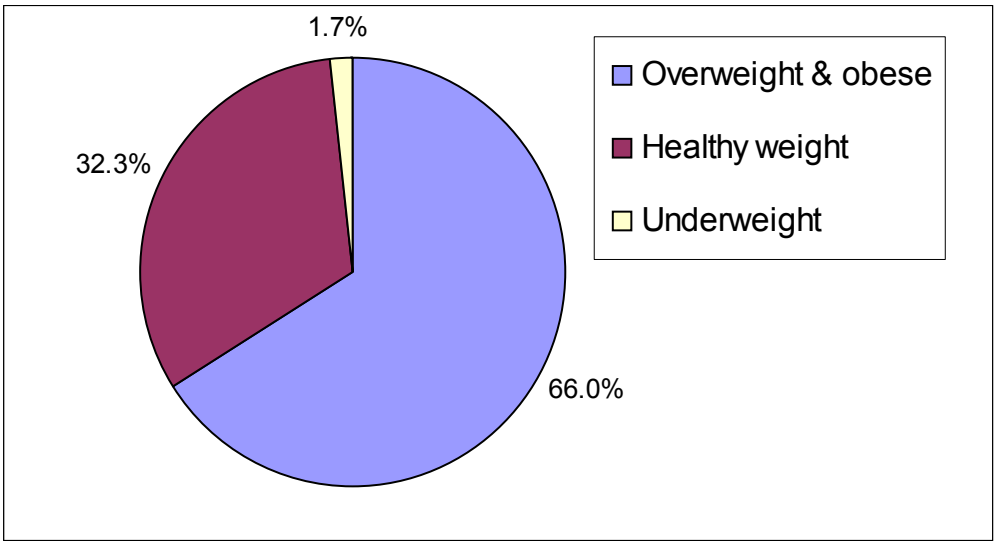

Figure 1.1. Prevalence of overweight and obesity in the United States based on body mass index.

White adipose tissue (WAT)

Structure and functions of WAT

The majority of WAT mass is composed of adipocytes and the rest is composed of many other cell types including endothelial cells, erythrocytes, and leukocytes such as monocytes, macrophages, T-lymphocytes, neutrophils, and B-lymphocytes. The primary functions of WAT include insulating and cushioning internal organs as well as storing energy in the form of TGs. In addition to these functions, WAT has an endocrine role, secreting many different adipokines and cytokines into the circulation. Leptin is a key hormone secreted by WAT that, together with gastrointestinal hormones, communicates with the central nervous system to regulate food intake (79). Lipolysis of TGs from adipocytes is also highly regulated, such that plasma non-esterified fatty acid levels are controlled

during fasting and feeding (174). A sufficient amount of properly functioning WAT is necessary for health. Lipodystrophy—a pathological condition in which WAT mass is insufficient—as well as obesity, are associated with insulin resistance and ectopic lipid storage (18). In this dissertation, we will focus on the effects of obesity on WAT.

Pathophysiology of WAT in obesity

As obesity progresses, WAT expands and becomes dysfunctional. Hypoxia within the rapidly growing tissue, adipocyte cell death, and secretion of cytokines by adipocytes, endothelial cells, or resident leukocytes cause both paracrine and endocrine effects (143). Locally, these changes signal for immune cells to enter the WAT to clear the debris and resolve the inflammation, however, the resulting influx of leukocytes can be detrimental and may interfere with adipocytes' sensitivity to insulin. WAT mediates its influence over other tissues in an endocrine manner also, as seen by elevated circulating leptin and decreased release of the insulin-sensitizing hormone adiponectin, and altered secretion of other adipokines. Although WAT has the capacity to expand even 100-fold in adults, ectopic lipid storage in the liver and skeletal muscle is a common feature of excessive weight gain and can disrupt the function of these other tissues (82). In this dissertation, we investigate the local and systemic consequences of obesity, focusing on the adipokines leptin and macrophage inflammatory protein-1α (MIP-1α), which is a chemotactic cytokine (or chemokine). Our underlying hypothesis is that elevated secretion of leptin

(Chapter III) and MIP-1α (Chapters IV and V) from WAT during obesity significantly influences development of obesity-related atherosclerosis, WAT inflammation, and systemic insulin resistance (Figure 1.2).

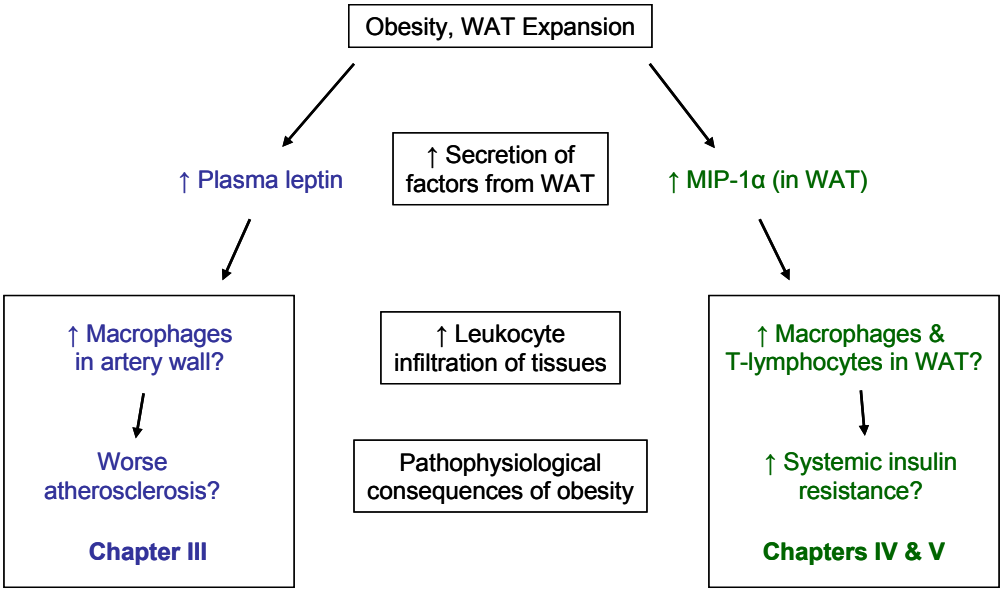

Figure 1.2. Overview of hypotheses tested in dissertation.

Leptin

Leptin and its receptor

Leptin is a 16kD protein secreted by WAT. In healthy weight humans, both free and bound leptin are present in the plasma and total plasma leptin averages about 0.1 – 1 nmol/l (~1.6 – 16 ng/ml) (91, 126). However, in obese individuals, the proportion of free leptin increases and total plasma leptin can be as high as 5 nmol/l (~80 ng/ml) or greater (91).

Leptin receptor (LepR) has 6 isoforms and exists in a soluble and membrane bound state. Soluble leptin receptor binds to and stabilizes circulating leptin. The membrane bound isoforms differ only in the length of their intracellular region, and isoform b (LepRb), unlike the other isoforms, has a 302-amino acid long cytosolic region capable of intracellular signaling. Leptin receptor has been detected on many cell types, but its function is best understood on neurons of the arcuate nucleus of the hypothalamus. Two sets of LepRb containing neurons are present within the arcuate nucleus—those that synthesize neuropeptide Y (NPY) and agouti related protein (AgRP) and those that express proopiomelanocortin (POMC), which is cleaved to form α-melanocyte stimulating hormone (α-MSH) (103). These function together in a feedback loop to regulate energy homeostasis. Leptin excites POMC neurons, which secrete α-MSH, an anorexic (appetite suppressing) factor, and leptin inhibits NPY/AgRP neurons, decreasing their secretion of the orexigenic (appetite stimulating) factors NPY and AgRP. Obese individuals lose sensitivity to leptin or become "leptin resistant", as described below.

History of leptin

In the 1950s and '60s, two spontaneously generated mouse mutations with similar obese phenotypes were discovered (59, 60). Based on parabiosis experiments in the 1970s (24, 25), mice with one of the mutations (later identified as $Lep^{ob/ob}$ mice) were proposed to lack a soluble satiety factor and mice with the other mutation ($LepR^{db/db}$ mice) to lack its receptor. In 1994, the gene *obese* was

cloned and its sequence suggested that it encoded a secreted factor, which was named leptin after the Greek word *leptos* meaning thin (172). Its receptor was identified and cloned shortly after (144). $LepR^{db/db}$ mice have a mutation in their leptin receptor and a nearly identical phenotype to $Lep^{ob/ob}$ mice with the exception of their exceedingly high plasma leptin concentrations.

The cloning of leptin initially generated much excitement because injection of leptin into $Lep^{ob/ob}$ mice induced dramatic weight loss (16, 50, 116). Researchers hoped leptin could be used to pharmacologically treat obese individuals; however, most humans are hyperleptinemic rather than leptin deficient, and the potential therapeutic uses of leptin are being reconsidered. Many clinical uses of leptin target thin, rather than obese, individuals. Humans in a state of negative energy balance—such as those with anorexia nervosa or highly training women athletes—can experience amenorrhea, compromised immunity, and other health deficiencies because of insufficient leptin levels. Therefore, clinical trials are underway to test the effectiveness of therapeutic leptin interventions (7). Centrally administered leptin has also been suggested as a therapy for diabetes because leptin can regulate β-cell secretion of insulin and glucose metabolism (64). It is critical to determine leptin's roles in CVD, not only for appropriate care of patients with CVD but also to understand the consequences of its various clinical uses.

Leptin resistance

Healthy, lean individuals can respond properly to leptin's appetite suppressing effects, but obese individuals lose sensitivity to the anorexic effects of leptin, becoming "leptin resistant". This term has been used to refer to a range of concepts, but one of the main mechanisms by which leptin resistance occurs is cellular resistance in the arcuate nucleus of the hypothalamus. Upon leptin binding to homodimerized LepRb, tyrosine kinase Jak2 associates with LepR and phosphorylates tyrosines 985, 1077, and 1138. Phosphorylation of Y_{985} attenuates leptin signaling as part of a negative feedback loop. Amplification of this feedback or removal of LepR from the plasma membrane can mediate cellular resistance in obese individuals (103). Leptin has pleiotropic effects, not all of which are inhibited in obese individuals. Selective leptin resistance is defined as resistance to the anorexic effects of leptin while retaining the response to leptin's other effects. For example, elevated stimulation of sympathetic nerve activity by hyperleptinemia is thought to aggravate hypertension in obese individuals (94). The hypothesis we test in Chapter III is based on the concept of selective leptin resistance since we propose that macrophages retain responsiveness to leptin despite resistance to leptin at the level of the hypothalamus.

Atherosclerosis

Atherosclerosis is a chronic inflammatory disease in which lipids accumulate within the intima of the artery wall and form a lesion or plaque. Many cell types participate in the development of atherosclerotic lesions including various subsets of monocytes/macrophages and T-lymphocytes, neutrophils, mast cells, B-lymphocytes, and progenitor cells (157), although in this dissertation we will focus on the role of monocytes/macrophages. Formation of atherosclerotic lesions can lead to hazardous consequences incuding myocardial infarction and stroke (Figure 1.3) (86).

Progression of atherosclerosis is strongly associated with hypercholesterolemia and is also associated with hypertriglyceridemia, although elevated plasma TGs alone is usually insufficient to drive the disease (41). An extreme illustration of the association between hypercholesterolemia and atherosclerosis is homozygous familial hypercholesterolemia (HFHC), caused by a genetic mutation in the low density lipoprotein receptor (LDLR) gene. HFHC causes extremely high plasma LDL cholesterol concentrations and severe atherosclerosis before age 10 (93).

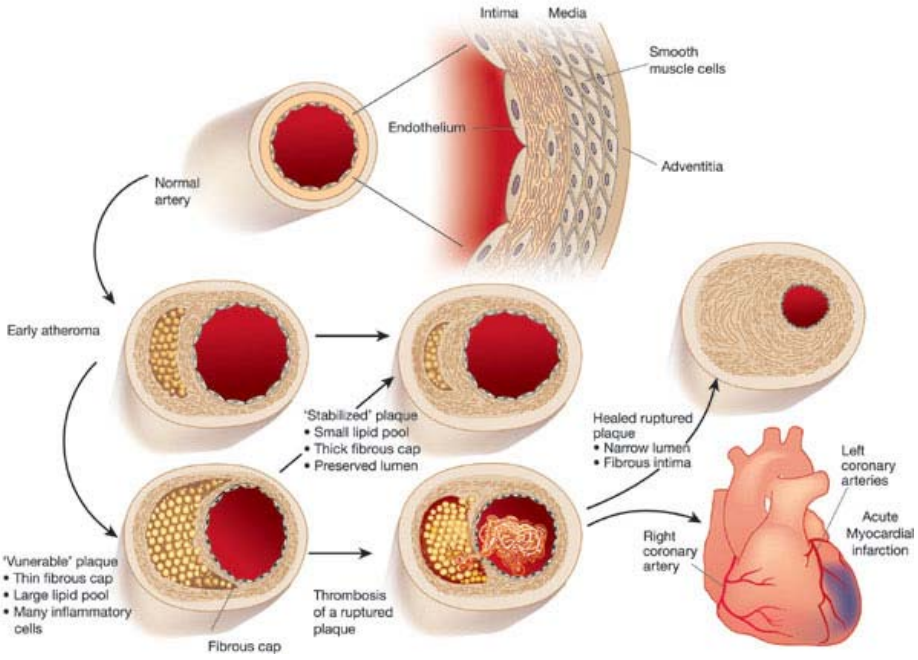

Figure 1.3. Schematic of the life history of an atheroma. Progression from a healthy artery to an atheroma and the different fates of the plaque including rupture, thrombosis, and the resultant myocaridial infarction. From Libby P, *Nature.* 2002 Dec 19-26;420(6917):868-74. For a detailed description of figure please see the original review.

The initiator of “fatty streaks” or early atherosclerotic lesions is not fully understood but involves endothelial cell dysfunction—often under conditions of hyperlipidemia—as well as inflammation. Endothelial cell injury can increase the adhesion of leukocytes and activated platelets to the endothelium and increases its permeability to lipids (157). Monocyte infiltration into the lesion may occur because of their increased adherence to endothelial cells as well as in response to lipid accumulation, and it is also an early step in lesion formation. As shown in Figure 1.4, circulating monocytes attach to various cell adhesion molecules, roll along the endothelium, firmly attach via integrin binding, and then diapadese

through the endothelial cell layer and into the artery wall. After exiting the circulation, these monocytes differentiate into macrophages and phagocytose lipids through their scavenger receptors. These macrophages become “foam cells”, so named because their high lipid content (which is mainly composed of cholesterol) gives them a foamy appearance. The macrophages within the nascent plaque secrete reactive oxygen species and matrix metalloproteinases, as well as proinflammatory cytokines, which recruit more leukocytes to the site of inflammation in the artery wall. In Chapter III, we will investigate whether leptin signaling through macrophage LepRb is involved in atherosclerotic lesion development.

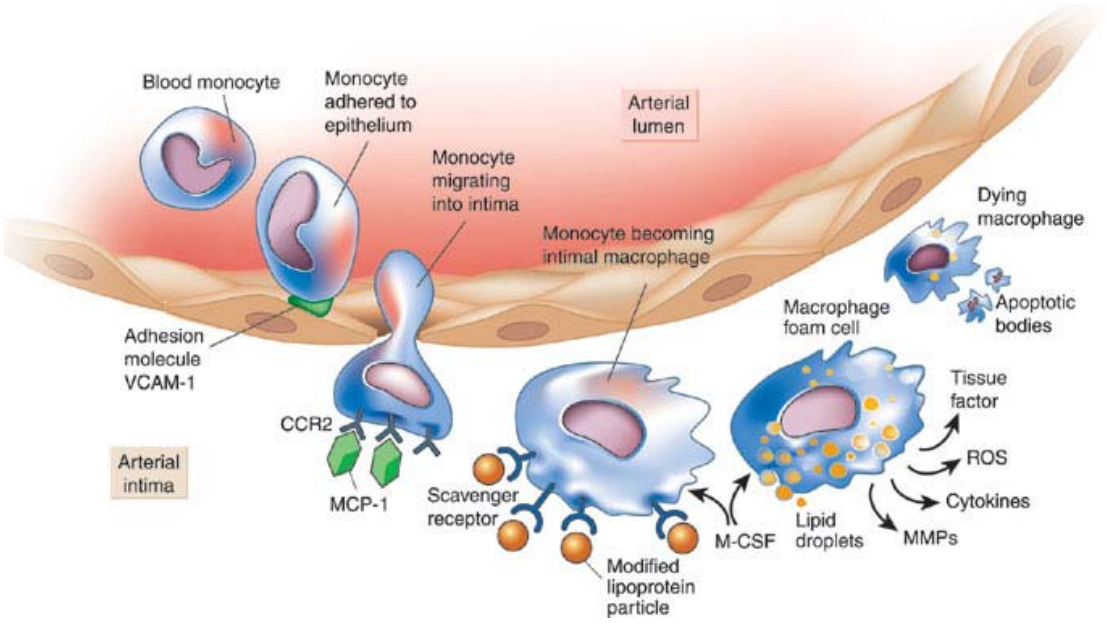

Figure 1.4. Recruitment of monocytes to artery wall and their differentiation into macrophages. Figure is from Libby P, *Nature.* 2002 Dec 19-26;420(6917):868-74. Please see reference for detailed description of figure.

Mouse models of atherosclerosis

Wild type C57BL/6 mice normally clear LDL and VLDL efficiently and, consequently, even when fed a high cholesterol diet such as the Western Diet (WD, see Chapter II for details) they develop virtually no atherosclerotic lesions. Thus, the most common mouse models of atherosclerosis are mice with mutations in the main lipoprotein clearance pathway. Apolipoprotein E deficient ($apoE^{-/-}$) mice do not produce apoE (117), a protein which is normally packaged with lipids to aid in their clearance from the plasma. apoE preferentially binds LDL receptors to clear chylomicron remnants and very low density lipoprotein (VLDL) but is also a ligand for LDL receptor-related protein (LRP). $apoE^{-/-}$ mice have hypercholesterolemia and develop atherosclerotic lesions spontaneously, even when fed a chow diet (171). Mice lacking LDL receptor ($LDLR^{-/-}$) are also a commonly used model of atherosclerosis. Chow diet fed $LDLR^{-/-}$ mice have a much greater amount of circulating LDL and VLDL so that their lipoprotein profile resembles that of humans (see Figure 1.5). When fed WD, $LDLR^{-/-}$ mice become severely hypercholesterolemic (62) and begin to develop arterial plaques. We will use the WD-fed $LDLR^{-/-}$ mouse model throughout this dissertation.

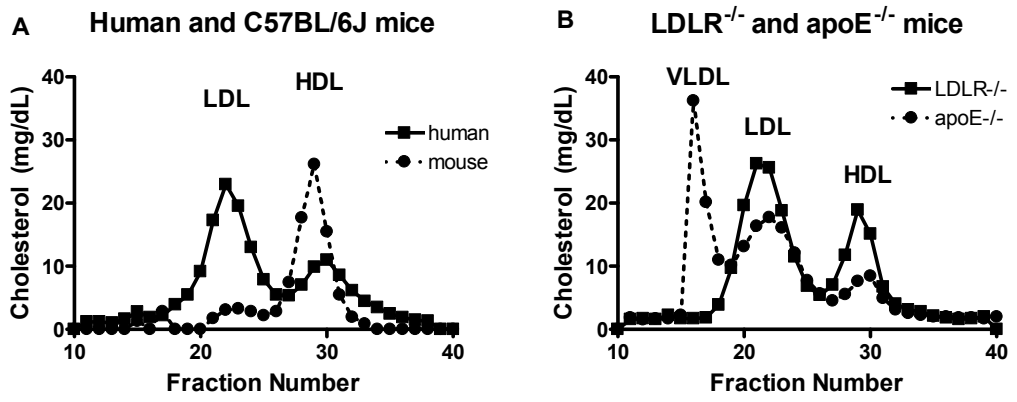

Figure 1.5. Cholesterol fractionation by FPLC in human and mouse plasma.

Monocytes and macrophages

In adult mammals, hematopoietic stem cells reside in the bone marrow where they regenerate themselves and produce cells which differentiate into various myeloid and lymphoid progenitor cells. Downstream of common myeloid progenitor cells are erythrocytes and numerous leukocytes including monocytes, which can differentiate into macrophages once they have exited the circulation to enter a tissue (Figure 1.6). Macrophages are antigen presenting cells and are part of the innate immune system. Expression of cell surface markers is used to identify macrophages and classify them into subgroups. F4/80 and CD68 are both cell surface glycoproteins which are commonly used to identify macrophage populations and are more specific for macrophages than other markers such as CD11b (Mac1) (87).

Like T-lymphocytes, macrophages are now understood to be a heterogeneous population of cells that can be polarized toward an M1 “classically activated” or an M2 “alternatively activated” phenotype (reviewed in (46, 92)).

The M1 macrophage phenotype is induced by inflammatory stimuli and results in secretion of pro-inflammatory cytokines, whereas the M2 phenotype is induced by exposure to IL-4 and IL-13 and results in the secretion of anti-inflammatory cytokines. One hallmark feature of M2 macrophages is the production of arginase, which blocks iNOS activity and may allow M2 macrophages to contribute to tissue repair (133).

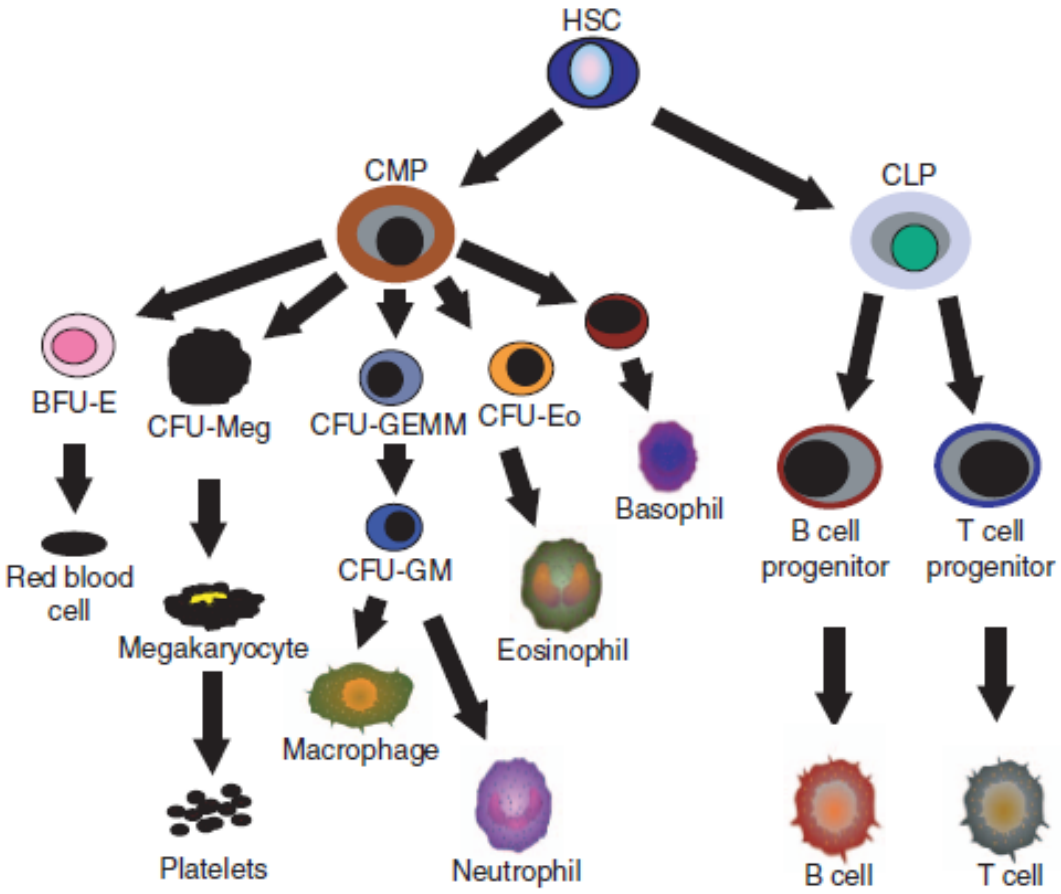

Figure 1.6. Haematopoietic hierarchy. Figure shows the generation of blood and immune cells from the HSCs. BFU: Blast-forming unit; CFU: Colony-forming unit; CLP: Common lymphoid progenitor; CMP: Common myeloid progenitor; GEMM: granulocyte/erythrocyte/monocyte/ megakaryocyte; GM: Granulocyte-macrophage; HSC:Haematopoietic stem cell. Figure and legend text from Ramkissoon SH et al. *Expert Opin. Biol. Ther.* (2006) 6(2):109-120.

WAT inflammation in obese individuals and subsequent insulin resistance

WAT is an insulin responsive tissue. Insulin both inhibits lipolysis and promotes the delivery of glucose to adipocytes via the glucose transporter GLUT4. In insulin resistant individuals, elevated secretion of insulin by the pancreas can overcome insulin resistance to maintain relatively normal blood glucose concentrations; however, elevated secretion of insulin does not prevent the increased flux of NEFAs into and out of WAT that is observed in obese individuals (135). During obesity, disruption of WAT's sensitivity to insulin can lead to uncontrolled release of non-esterified fatty acids (NEFAs). This increases the liver, pancreas, and skeletal muscle's exposure to NEFAs and provides more substrate for liver VLDL synthesis (135). Therefore, insulin resistance in WAT can lead to lipid deposition in other tissues as well as systemic insulin resistance. ATMs and T-lymphocytes present in WAT contribute to the dysfunction of adipocytes during obesity, and subsequently, to insulin resistance, as described below.

Monocyte recruitment to WAT

Monocyte recruitment into WAT is an area of intense investigation (49, 65, 67, 70, 131, 147, 158). Macrophage accumulation in WAT correlates positively with obesity, as measured by BMI and adipocyte size (159) and is increased in obesity in both humans and rodents (166). Microarray analysis of perigonadal WAT from multiple models of obese mice was used to identify genes correlated with obesity, and 30% of the 100 most significant positively correlated genes

were macrophage associated genes (159). Within WAT, macrophages surround dead adipocytes in “crown-like structures” (22, 101, 140), which stain positive for F4/80, MAC-2, TNF-α, and IL-6—indicative of their macrophage content and inflammatory properties (22, 101, 140). The macrophages in the crown-like structures are indeed recruited to the WAT. It has been shown that during the development of obesity in mice, monocytes exit the bone marrow and enter the circulation (159), from which they enter the WAT and differentiate into pro-inflammatory (M1) macrophages (89). Resident alternatively activated (M2) macrophages are retained in the WAT but do not collect around the dead adipocytes.

ATMs have been proposed to contribute to whole body insulin resistance by inducing inflammation and local insulin resistance. Xu et al. demonstrated that in mice with diet induced obesity (DIO), macrophage accumulation temporally precedes an increase in circulating insulin levels (166), and treatment with the insulin-sensitizing drug rosiglitazone decreases the expression of macrophage-originated genes in visceral fat (166). This paracrine effect between macrophages and adipocytes is thought to be partially mediated by TNFα and IL-6. Mice with an absence of macrophage-derived TNFα exhibit reduced epididymal fat pad weight and enhanced insulin sensitivity in comparison to control mice (35). Using *in vitro* studies, Suganami et al. showed that macrophage secreted TNFα induces lipolysis and inhibits adipocyte insulin signaling via serine phosphorylation of insulin receptor substrate-1 (IRS-1) (141). TNFα’s induction of lipolysis causes increased NEFA release by adipocytes,

which further exacerbates the inflammatory phenotype of the macrophages, creating a vicious cycle of inflammation and insulin resistance (141). Thus, it is widely believed that macrophage infiltration into WAT leads to increased local inflammation, which in turn reduces insulin sensitivity both in the WAT and systemically.

T-lymphocyte populations in WAT

T-lymphocytes are recruited to WAT within 2 weeks of high fat diet feeding in mice (105), and numerous groups are currently investigating their role in WAT inflammation and insulin resistance (39, 72, 105, 124, 162, 164). *In vitro* migration experiments support the idea that adipocyte-secreted chemokine RANTES is involved in T-lymphocyte recruitment to the WAT (164), and the arrival of neutrophils in WAT within the first week of high fat diet feeding suggests that they, too, may be involved in initiating the recruitment of other leukocytes (38).

T-lymphocytes can be characterized according to their cell surface markers. Cytotoxic CD3+/CD8+/CD4- T-lymphocytes are increased in the WAT of both DIO and $Lep^{ob/ob}$ mice (105, 124). In contrast, CD3+/CD8-/CD4+ T-lymphocytes and Foxp3+ T-regulatory (T_{reg}) lymphocytes are decreased in the WAT of obese mice in comparison to WAT from lean mice (39, 105). T_{reg} lymphocytes are also less frequent in visceral WAT from obese versus lean humans (162), but in regard to CD4+ and CD8+ T-lymphocytes the data from humans and mice are not yet reconciled. In patients with type 2 diabetes,

Kintscher et al. detected only moderate expression of CD8 in WAT, but demonstrated the presence of CD4+ T-lymphocytes and a positive correlation between CD4 expression and body weight (72). Kintscher et al. also demonstrated that the majority of the ATMs were HLA-DR-positive, suggesting that they may have been activated by interferon-γ, a cytokine released by CD4+ helper T-lymphocytes (72). These variances might be due to species differences; however, the interaction of inflammatory cells within WAT is dynamic, and perhaps the CD8+ T-lymphocytes are common during the early stages of human obesity.

Macrophage infiltration of the WAT has been shown to temporally precede systemic insulin resistance in mice with DIO (166), but the converse has also been demonstrated. T-lymphocyte accumulation in WAT, as well as impaired glucose tolerance and insulin sensitivity can occur before macrophage accumulation in mice with DIO (72). Thus, the sequence in which immune cells infiltrate WAT and the sequence of events leading to insulin resistance in humans is not yet clearly defined. In Chapters IV and V, we investigate the role of MIP-1α, a chemoattractant for both T-lymphocytes and monocytes, in obesity-related WAT inflammation. This dissertation will conclude with a discussion of the timeline of the events in obesity-related WAT inflammation (Chapter VI).

Initiation of leukocyte recruitment to WAT during weight gain

Both adipocyte hyperplasia and hypertrophy can contribute to WAT expansion; however, in adults, hypertrophy appears to predominate. Some of

the consequences of hypertrophy include increased fatty acid flux from adipocytes, increased leptin secretion, hypoxia, and adipocyte death. These adipocyte-related consequences of WAT expansion are all possible contributors to the initiation of monocyte and T-lymphocyte recruitment. Here we will highlight hypoxia and adipocyte death, two of the top candidates for initiation of leukocyte recruitment to WAT during obesity, as well as the potential role of leptin. Lastly, we will discuss models in which the correlation between WAT growth and leukocyte infiltration seems to be dissociated.

Hypoxia

At least three different obese mouse models (DIO, KKA^{y}, and $Lep^{ob/ob}$) have been used to demonstrate that hypoxia is present in obese WAT (54, 167). Decreased vascular density, which has been observed in obese mice (112, 153), may contribute to this. Furthermore, protein and mRNA levels of hypoxia-inducible factor-1α (HIF-1α) are elevated in WAT from obese mice, as are mRNA levels for other hypoxia inducible genes (54, 167). Evidence suggests that hypoxia may initiate an inflammatory response as *in vitro* exposure of primary adipocytes and macrophages to hypoxia increases their expression of multiple inflammatory genes (167).

Human adipocytes, like murine adipocytes, also have increased expression of HIF-1α and other hypoxia related genes when exposed to low oxygen levels (1%) (156). Human preadipocytes exposed to hypoxia had elevated HIF-1α mRNA, increased secretion of vascular endothelial growth

factor, and although leptin expression and secretion was nearly absent in preadipocytes under normal oxygen conditions, hypoxia stimulated their expression and secretion of leptin (155). Therefore, hypoxia is potentially involved in several of the initiating factors of macrophage recruitment including leptin secretion and adipocyte death (discussed below), as well as an initial upregulation of inflammatory genes.

Adipocyte death

Adipocyte death does occur in WAT from lean individuals, but its frequency increases with obesity and it positively correlates with adipocyte hypertrophy (22, 101, 118, 140). Therefore, it is believed that the influx of macrophages to the WAT is partially in response to adipocyte death and the need for these dying cells to be phagocytosed. Support for this comes from hormone sensitive lipase deficient mice, which have hypertrophic adipocytes and increased adipocyte cell death despite their being lean (110). Epididymal and visceral WAT contain more dead adipocytes and inflammation as well as a greater accumulation of ATMs than subcutaneous WAT (14, 100, 101, 108, 140). Thus, it is likely that adipocyte cell death, which may be caused by the hypoxic conditions that occur during rapid tissue expansion (reviewed in (45)), is a signal that attracts phagocytic macrophages.

Leptin's potential roles in WAT inflammation

Leptin, which like IL-6 is a class-I cytokine, is a chemoattractant for multiple cell types. We have shown *in vitro* that leptin can induce monocyte migration (47). In addition, leptin negatively regulates the proliferation of T_{reg} lymphocytes (34), which are much more abundant in lean than in obese individuals. Therefore, this evidence suggests that leptin can both actively recruit new monocytes to WAT while at the same time inhibiting the proliferation of T_{reg} lymphocytes, which suppress WAT inflammation.

Correlation between WAT mass and inflammation

Although expansion of WAT is typically associated with an increased accumulation of inflammatory leukocytes, situations in which these two parameters are disconnected can provide insight into the commonly observed correlation between obesity and leukocyte accumulation within WAT. Two recent publications have examined the effect of the PPARγ agonists thiazolidinediones (TZDs) on WAT and insulin sensitivity (78, 136). TZD administration increases insulin sensitivity in people with type 2 diabetes but simultaneously causes weight gain and increases the size of subcutaneous adipocytes (40, 78). In addition, patients who become more insulin sensitive in response to TZDs have increased intramyocellular adipocytes and fewer inflammatory macrophages within their WAT (136). These data suggest that treatment with TZDs increases the capacity for healthy storage of TGs and that WAT inflammation—not merely the presence of more or larger adipocytes—is responsible for obesity-associated

insulin resistance. Similarly, fish oil supplementation in high fat diet fed mice increases WAT mass but decreases macrophage infiltration and inflammation in the WAT, and this is associated with increased insulin sensitivity (131).

Collagen VI knockout mice demonstrate another facet to the relationship between adipocyte size and insulin sensitivity. Within WAT, the extracellular matrix usually becomes denser during obesity, and collagen VI is one of the main components of this matrix. In the absence of collagen VI, individual adipocyte growth is uninhibited, and, in this context, larger adipocytes are associated with reduced WAT inflammation and increased systemic insulin sensitivity (69).

As another example, individuals with lipodystrophy—like many obese individuals—are insulin resistant and have increased WAT inflammation (18, 137). Thus, in this example as well as the previous, WAT inflammation and insulin resistance are positively correlated, and proper functioning of adipocytes is more important than their size. The amount of adiponectin secreted appears to be an important factor in this relationship. In fish oil-fed mice and in TZD-treated patients secretion of more adiponectin—even if by larger adipocytes—is associated with an improvement in insulin sensitivity and reduced WAT inflammation (131). In agreement with this, adiponectin transgenic mice have improved insulin sensitivity and less WAT macrophage infiltration even though their adipocytes are smaller than those of wild type mice, indicating once again that adipocyte function and the adipokines secreted are more important than cell size.

Chemokines as propagators of WAT inflammation

Similar to how chemokines direct leukocytes into the artery wall in atherosclerosis, evidence suggests that they also propagate inflammation in WAT (Figure 1.7). Initial reports indicated that the chemokines MIP-1α and MCP-1 as well as the inflammatory cytokine TNFα were mainly derived from stromal vascular cells rather than adipocytes (14, 159, 166). However, other reports have indicated that adipocytes, not stromal vascular cells, secrete more chemokines during weight gain (63, 84) and that 3T3-L1 adipocytes increase secretion of chemokines in response to free fatty acid administration (63). Therefore, both adipocytes and leukocytes appear to produce chemokines in WAT and the proportion of inflammatory mediators being produced by each likely changes during the development of obesity. Evidence for the importance of chemokines in WAT inflammation in obese mice and humans is discussed below.

The role of chemokines in WAT inflammation: Mouse studies

Numerous chemokines exhibit elevated mRNA and protein levels in the WAT and plasma of mice with genetic or diet-induced obesity. Expression of macrophage chemokines monocyte chemotactic protein-1 (MCP-1) and MIP-1α are increased in the WAT of $LepR^{db/db}$, $Lep^{ob/ob}$, and diet induced obese mice (19, 61, 65, 66, 104, 166, 168). Other chemokines upregulated in WAT from diet induced obese and/or $Lep^{ob/ob}$ mice are MCP-2 (158), MCP-3 (158), RANTES (164), and CXCL14 (104). Receptors for these chemokines such as CCR2, CCR3, and CCR5 are also elevated in the WAT of mice with DIO (158, 164).

Furthermore, in comparison with WAT from lean mice, epididymal and inguinal WAT from diet induced obese mice have altered gene expression of 60 inflammatory genes, including MCP-1 and MCP-3, which were the two most highly upregulated inflammatory genes (19).

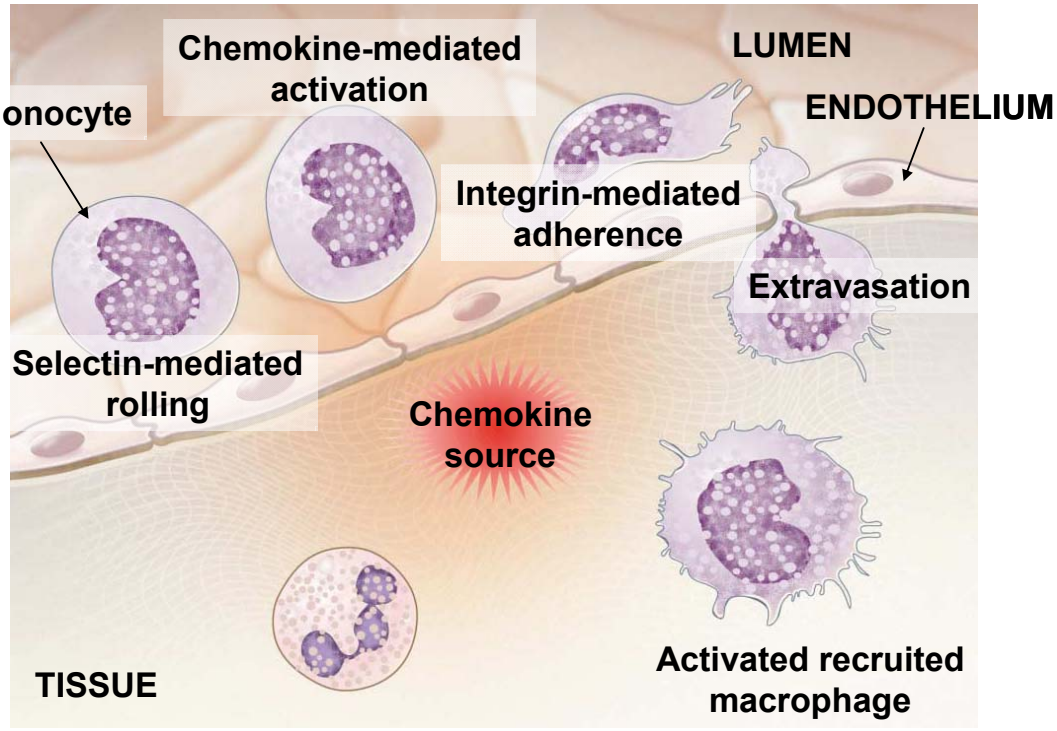

Figure 1.7. Recruitment of macrophages to tissues in response to inflammatory signal. This process is well-documented in the recruitment of leukocytes to the artery wall and is a model for what is thought to occur in WAT. Monocytes and macrophages are shown above, but the process for other leukocytes is similar. Adapted from Luster AD, *N Engl J Med.* 1998 Feb 12;338(7):436-45.

It is clear that obese mice have elevated chemokines in their WAT. However, some of their functions may overlap, such that alteration of only one chemokine or chemokine receptor at a time may have only minor effects on ATM accumulation (143). More work needs to be done to clarify which chemokines are important in the recruitment of macrophages and the mechanisms by which

they induce insulin resistance. In Chapter IV we investigate the role of MIP-1α in recruitment of leukocytes to WAT.

The role of chemokines in WAT inflammation: Human studies

Multiple human studies have demonstrated an elevation in gene expression of various chemokines in WAT in obesity, including MCP-1, MIP-1α, MIP-1β, MCP-2, MCP-4, MIP-2α, and pulmonary and activation-regulated chemokine (PARC) (14, 31, 102, 160). Insulin resistant humans have increased expression of macrophage markers in WAT in comparison to insulin sensitive individuals, and WAT expression of MIP-1α and MCP-1 is elevated during hyperinsulinemic euglycemic clamps in people with insulin resistance (160). Furthermore, a significant positive correlation has been observed between WAT gene expression of the chemokines MIP-1α, MCP-1, and MCP-2 and fasting serum insulin as well as whole body glucose disposal rate (102). Finally, in a comparison of obese versus lean individuals, expression of 6 different chemokines and their receptors was higher in obese humans, and the expression of MIP-1α and RANTES positively correlated with fasting plasma insulin levels independent of waist circumference (56). Thus, analysis of human WAT has demonstrated a potential role for chemokines, including MIP-1α, in the propagation of macrophage recruitment and in obesity-related insulin resistance.

Macrophage inflammatory protein-1α (MIP-1α)

MIP-1α is a classic chemokine of 69 amino acids in length in its mature state. It is a member of the CC chemokine family, named so because of their two sequential cysteine residues near the N-terminus. In mice, standard nomenclature for MIP-1α is CC chemokine ligand 3, or CCL3. In humans, MIP-1α is encoded by two genes: *CCL3* and *CCL3L* (115). Although MIP-1α can be expressed in adipocytes, platelets, osteoblasts, astrocytes, and epithelial cells, mature hematopoietic cells tend to be its major source. Bacterial lipopolysaccharide, viral infection, TNFα and other pro-inflammatory cytokines induce MIP-1α expression (44, 96). Our laboratory has also shown that its expression in macrophages is greatly increased upon exposure to human very low density lipoprotein (Figure 1.8) (132). MIP-1α signals through the G protein coupled CC chemokine receptors CCR1, CCR3, and CCR5 (98). MIP-1α has been shown to induce the chemotaxis of monocytes (150), activated T-lymphocytes (especially CD8+ cells), B-lymphocytes, NK cells, basophils, and eosinophils (6, 30, 128, 134, 145, 146, 148). Expression of MIP-1α and its receptors is upregulated in the WAT of obese humans and rodents (see below for more details) (57, 63, 84, 166). The importance MIP-1α in the recruitment of leukocytes to WAT in obese mice will be addressed in Chapters IV and V.

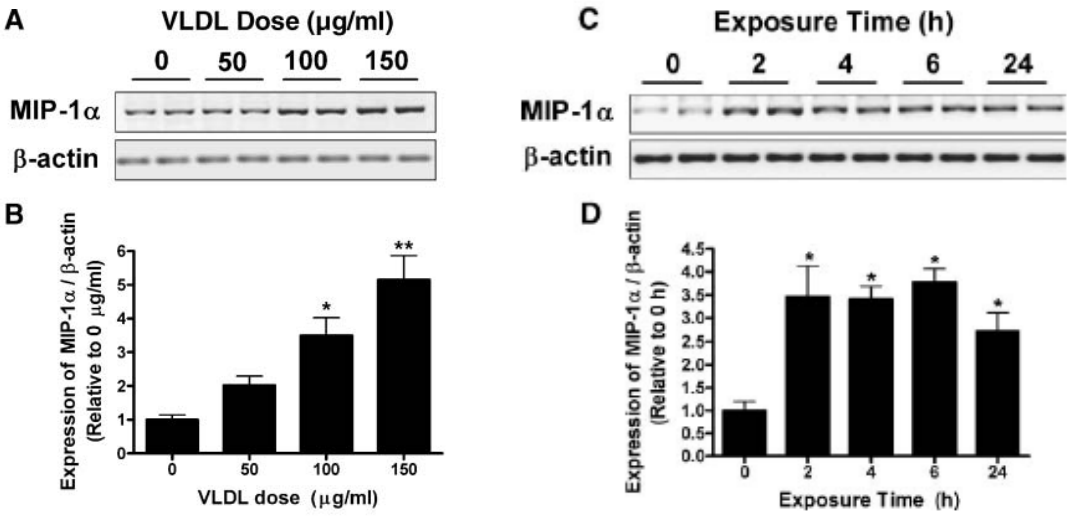

Figure 1.8. Dose- and time-dependent effects of VLDL on MIP-1α expression in mouse peritoneal macrophages. A, B: Mouse primary peritoneal macrophages were incubated with 0, 50, 100, or 150 mg/ml VLDL for 6 h. RNA was isolated, and MIP-1α gene expression was measured by RT-PCR. B-Actin was used as a control to confirm equal RNA concentrations. A: Representative amplification of duplicate samples. B: Band intensities from six samples were quantified using Quantity One software and plotted as means 6 SEM. C, D: Mouse primary peritoneal macrophages were incubated with 100 mg/ml VLDL for 0, 2, 4, 6, or 24 h. C: RNA was isolated from cells and analyzed for MIP-1α expression by RT-PCR. D: Band intensities from six samples were quantified using Quantity One software and plotted as means ± SEM. *p<0.01 compared with 0 mg/ml VLDL; **p<0.001 compared with 0 and 50 mg/ml VLDL. Figure and legend text from Saraswathi and Hasty. *J Lipid Res.* 2006 Jul;47(7):1406-15. Epub 2006 Apr 25.

The role of chemokines and chemokine receptors in CVD

Predictive and diagnostic potential of chemokine levels for CVD

Several chemokines are significantly elevated in the circulation of individuals with coronary artery disease (CAD), and although increased inflammation is not unique to atherosclerosis, a recent publication suggests

measurement of a combination of chemokines can be helpful for predicting disease. Inclusion of circulating CXCL10, MIP-1α, and CCL7 with the traditional risk factors of waist circumference and smoking in a linear regression model has better diagnostic potential than linear regression models based only on traditional risk factors (3). In patients with unstable angina pectoris, circulating MIP-1α, RANTES, and CCL18 transiently increase during ischemia, and plasma MIP-1α is a potential predictor of future ischemic events (32, 80). Plasma MIP-1α as well as MCP-1 and RANTES are also elevated in patients with severe acute myocardial infarction (77, 113). These and other clinical studies demonstrate that measurement of circulating chemokines such as MIP-1α may assist in early detection of CVD and improve patient care.

Secretion of chemokines by peripheral blood mononuclear cells (PBMCs) is altered by some CVDs. PBMCs from CAD patients spontaneously secrete more MCP-1, IL-8, GROα, CXCL9, and CXCL10 than PBMCs from controls, and they release greater amounts of MCP-1 and IL-8 when stimulated with oxLDL relative to controls (13, 33). Unstimulated PBMCs from hypercholesterolemic HFHC patients release more MIP-1α, MIP-1β, and IL-8 than control PBMCs, and this spontaneous release is positively correlated with plasma total and LDL cholesterol (53). MIP-1α, MIP-1β, and IL-8 may be especially important mediators of inflammation in individuals with high LDL cholesterol. As shown in Chapter V, we measured atherosclerotic lesion area and determined the consequences of MIP-1α deficiency in $LDLR^{-/-}$ mice to test the combined importance of MIP-1α and hyperlipidemia.

Chemokine receptors CCR5 and CCR1 and atherosclerosis

Several studies have investigated the roles of CCR5 and CCR1, receptors for MIP-1α, macrophage inflammatory protein-1β (MIP-1β/CCL4) and RANTES. CCR5 deficiency reduces atherosclerotic lesion area and inflammation in both apoE$^{-/-}$ and LDLR$^{-/-}$ mice (12, 120, 121), although CCR5 deficiency is not protective during early atherosclerosis in apoE$^{-/-}$ mice (81). Furthermore, CCR5 deficiency protects against neointima formation induced by arterial wire injury in apoE$^{-/-}$ mice (169). Some of these beneficial effects can be accounted for by the upregulation of anti-inflammatory cytokine IL-10 in CCR5$^{-/-}$ mice (12, 169). The atherogenic effects of CCR5 appear to be independent of the well-studied chemokine MCP-1 and the chemokine receptor CX_3CR1, since CCR5 antagonism further decreases lesion area in apoE$^{-/-}$ mice that are also deficient in MCP-1 and CX_3CR1 (apoE$^{-/-}$;MCP-1$^{-/-}$;$CX_3CR1^{-/-}$ mice) (26). In contrast to CCR5, CCR1 deficiency increases lesion area in atherosclerosis prone mice (12, 119), suggesting that CCR1 is protective against lesion formation. In Chapter V we examine the role of MIP-1α, a CCR5/CCR1 ligand, in atherosclerotic lesion formation.

Significance

Approximately two-thirds of American adults are overweight or obese (2). Obesity is recognized as a strong risk factor for CVD and type 2 diabetes, partially because of altered release of various hormones and cytokines from

WAT. The potential role of these secreted factors in the health conditions associated with obesity has only begun to be addressed. The following chapters will describe our research regarding how leptin/LepRb signaling in macrophages influences atherosclerosis (Chapter III) and the role of MIP-1α in diet-induced obesity, WAT inflammation, and systemic insulin resistance (Chapters IV and V, see Figure 1.2). Understanding the roles of leptin and MIP-1α in obesity will potentially enhance clinicians' ability to assist patients with obesity, hyperlipidemia, and CVD.

CHAPTER II

MATERIALS AND METHODS

Mouse care

Ethics Statement

All procedures were performed according to and with approval by Vanderbilt University's Institutional Animal Care and Use Committee.

Diets

Mice were fed a standard rodent chow diet (LabDiet 5001; 12% kcal from fat, 28% kcal from protein, 60% kcal from carbohydrates) unless otherwise indicated. Western Diet (WD; TD.88137, Harlan Teklad; Madison, WI) is composed of 42% kcal from fat, 15% kcal from protein, and 43% kcal from carbohydrates with 0.15% added cholesterol.

Mice used in Chapter III

All mice were originally purchased from Jackson Laboratories (Bar Harbor, ME) and were on the C57BL/6 background. Donor and recipient mice for all experiments were LDL receptor deficient ($LDLR^{-/-}$, strain B6.129S7-*Ldlr* ^{tm1Her}/J). $LDLR^{-/-}$ mice heterozygous for LepR deficiency were crossed to generate homozygous $LepR^{db/db}$;$LDLR^{-/-}$ mice.

Mice used in Chapter IV

MIP-1α deficient (MIP-1α$^{-/-}$) mice on a C57BL/6 background were purchased from Jackson Laboratory (strain B6.129P2-*Ccl3*^{tm1Unc}*/J*) and crossed with C57BL/6 mice from our colony (originally purchased from Jackson Laboratory) to obtain MIP-1α$^{+/-}$ mice. Mice from this F1 generation were bred to yield MIP-1α$^{+/+}$, MIP-1α$^{+/-}$, and MIP-1α$^{-/-}$ littermates, and the colony was maintained by breeding MIP-1α heterozygous mice. We obtained female mice at the expected Mendelian ratio (24% MIP-1α$^{+/+}$, 49% MIP-1α$^{+/-}$, and 27% MIP-1α$^{-/-}$, n=119), in agreement with the publication in which these mice are first described (29). However, we obtained fewer MIP-1α$^{+/+}$ male littermates than predicted (17% MIP-1α$^{+/+}$, 57% MIP-1α$^{+/-}$, and 26% MIP-1α$^{-/-}$, n=132).

At 8 wks of age, male and female littermates were switched from CD to WD, which they were fed for a total of 16 wks. A second cohort of mice was kept on chow diet throughout the duration of the study. In both the WD- and CD-fed groups, mice were weighed weekly for a 16 wk period and were bled at 24 wks of age. Their total lean and fat mass was measured every 4 wks, from wks 8 to 24 using nuclear magnetic resonance (NMR) with a Bruker Minispec (Woodlands, TX) housed in Vanderbilt University's Mouse Metabolic Phenotyping Center (MMPC).

Mice were genotyped using DNA extracted from ear tissue. The PCR protocol was obtained from Jackson Laboratory's website, and the following primers were used: 5'–ctt ggg tgg aga ggc tat tc–3' (mutant forward), 5'–agg tga

gat gac agg aga tc–3' (mutant reverse), 5'–atg aag gtc tcc acc act gc–3' (wild type forward), and 5'–agt caa cga tga att ggc g–3' (wild type reverse).

Mice used in Chapter V

LDLR$^{-/-}$ and MIP-1α$^{-/-}$ mice were originally purchased from Jackson Laboratories and were propagated within our colony. We crossed MIP-1α$^{-/-}$ and LDLR$^{-/-}$ mice to generate MIP-1α$^{+/-}$;LDLR$^{+/-}$ mice, which we bred to generate littermate MIP-1α$^{+/+}$;LDLR$^{-/-}$, MIP-1α$^{+/-}$;LDLR$^{-/-}$, and MIP-1α$^{-/-}$;LDLR$^{-/-}$ mice.

Genotyping protocol (Chapter V)

To genotype the mice used Chapter V, we chose primer pairs that allowed us to discriminate between mutations in the LDLR and MIP-1α genes, which both contained inserted neo cassettes. To determine the LDLR genotype, we used 3 primer sequences from Jackson Labs' website: 5'-AAT CCA TCT TgT TCA ATg gCC gAT C-3' (within the neo region), 5'-CCA TAT gCA TCC CCA gTC TT-3' (primer common to wild type and mutant mice), and 5'-gCg ATg gAT ACA CTC ACT gC-3' (within exon 4, only present in wild type mice). The MIP-1α genotype was determined according to the methods of Wu and Proia (165) using 2 pairs of primers: 5'-ATGAAGGTCTCCACCACTGC-3' (wild type, exon 1), 5'-AGTCAACGATGAATTGGCG-3' (wild type, exon 2), 5'-TAAAGCATGCTCCAGACT-3' (mutant, neo cassette), and 5'-CAAAGGCTGCTGGTTTCAAA-3' (mutant, exon 2). Primers were synthesized by Invitrogen (Carlsbad, CA), and REDExtract-N-Amp Tissue PCR Kit (Sigma,

St. Louis, MO) was used to amplify the DNA fragments, which were run on a 1.5% agarose gel.

Plasma analyses

Following a 5 h fast, mice were anesthetized with isoflurane and bled retro-orbitally using heparinized glass capillary tubes. Fasting glucose was measured on whole blood using a One-Touch glucometer (Lifescan, Inc., Milpitas, CA). Plasma was separated by centrifugation (12,000 rpm at 4˚C), aliquotted, and frozen at -20˚C for short term storage or -70˚C for long term storage. Plasma total cholesterol and triglycerides (TGs) were measured by enzymatic colorimetric assays according to manufacturers' directions adapted to a microtiter plate (Raichem, San Diego, CA). Fast performance liquid chromatography (FPLC) was performed as described (48). Plasma non-esterified fatty acids (NEFAs) were also measured by enzymatic colorimetric assays from Wako (NEFA-C kit for Chapter III, NEFA-HR (2) kit for Chapters IV-V; Richmond, VA). Plasma fasting insulin was measured by radioimmunoassay (Chapters III and V) in Vanderbilt University's MMPC Hormone Assay Core or by ELISA (Rat/Mouse Insulin ELISA Kit; Linco Research, Inc.; St. Charles, MO; Chapter IV).

Harvesting of tissues

At the conclusion of each study, mice were euthanized with isoflurane followed by cervical dislocation and were perfused with PBS. Cervical

dislocation was not performed when aortas were being collected (Chapter III and V). Tissues were then harvested, weighed, frozen immediately in liquid nitrogen, and stored at -70˚C, unless otherwise specified.

Bone marrow transplantation (Chapter III)

Donor mice were killed by cervical dislocation under anesthesia, and bone marrow was collected from the femurs and tibias. Approximately 2-5 x 10^6 bone marrow cells were injected into lethally irradiated recipient mice via the retroorbital venous plexus. Recipient mice were given antibiotic water (5 mg neomycin and 25,000 units polymyxin B sulfate per liter) for 1 week prior to and 2 weeks following BMT. Three separate BMT experiments were conducted as described below and diagrammed in Figure 3.1.

BMT #1

Male and female $LepR^{+/+}$;$LDLR^{-/-}$ mice were lethally irradiated at 6-9 weeks of age and transplanted with marrow from $LepR^{+/+}$;$LDLR^{-/-}$ or $LepR^{db/db}$;$LDLR^{-/-}$ donors. Eight weeks post-BMT, mice were fed WD. Mice were killed 21 weeks post-BMT.

BMT #2

Female $LepR^{+/+}$;$LDLR^{-/-}$ mice were lethally irradiated at 9-16 weeks of age and transplanted with marrow from $LepR^{+/+}$;$LDLR^{-/-}$ or $LepR^{db/db}$;$LDLR^{-/-}$ donors. Starting 4 weeks post-BMT, mice were fed WD through the end of the study (8

weeks total). Mice were assessed for adipose and muscle mass by NMR as described above. After 4 weeks of WD feeding, mice began to receive daily injections of leptin or PBS control (see below) for 4 weeks and were then killed.

BMT #3

Male and female obese, hyperleptinemic $LepR^{db/db}$;$LDLR^{-/-}$ mice were lethally irradiated at 9-13 weeks of age and transplanted with marrow from $LepR^{db/db}$;$LDLR^{-/-}$ or $LepR^{+/+}$;$LDLR^{-/-}$ donors. Mice remained on chow diet throughout the study and were killed 16 weeks post-BMT.

Leptin injections (Chapter III)

Mice in BMT protocol #2 received leptin or vehicle injections daily for 4 weeks. Murine recombinant leptin (National Hormone & Peptide Program, Torrance, CA) was dissolved in PBS, and 125 µg was injected intraperitoneally in a volume of 200 µl, as previously used by Bodary et al. (8). Leptin solution was made fresh each week and frozen at -20°C until use.

For the leptin half-life study, 9-week-old $LepR^{+/+}$;$LDLR^{-/-}$ female mice were injected with leptin (125 µg) one time. Plasma samples were obtained at baseline (2 h before injection), 30 min, 1 h, 3 h, 12 h, and 22 h post-leptin injection.

Atherosclerosis quantification (Chapters III and V)

Hearts were preserved in OCT and immediately frozen on dry ice. Fifteen 10 μm sections were collected over a 300 μm range beginning at the aortic root, according to the method of Paigen et al. (111). Aortic root sections were then stained for neutral lipids with Oil Red O (ORO) and counterstained with hematoxylin according to standard protocol. Lesions were captured with a Q-Imaging Micropublisher camera and quantified using Kinetic Histometrix 6 imaging and analysis software (Kinetic Imaging, Durham, NC).

Energy expenditure (Chapter IV)

After 8 wks on WD, representative male MIP-1α$^{-/-}$, MIP-1α$^{+/-}$, and MIP-1α$^{+/+}$ mice were housed individually in OxyMax cages (in Vanderbilt's MMPC) and kept on a light/dark cycle of 12 h light, 12 h dark. After an acclimation period of approximately 15 h, oxygen consumption data was recorded for a 24 h period, and energy expenditure (kcal/h) was calculated based on the (Vo_2 rate)/(Vco_2 rate) ratio using software provided by Columbia Instruments. Mice were weighed before and after being housed individually, and the initial body mass was used for energy expenditure/body mass calculations. The food in each cage was weighed at the beginning and end of the experiment to calculate food consumption per mouse.

Staining of WAT and liver sections

Perigonadal WAT was harvested from mice, weighed, and a portion was fixed overnight in 10% formalin, transferred to 70% ethanol, and paraffin embedded. Tissue was cut into 7μm sections (HM325 microtome, Microm) and stained with 0.1% w/v toluidine blue solution (Newcomer Supply, Middleton, WI). Representative sections are shown. Images were taken at 100x magnification. Liver sections were stained with oil red O and hematoxylin as previously described (23).

Hepatic triglyceride content

After mice were killed, livers were weighed and frozen in liquid nitrogen. Measurement of TG content was conducted by the Lipid Core Lab of Vanderbilt's MMPC as previously described (132).

Real time polymerase chain reaction (PCR)

Tissues for RNA extraction were harvested and immediately frozen in liquid nitrogen before being stored at -70˚C. RNA was isolated from tissues using the RNeasy Mini Kit (Qiagen) and RNA concentration was quantified by measuring optical density at 260 nm. BioRad's iScript cDNA Synthesis kit was used to synthesize cDNA. An iQ5 thermal cycler (BioRad) was used in conjunction with iQ Supermix (BioRad) and individual Assay-on-Demand (Applied Biosystems) primer/probe sets for each gene. The following genes were assessed: *18S* (4352930E), *Ccl2* (Mm00441242_m1),

Ccl3 (Mm00441258_m1), *Ccl4* (Mm00443111_m1), *Ccl5* (Mm01302428_m1), *Emr1* (Mm00802530_m1), *Cd68* (Mm00839636_g1), *Cd3e* (Mm00599683_m1), *Saa1* (Mm00656927_g1), *Tnfa* (Mm00443258_m1), *Il-10* (Mm99999062_m1), *Arg1* (Mm01190441_g1), *Adipoq* (Mm00456425_m1), *Foxp3* (Mm00475156_m1), *Mgl1* (Mm00546124_m1), *Mgl2* (Mm00460844_m1), *Ccr1* (Mm00438260_s1), *Ccr5* (Mm01216171_m1), *Srebp-1c* (Mm00550338_m1), and *Scd-1* (Mm01197142_m1). Relative expression was calculated by the ΔΔCt method using 18S expression to normalize the results.

Migration assays

Thioglycollate-elicited recruitment of immune cells to the peritoneal cavity

Mice were injected intraperitoneally with 3 ml of 3% thioglycollate (Sigma) to induce sterile inflammation. Three days later, peritoneal cells were harvested by lavage with 10 ml of serum-free DMEM, washed, and counted to determine the number of macrophages recruited to the peritoneal cavity. Cells collected in this manner were used for the Boyden chamber assays.

Boyden chamber migration assay

The chemoattractants and vehicle control were loaded into the bottom wells of the Boyden chamber, covered by a cell-permeable membrane, and primary peritoneal macrophages from C57BL/6 (MIP-1$\alpha^{+/+}$) or MIP-1$\alpha^{-/-}$ mice

were loaded on top of the membrane. After a 2 h incubation at 37˚ with 5% CO_2, cells that migrated to the bottom side of the membrane were fixed for 10 minutes in cold methanol, stained with crystal violet, and counted using a light microscope. Five high powered fields were counted per well.

Statistics

Chapter III

The unpaired Student's *t*-test was used to assess statistical significance. A p value of <0.05 was considered to be statistically significant. Results are shown as mean ± standard error of mean (SEM).

Chapters IV and V

GraphPad Prism software (version 4.01) was used for all statistical analyses. Data was analyzed with 2-way ANOVA and Bonferroni's post hoc test or by 1-way ANOVA followed by Tukey's multiple comparison post hoc test, as indicated. Two-way ANOVA was used to assess the relative contribution of multiple effects and to check for interactions between different conditions. Outliers were removed from the data if outside the range of the mean ± 2SD. $p \leq 0.05$ was considered significant.

CHAPTER III

THE ROLE OF MACROPHAGE LEPTIN RECEPTOR IN AORTIC ROOT LESION FORMATION

Introduction

In the current worldwide obesity epidemic, over 1 billion adults are overweight, and at least 300 million of these individuals are obese. In the United States, cardiovascular disease (CVD) is the number one cause of death, and over 80% of deaths from CVD are due to atherosclerosis-related diseases. Due to the compounding effect of obesity on atherosclerosis (37, 97, 127, 151, 161), understanding mechanisms by which obesity increases risk of atherosclerosis is critical to providing knowledgeable treatment and prevention of this deadly disease.

Leptin is a 16-kD protein secreted by adipocytes and represents one potential molecular link between obesity and atherosclerosis. Circulating plasma leptin levels correlate with the percentage of body fat and/or body mass index in normal-weight and obese rodents and humans (28, 90). Although leptin is a satiety factor that normally reduces appetite and promotes energy expenditure, many obese humans display hyperleptinemia and are considered leptin resistant (4). Leptin has multiple biologic effects, both centrally and peripherally, and there is evidence that hyperleptinemia is an independent risk factor for myocardial infarction and atherosclerosis (139, 154).

There are six leptin receptor (LepR) isoforms. Unlike the other isoforms, the long form of the receptor, isoform b, has a 302-amino acid cytoplasmic tail

and participates in intracellular signaling. The long form of the LepR is primarily expressed on hypothalamic neurons, and LepR deficient ($LepR^{db/db}$) mice develop extreme obesity and hyperleptinemia. Peripheral cells such as macrophages also express this isoform (95, 106). Leptin has been shown to have several potentially atherogenic effects in macrophages. Treatment of macrophages with recombinant leptin affects their cytokine production (88, 129, 130), lipid metabolism (42, 106), phagocytic function (42, 88), proliferation (42, 88, 129, 130), and oxidative stress (5, 83). Because macrophages are key in the development and progression of atherosclerosis (85), it is possible that hyperleptinemia could promote atherogenesis via some of these macrophage-specific effects.

Recently, Bodary et al. (8) investigated the possible role of hyperleptinemia in atherosclerosis and thrombosis. In their study, atherosusceptible apolipoprotein E deficient ($apoE^{-/-}$) mice were injected daily with recombinant leptin for 4 weeks. Mice receiving the leptin injections had a significant increase in lesion surface area in their brachiocephalic and carotid arteries as well as their thoracic aorta. Although these experiments indicated that leptin may be a molecular link between obesity and CVD, the cell type mediating leptin's effect was not identified. In the experiments described in our current study, we have tested the hypothesis that hyperleptinemia promotes atherosclerosis at the aortic root via macrophage LepRs.

Results

To test our hypothesis that hyperleptinemia promotes atherosclerosis via macrophage LepR, three different BMT experiments were conducted (Figure 3.1), and they will be discussed in detail below. All donor and recipient mice were LDLR deficient, with or without LepR. After transplantation, reconstitution with the correct donor marrow was confirmed by performing PCR for the LepR on DNA from whole blood or spleen tissue from recipient mice. As shown in 3.2, mice were completely reconstituted and expressed the LepR genotype of the donor marrow.

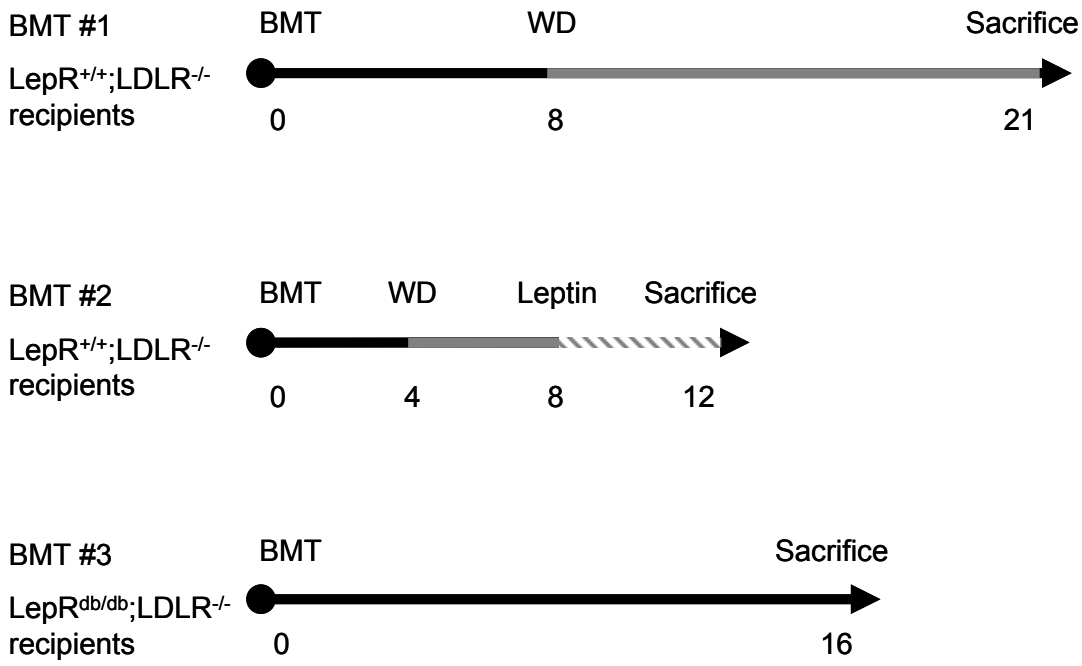

Figure 3.1. Time course diagrams for bone marrow transplantation experiments. In each BMT, mice were lethally irradiated and transplanted with bone marrow from $LepR^{+/+}$;LDLR-/- or $LepR^{db/db}$;$LDLR^{-/-}$ mice. Numbers represent the weeks post-BMT. "WD" represents the start of Western diet feeding. In BMT #2, "Leptin" indicates the start of daily injections of recombinant leptin (125 µg) or vehicle control.

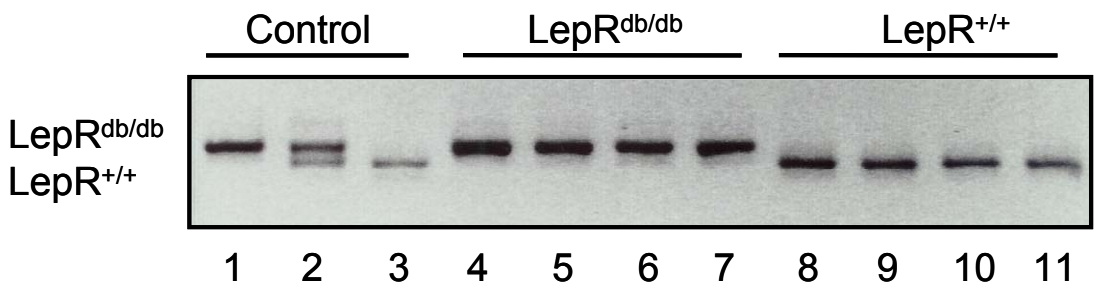

Figure 3.2. PCR analysis of recipient blood DNA. DNA was isolated from blood collected from transplanted mice. PCR analyses for the LepR were performed as described in Chapter II. Lanes 1–3 are the PCR products of tail DNA from $LepR^{db/db}$, $LepR^{db/+}$, and $LepR^{+/+}$ mice, respectively. Lanes 4–7 are PCR products from blood DNA of mice receiving LepRdb/db marrow, and lanes 8–11 are PCR products from blood DNA of mice receiving $LepR^{+/+}$ marrow.

Bone Marrow Transplantation #1: Mice with an absence of macrophage LepR and mild hyperleptinemia

The first BMT was designed to test the hypothesis that the absence of macrophage LepRs would be atheroprotective in a setting of mild hyperleptinemia. At 6-9 weeks of age, $LepR^{+/+}$;$LDLR^{-/-}$ mice were lethally irradiated and transplanted with bone marrow from $LepR^{+/+}$ or $LepR^{db/db}$ donors. This BMT design resulted in mice with an absence of functional LepR in their hematopoietic cells, including macrophages. Comparisons were made for male and female recipients separately (Table 3.1, which can be found at the end of the Results). At sacrifice, body weight, glucose, NEFA, insulin and leptin levels were not different between the recipients of $LepR^{+/+}$;$LDLR^{-/-}$ or $LepR^{db/db}$;$LDLR^{-/-}$ marrow. TC and TG levels in male mice receiving $LepR^{db/db}$;$LDLR^{-/-}$ marrow were increased compared to controls ($p<0.05$); however, no differences in plasma lipids were noted in female mice. Measurement of aortic root lesion area by

ORO staining revealed an increase in lesion area in female compared to male mice (Figure 3.3); however, within each gender the absence of LepR on hematopoietic cells did not affect lesion area.

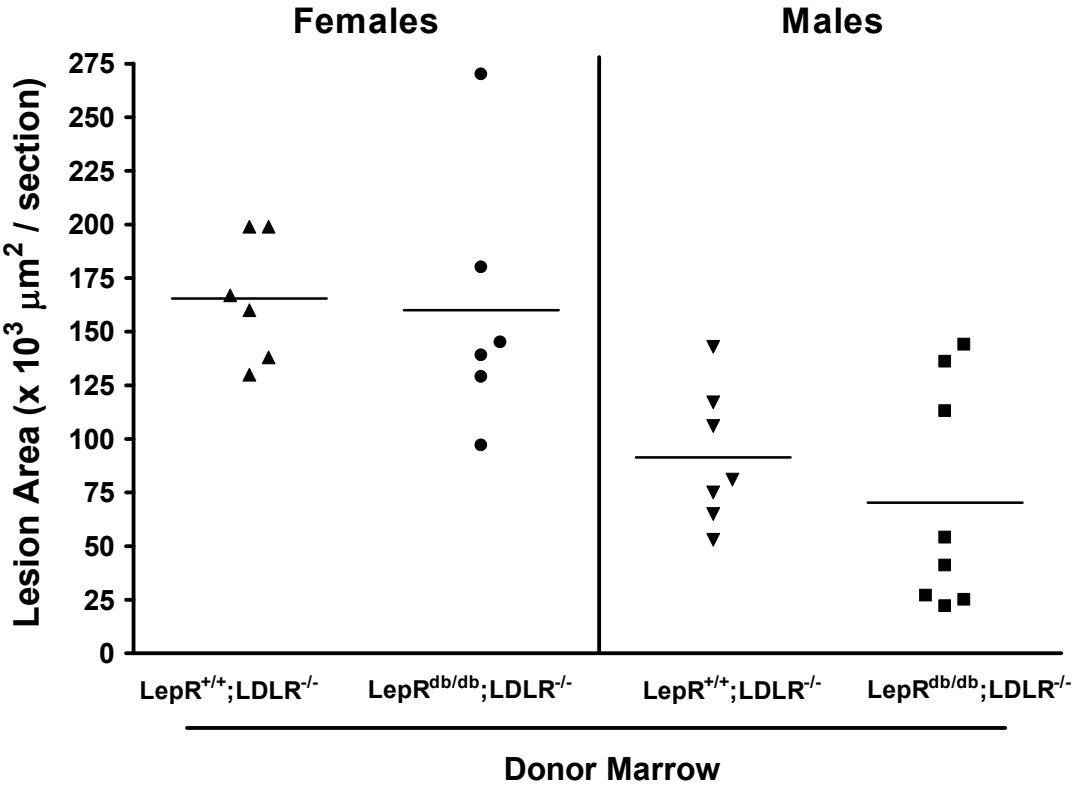

Figure 3.3. Aortic root lesion area in LepR+/+;LDLR-/- mice from BMT #1. Lethally irradiated $LepR^{+/+}$;$LDLR^{-/-}$ recipients were reconstituted with $LepR^{+/+}$;$LDLR^{-/-}$ or $LepR^{db/db}$;$LDLR^{-/-}$ bone marrow and placed on WD starting 8 wks post-BMT and sacrificed 5 months post-BMT. Aortic root lesions were stained with oil red O and quantified as described in the Methods section. Mouse gender and bone marrow genotype of the recipients are as follows: female $LepR^{+/+}$;$LDLR^{-/-}$ (▲), female $LepR^{db/db}$;$LDLR^{-/-}$ (●), male $LepR^{+/+}$;$LDLR^{-/-}$ (▼), and male $LepR^{db/db}$;$LDLR^{-/-}$ (■). n=6-8 mice per group.

Bone Marrow Transplantation #2: Mice with an absence of macrophage LepR and pharmacologically-induced extreme hyperleptinemia

As the presence or absence of LepR on hematopoietic cells did not impact atherosclerotic lesion area in $LepR^{+/+}$;$LDLR^{-/-}$ recipient mice when they were exposed to only mild elevations in leptin, a similar experiment was conducted using daily injections of leptin to induce extreme hyperleptinemia. At 9-16 weeks of age, female $LepR^{+/+}$;$LDLR^{-/-}$ recipients were lethally irradiated and transplanted with bone marrow cells either with or without LepR expression. After 4 weeks on WD, mice began receiving leptin (125 μg) or vehicle (PBS) injections for an additional 4 weeks. The resulting groups are labeled according to the genotype of their bone marrow and their injection treatment type: 1) $LepR^{+/+}$;$LDLR^{-/-}$ Vehicle, 2) $LepR^{db/db}$;$LDLR^{-/-}$ Vehicle, 3) $LepR^{+/+}$;$LDLR^{-/-}$ Leptin, and 4) $LepR^{db/db}$;$LDLR^{-/-}$ Leptin.

Body weight, abdominal adipose tissue and liver mass, as well as total body adipose tissue and muscle mass, were measured (Figure 3.4). At baseline, no differences in body weight were observed among the four groups (Figure 3.4A). All groups had increased body weight after 4 weeks on WD. After initiation of leptin injection, both groups receiving leptin had a significant decrease in body weight ($p<0.05$ at 2 and 4 weeks post-injection; Figure 3.4A and Table 3.2). Both leptin-treated groups had significantly less abdominal adipose tissue compared to vehicle-treated groups at sacrifice ($LepR^{+/+}$;$LDLR^{-/-}$ Leptin vs. $LepR^{+/+}$;$LDLR^{-/-}$ Vehicle, $p<0.005$; $LepR^{db/db}$;$LDLR^{-/-}$ Leptin vs. $LepR^{db/db}$;$LDLR^{-/-}$ Vehicle, $p=0.0001$; Figure 3.4B). Liver mass was also

decreased in both leptin-treated groups, although this reached significance only for the $LepR^{db/db}$;$LDLR^{-/-}$ Leptin group (p<0.005; Figure 3.4B). Total body adipose tissue mass (as measured by NMR) was decreased by 45% in the $LepR^{+/+}$;$LDLR^{-/-}$ Leptin group and by 49% in the $LepR^{db/db}$;$LDLR^{-/-}$ Leptin group compared to their respective controls (p<0.0001; Figure 3.4C). Muscle mass decreased non-significantly by 3% in mice receiving leptin.

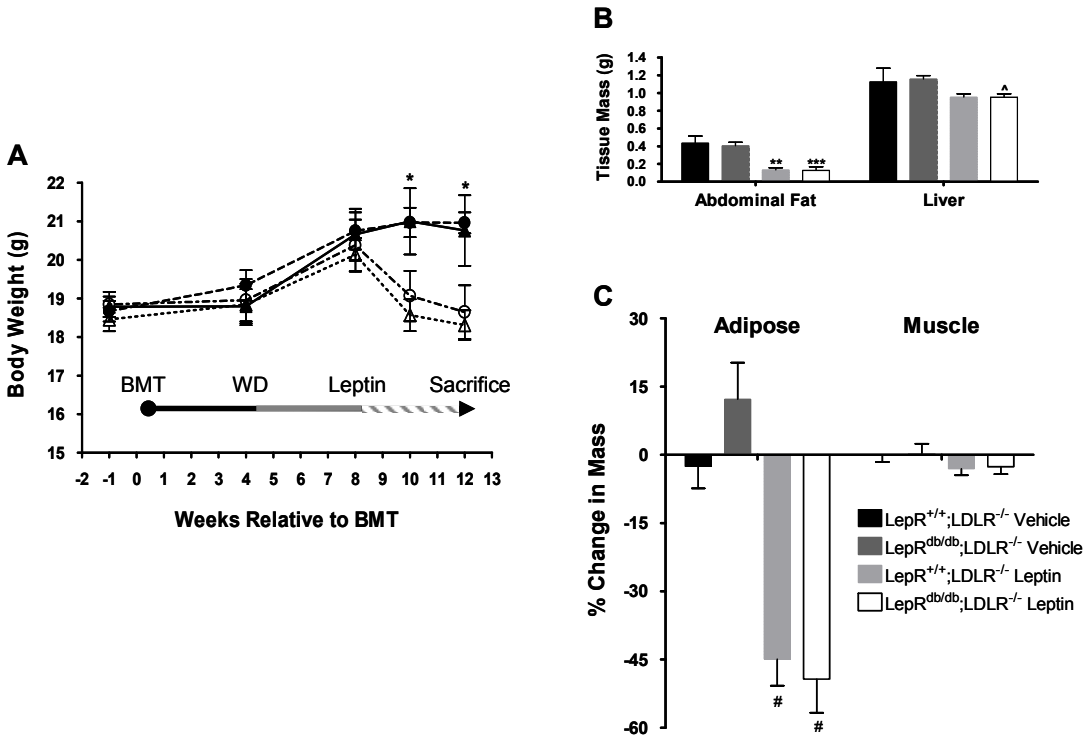

Figure 3.4. Differences in body weight and tissue mass in LepR+/+;LDLR-/- mice during the BMT #2 experiment. Lethally irradiated female LepR+/+;LDLR-/- recipients were reconstituted with LepR+/+;LDLR-/- or LepRdb/db;LDLR-/- bone marrow, fed WD for 8 weeks, followed by daily leptin injections for 4 of the 8 weeks. Bone marrow genotype of the recipients and injection treatment are indicated as follows: LepR+/+;LDLR-/- Vehicle (▲), LepRdb/db;LDLR-/- Vehicle (●), LepR+/+;LDLR-/- Leptin (∆), and LepRdb/db;LDLR-/- Leptin(○). n=7-10 mice per group. (A) Body weight over the time course of the experiment. *p<0.05 vs. respective leptin-treated groups. (B) Tissue mass at sacrifice. **p<0.005, ***p=0.0001, and ^p<0.005 vs. respective vehicle-treated groups. (C) Percent change in mass of adipose and muscle tissue over the 4 week injection period. #p<0.0001 vs. respective vehicle-treated groups.

The presence or absence of macrophage LepRs did not impact any plasma parameters when comparing mice within the vehicle- or leptin-treated groups (Table 3.2). When comparing leptin- versus vehicle-treated recipients of the same marrow, some differences in plasma parameters were noted (Table 3.2). Leptin-treated $LepR^{db/db}$;$LDLR^{-/-}$ recipients demonstrated a reduction in TC

and TG levels compared to vehicle-treated controls ($p<0.05$). Leptin-treated $LepR^{+/+}$;$LDLR^{-/-}$ recipients displayed a reduction in TC and an increase in NEFA levels compared to vehicle-treated controls ($p<0.01$). Plasma insulin levels were lower in the leptin-treated $LepR^{db/db}$;$LDLR^{-/-}$ and $LepR^{+/+}$;$LDLR^{-/-}$ groups ($p<0.05$ for $LepR^{+/+}$;$LDLR^{-/-}$ group) compared to their respective vehicle controls. Surprisingly, a statistically significant decrease in plasma leptin levels was observed in both leptin-treated groups at sacrifice ($p<0.05$). No differences in aortic root lesion area were detected among the groups (Figure 3.5).

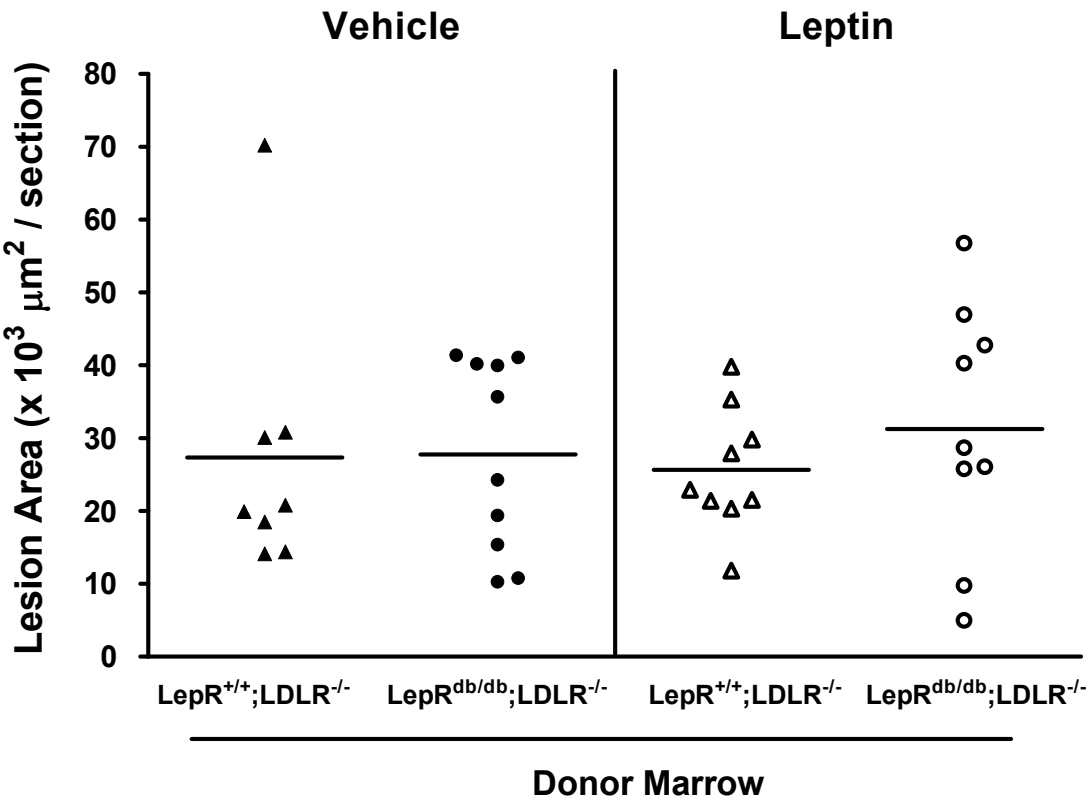

Figure 3.5. Aortic root lesion area in female LepR$^{+/+}$;LDLR$^{-/-}$ mice from BMT #2. Lethally irradiated female LepR$^{+/+}$;LDLR$^{-/-}$ recipients were reconstituted with LepR$^{+/+}$;LDLR$^{-/-}$ or LepR$^{db/db}$;LDLR$^{-/-}$ bone marrow, fed WD for 8 weeks, followed by daily leptin injections for 4 of the 8 weeks. Aortic root lesions were stained with ORO and quantified as described in the Methods section. Bone marrow genotype of the recipients and injection treatment are indicated as follows: LepR$^{+/+}$;LDLR$^{-/-}$ Vehicle (▲), LepR$^{db/db}$;LDLR$^{-/-}$ Vehicle (●), LepR$^{+/+}$;LDLR$^{-/-}$ Leptin (Δ), and LepR$^{db/db}$;LDLR$^{-/-}$ Leptin (○). n=8-10 mice per group.

Half-life of Injected Leptin

Because endpoint circulating leptin levels were significantly lower in mice injected with leptin, we sought to investigate the half-life of injected recombinant leptin. $LepR^{+/+}$;$LDLR^{-/-}$ mice were injected with 125 µg of leptin and plasma leptin concentrations measured for up to 22 h post-injection (Figure 3.6). Plasma leptin levels were dramatically elevated at 30, 60, and 180 minutes post-injection (p<0.0001). By 12 h post-leptin injection, plasma leptin levels had returned to baseline in all of the mice.

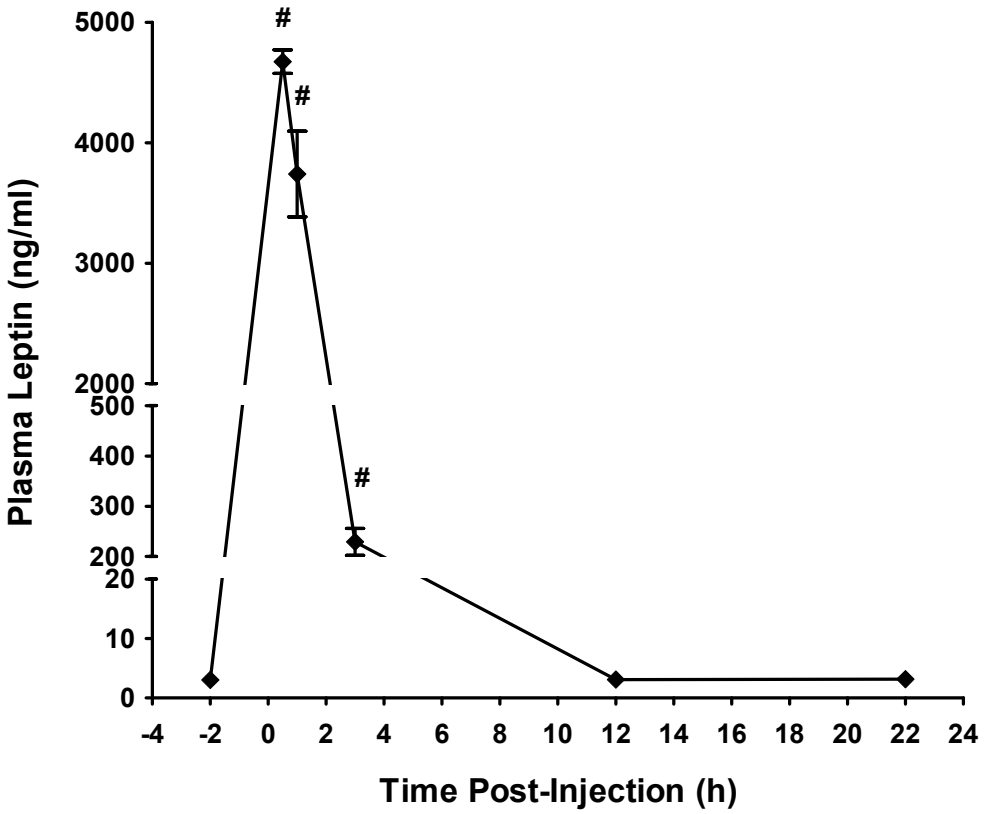

Figure 3.6. Measurement of plasma leptin following intraperitoneal leptin injection. Lean female LepR+/+;LDLR-/- mice were injected with recombinant leptin (125 µg). Blood samples were collected at baseline (2 h before injection) and at 30 min, 1 h, 3 h, 12 h, and 22 h after injection, and plasma leptin values were quantified. #p<0.0001 vs. baseline. n=3-5 mice per time point.

Bone Marrow Transplantation #3: Mice with the presence of macrophage LepR and severe hyperleptinemia

As a third test of our hypothesis, obese hyperleptinemic $LepR^{db/db}$;$LDLR^{-/-}$ mice were transplanted with bone marrow from $LepR^{db/db}$ or $LepR^{+/+}$ donors. The $LepR^{db/db}$; $LDLR^{-/-}$ recipients had naturally occurring hyperleptinemia (>100 ng/ml) due to their deficiency of LepR and were also hyperlipidemic, similar to leptin deficient $LDLR^{-/-}$ mice (48, 51). Thus they did not require the use of a high fat diet to induce atherosclerotic lesion formation. This BMT was designed to test the atherogenicity of LepR when it is only expressed on macrophages and other hematopoietic cells in the presence of obesity accompanied by high serum leptin levels. Mice were 9-13 weeks old at the time of transplantation, and were sacrificed 16 weeks post-BMT.

There were no differences in body weight, plasma lipids, or leptin levels between the two groups at sacrifice; however, plasma insulin levels were significantly lower in the $LepR^{+/+}$;$LDLR^{-/-}$ recipients ($p<0.05$; Table 3.3).

No sexual dimorphism was detected among the groups when aortic root lesions were quantified by ORO staining, therefore data from male and female mice were combined. Differences in lesion size were not observed between the mice with a global absence of LepR ($LepR^{db/db}$;$LDLR^{-/-}$ group) and those expressing LepR only on their hematopoietic cells ($LepR^{+/+}$;$LDLR^{-/-}$ group), as shown in Figure 3.7.

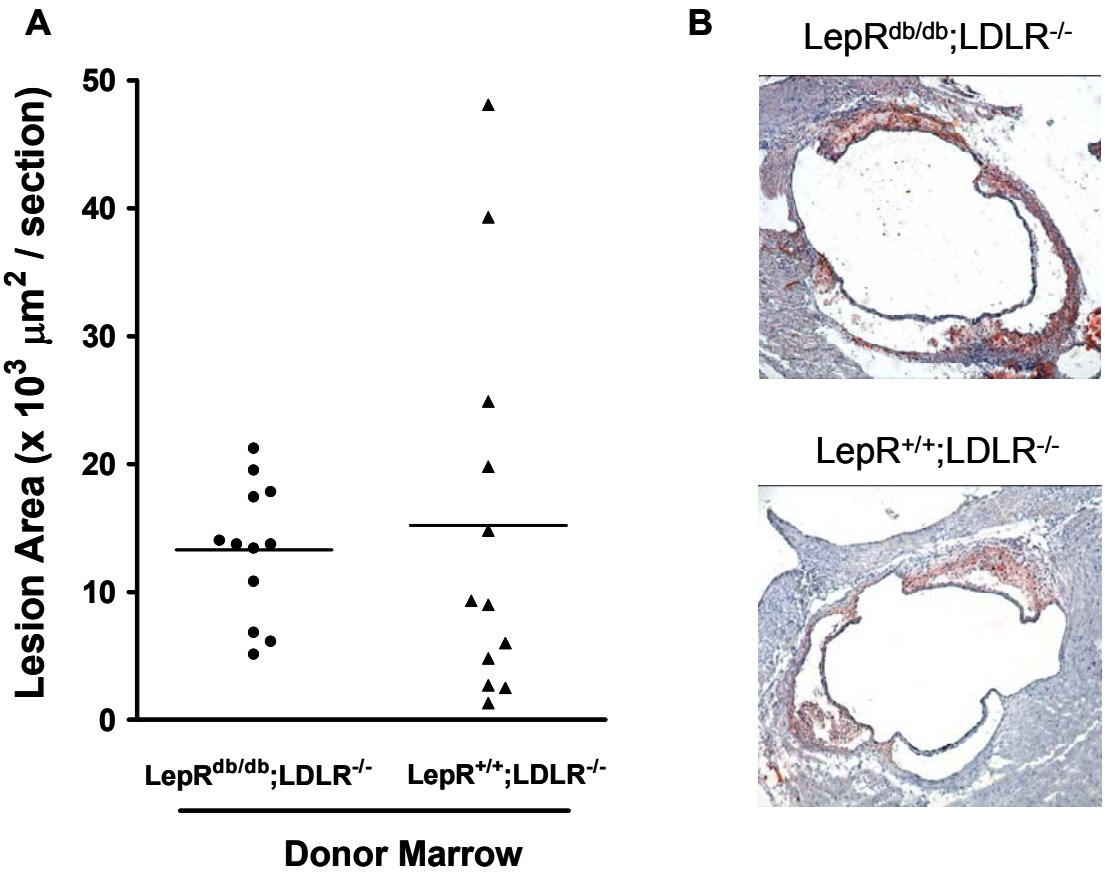

Figure 3.7. Aortic root lesion area in LepR$^{db/db}$;LDLR$^{-/-}$ mice from BMT #3. Lethally irradiated LepR$^{db/db}$;LDLR$^{-/-}$ recipients were reconstituted with LepR$^{db/db}$;LDLR$^{-/-}$ or LepR$^{+/+}$;LDLR$^{-/-}$ marrow by BMT. Mice were kept on a standard chow diet for the duration of the study, and sacrificed 16 weeks post-BMT. (A) Aortic root lesions were stained with ORO and quantified as described in the Methods. Groups are labeled according to the bone marrow genotype of the recipients: LepR$^{db/db}$;LDLR$^{-/-}$ (●) and LepR$^{+/+}$;LDLR$^{-/-}$ (▲). n=12-13 mice per group. (B) Representative ORO stained sections.

Table 3.1 Plasma parameters and body weight for $LepR^{+/+};LDLR^{-/-}$ recipients from BMT #1 at sacrifice

	Females		Males	
Donor Marrow	**$LepR^{+/+};LDLR^{-/-}$**	**$LepR^{db/db};LDLR^{-/-}$**	**$LepR^{+/+};LDLR^{-/-}$**	**$LepR^{db/db};LDLR^{-/-}$**
n	6	6	7	8
Body weight (g)	21.4 ± 1.1	20.8 ± 1.0	26.6 ± 1.3	25.0 ± 0.5
Cholesterol (mg/dl)	873 ± 59	765 ± 44	904 ± 37	1093 ± 72*
Triglycerides (mg/dl)	357 ± 38	276 ± 50	323 ± 65	568 ± 53*
NEFAs (mEq/L)	0.71 ± 0.08	0.87 ± 0.07	0.88 ± 0.10	1.04 ± 0.12
Glucose (mg/dl)	146 ± 11	147 ± 12	118 ± 5	130 ± 8
Insulin (ng/ml)	3.43 ± 1.58	1.13 ± 0.20	3.40 ± 1.53	0.73 ± 0.11
Leptin (ng/ml)	16.9 ± 2.9	12.8 ± 1.8	18.9 ± 3.9	12.4 ± 1.6

$LepR^{+/+};LDLR^{-/-}$ recipients were transplanted with $LepR^{+/+};LDLR^{-/-}$ or $LepR^{db/db};LDLR^{-/-}$ bone marrow. Mice were placed on WD 8 weeks post-BMT and sacrificed 21 weeks post-BMT. Plasma parameters were assayed as described in the Methods section. Statistics were performed using a Student's *t*-test to compare parameters of $LepR^{+/+}$ and $LepR^{db/db}$ recipients within each gender. * $p<0.05$ vs. $LepR^{+/+};LDLR^{-/-}$ group.

Table 3.2 Plasma parameters and body weight for $LepR^{+/+};LDLR^{-/-}$ recipients from BMT #2

	Vehicle		Leptin	
Donor Marrow	**$LepR^{+/+};LDLR^{-/-}$**	**$LepR^{db/db};LDLR^{-/-}$**	**$LepR^{+/+};LDLR^{-/-}$**	**$LepR^{db/db};LDLR^{-/-}$**
n	8	10	9	9
Body weight (g)	20.8 ± 0.9	21.0 ± 0.3	18.3 ± 0.4*	18.6 ± 0.7§
Cholesterol (mg/dl)	820 ± 59	817 ± 46	691 ± 35	662 ± 34†
Triglycerides (mg/dl)	281 ± 14	287 ± 24	216 ± 8‡	226 ± 16†
NEFAs (mEq/L)	0.96 ± 0.08	1.11 ± 0.19	1.36 ± 0.10‡	1.16 ± 0.11
Glucose (mg/dl)	108 ± 10	127 ± 7	105 ± 6	107 ± 10
Insulin (ng/ml)	1.15 ± 0.21	0.89 ± 0.13	0.67 ± 0.06*	0.63 ± 0.04
Leptin (ng/ml)	10.6 ± 2.3	9.3 ± 1.4	4.8 ± 0.6*	4.7 ± 0.9†
Estimated average daily leptin (ng/ml)	10.6 ± 2.3	9.3 ± 1.4	348.6	348.5

Female $LepR^{+/+};LDLR^{-/-}$ recipients were transplanted with $LepR^{+/+};LDLR^{-/-}$ or $LepR^{db/db};LDLR^{-/-}$ bone marrow. Mice were placed on WD 4 weeks post-BMT. Eight weeks post-BMT, mice were injected daily with leptin (125 µg) or vehicle (PBS) for 4 weeks. Mice were injected with leptin or vehicle 21-25 h before sacrifice. Student's *t*-tests were used to compare recipients of different bone marrow within treatment groups, and recipients of the same bone marrow in different treatment groups. The average daily leptin levels were estimated using the area under the curve from Figure 3.6 to calculate the average elevation above basal leptin levels in leptin-injected mice. * $p<0.05$ vs. $LepR^{+/+};LDLR^{-/-}$ Vehicle group; † $p<0.05$ vs. $LepR^{db/db};LDLR^{-/-}$ Vehicle group; ‡ $p<0.01$ vs. $LepR^{+/+};LDLR^{-/-}$ Vehicle group; § $p<0.01$ vs. $LepR^{db/db};LDLR^{-/-}$ Vehicle group.

Table 3.3 Plasma parameters and body weight for $LepR^{db/db}$;$LDLR^{-/-}$ recipients from BMT #3

Donor Marrow	$LepR^{db/db}$;$LDLR^{-/-}$	$LepR^{+/+}$;$LDLR^{-/-}$
n	12	13
Body weight (g)	48 ± 1	47 ± 1
Cholesterol (mg/dl)	775 ± 29	723 ± 42
Triglycerides (mg/dl)	430 ± 41	352 ± 30
NEFAs (mEq/L)	0.86 ± 0.06	0.90 ± 0.08
Glucose (mg/dl)	200 ± 28	234 ± 25
Insulin (ng/ml)	17.8 ± 2.3	11.6 ± 1.5*
Leptin (ng/ml)	153 ± 10	130 ± 13

$LepR^{db/db}$;$LDLR^{-/-}$ recipients were transplanted with $LepR^{db/db}$;$LDLR^{-/-}$ or $LepR^{+/+}$;$LDLR^{-/-}$ bone marrow and sacrificed 16 weeks post-BMT. * $p<0.05$ vs. $LepR^{db/db}$;$LDLR^{-/-}$ group.

Discussion

We have addressed the role of macrophage LepR in aortic root atherosclerotic lesion formation through three distinct bone marrow transplantation studies. First, we tested the hypothesis that an absence of LepR on macrophages would be atheroprotective in lean $LDLR^{-/-}$ mice (BMT #1). Second, we tested this same hypothesis under pharmacologically induced hyperleptinemia (BMT #2). Finally, we tested the hypothesis that the presence of LepR only on hematopoietic cells such as macrophages would be pro-atherogenic in obese hyperleptinemic mice (BMT #3). Despite the use of these three approaches to test our overall hypothesis, analysis of aortic root cross sections did not reveal alterations in atherosclerotic lesion area due to the presence or absence of macrophage LepR.

There is evidence that hyperleptinemia is associated with increased risk of cardiovascular disease in humans (139, 154). Recent mechanistic studies related to the role of leptin in vascular health have focused on the four major cell types involved in atherogenesis: endothelial cells, smooth muscle cells, T lymphocytes, and macrophages. Full-length LepR has been shown to be expressed on and capable of signal transduction in all four of these cell types (107, 114, 138). Potential means by which leptin could cause macrophages to become pro-atherogenic include: increased inflammatory cytokine secretion (88, 130), proliferation (42, 88, 129, 130), and oxidative stress (5, 83), as well as impaired lipid metabolism (15, 106). Thus, we speculated that macrophages could be the cell type responsible for increased lesion formation in a setting of

hyperleptinemia. However, our data, derived from three separate bone marrow protocols, do not support a role for macrophages in hyperleptinemia-associated aortic root lesion formation.

Bodary et al. has shown significantly increased total lesion area in the thoracic aorta as well as the brachiocephalic and carotid arteries in apoE$^{-/-}$ mice receiving recombinant leptin (8). One possible explanation for the differences between this and our current studies is that macrophages may not be the primary cell type responsible for hyperleptinemia-induced aortic root lesion formation. In fact, recent studies by Bodary and colleagues have shown that leptin's effects on neointimal formation after vascular injury are not attributable to bone marrow-derived cells (9). However, other possibilities exist. First, the animal model used was different. We cannot rule out the possibility that leptin interacts with apoE, and that the combined deficiency of both is required to detect the atherogenic potential of leptin. Second, it is possible that leptin has a greater effect in more advanced lesions. The lesions in apoE$^{-/-}$ mice fed Western diet for 8 weeks are more advanced than those in LDLR$^{-/-}$ mice under the same conditions. Third, the location of the lesions quantified was different between the two studies. It is possible that leptin mediates more potent effects at sites other than the aortic root.

In both the study by Bodary and colleagues (8), as well as a recent study by Chiba et al. (21) leptin was shown to mediate changes in the abdominal and thoracic aorta as well as smaller arteries such as the brachiocephalic. This difference from our current finding in the aortic root is important to note because

these other vessels are encompassed by adipose tissue. Leptin can be secreted from perivascular adipose tissue (52) and could modulate the activity of macrophages more directly in these vessels. Our original hypothesis was that leptin would increase macrophage-driven atherogenesis by mediating inflammatory or lipid-related processes. However, recent data from our lab has shown that leptin is a potent monocyte/macrophage chemoattractant (47). Our current studies in the aortic root are unable to address the question of whether perivascular-derived leptin can influence macrophage recruitment to the artery wall.

Our current data leave open the possibility that non-bone marrow-derived cells such as endothelial cells and smooth muscle cells mediate the pro-atherogenic effects of leptin detected in other studies (4, 8). LepRs are expressed on coronary endothelial cells, and hyperleptinemia has been shown to induce endothelial dysfunction (76) and nitric oxide production (152). Other investigators have shown that leptin induces oxidant stress in endothelial cells as well as their proliferation and expression of matrix metalloproteinases, a process likely involved in plaque rupture (11). Oda et al. have shown that leptin stimulates the proliferation and migration of rat aortic smooth muscle cells, a process that is involved in both intermediate atherosclerotic lesion formation and in restenosis after balloon injury (107). Thus, it is possible that the atherogenic effects of leptin are via activation of these non-hematopoietic cells involved in lesion formation.

The leptin-treated mice in BMT #2 responded physiologically to the exogenously induced hyperleptinemia by losing weight, including a nearly 50% reduction in adipose tissue mass, which concurs with previous studies (8, 20). At sacrifice, despite 4 weeks of daily leptin treatment, both leptin-treated groups had significantly lower plasma leptin levels than the vehicle-treated groups. Thus, induction of hyperleptinemia via daily intraperitoneal injection resulted in reduced endpoint plasma leptin levels, probably due to the significant loss of adipose tissue, the main endogenous source of leptin. To test the length of time that injected leptin stayed in the circulation plasma leptin levels were measured for up to 22 h post-injection. Although this leptin half-life study did not indicate leptin's chronic effects, it suggested that the leptin-treated mice in BMT #2 were exposed to hyperleptinemia for less than 12 h out of each day during the 4 week treatment period. This short period of extreme hyperleptinemia was sufficient to induce loss of adipose tissue mass; however, the overall result was decreased plasma leptin levels at the end of the study. Other methods of leptin treatment—such as twice daily injections, mini osmotic pumps, or adenovirus vectors—might induce hyperleptinemia more effectively in lean mice (9, 20) and therefore allow obesity and hyperleptinemia to be separately assessed.

In conclusion, although *in vitro* data (15, 42, 106, 130) have suggested a role for macrophages in the leptin mediated development of atherosclerotic lesions, our results, from three different *in vivo* BMT studies, do not support a role for hematopoietic cell derived LepRb in aortic root lesion formation.

CHAPTER IV

IMPACT OF GLOBAL MACROPHAGE INFLAMMATORY PROTEIN-1α DEFICIENCY ON WHITE ADIPOSE TISSUE INFLAMMATION AND METABOLISM IN MICE

Introduction

Pro-inflammatory macrophages and T-lymphocytes accumulate in the white adipose tissue (WAT) of obese mice and humans (124, 159, 164, 166). Research within this field has focused on multiple topics related to adipose tissue macrophages (ATMs) and T-lymphocytes, but many questions remain unanswered. In particular, many of the factors that recruit immune cells to WAT during weight gain are still unknown.

One group of candidates for the recruitment of inflammatory cells into WAT is the family of "chemotactic cytokines", referred to as chemokines, which induce chemotaxis of leukocytes. According to their classic definition, chemokines are small, 8-10 kD proteins that share structural similarity. Chemokines have been implicated in chronic inflammatory diseases, such as atherosclerosis and rheumatoid arthritis, and, recently, obesity. Many chemokines, including those mentioned here, are within the "CC" chemokine category in reference to a characteristic pair of cysteine residues.

Macrophage inflammatory protein-1α (MIP-1α), referred to in standard nomenclature as CCL3, is a CC chemokine with increased expression in obese

WAT humans and mice. MIP-1α transcript and protein are significantly elevated in WAT of three different models of obese mice: $Lep^{ob/ob}$, $LepR^{db/db}$, and diet induced obese (63, 166). Expression of MIP-1α and its receptors CCR1 and CCR5 is increased in omental and subcutaneous WAT from obese humans as compared with normal weight individuals (55). Furthermore, expression of MIP-1α and CCR1 in WAT is positively correlated with fasting plasma insulin concentrations in humans (55, 102, 160). Therefore, as multiple reports have shown, WAT MIP-1α transcript and protein are elevated in obesity and correlated with fasting plasma insulin, but the consequences of this are unknown.

In order to determine the role of MIP-1α in the WAT of obese mice, we used a previously generated genetic model (29), MIP-1α deficient ($MIP\text{-}1\alpha^{-/-}$) mice. Although these mice have been used for immunology studies, to our knowledge, no one has characterized their metabolic phenotype. We hypothesized that secretion of MIP-1α from WAT increases recruitment of monocytes and T-lymphocytes during weight gain, and, therefore, that diet induced obese $MIP\text{-}1\alpha^{-/-}$ mice would have fewer macrophages and T-lymphocytes in their WAT as well as lower fasting plasma insulin when compared to $MIP\text{-}1\alpha^{+/+}$ mice. By measuring WAT gene expression, body composition, energy expenditure, and hepatic inflammation and lipid accumulation, we were able to address the role of MIP-1α in metabolism and, specifically, in WAT inflammation.

Results

Experimental design

Male and female MIP-1α$^{-/-}$, MIP-1α$^{+/-}$, and MIP-1α$^{+/+}$ mice were started on WD at 8 wks of age (Figure 4.1). Mice were weighed weekly and body composition was measured every 4 weeks. Mice were bled at baseline and after 16 wks on WD. Mice were killed and their tissues harvested after 16 wks of WD feeding.

Metabolic phenotype of diet induced obese mice

Total body mass, fat mass, and lean mass significantly increased during WD feeding (diet effect in males and females was $p<0.0001$ for each at 24 wks of age), but MIP-1α expression level did not affect these parameters in either gender (Figure 4.2). Perigonadal and perirenal WAT, liver, kidneys, and spleen masses were unaffected by MIP-1α genotype in male and female mice on either diet (Tables 4.1 and 4.2).

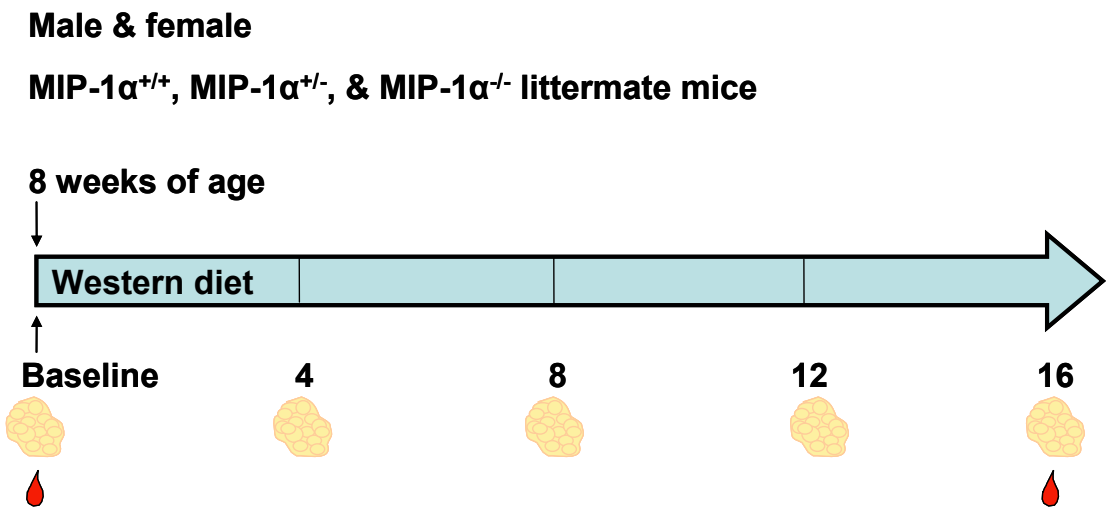

Figure 4.1. Experimental design (Chapter IV). Numbers indicate wks on WD. Body composition was measured at each week shown, and plasma parameters were determined at baseline and 16 wks post-WD. Mice were weighed weekly.

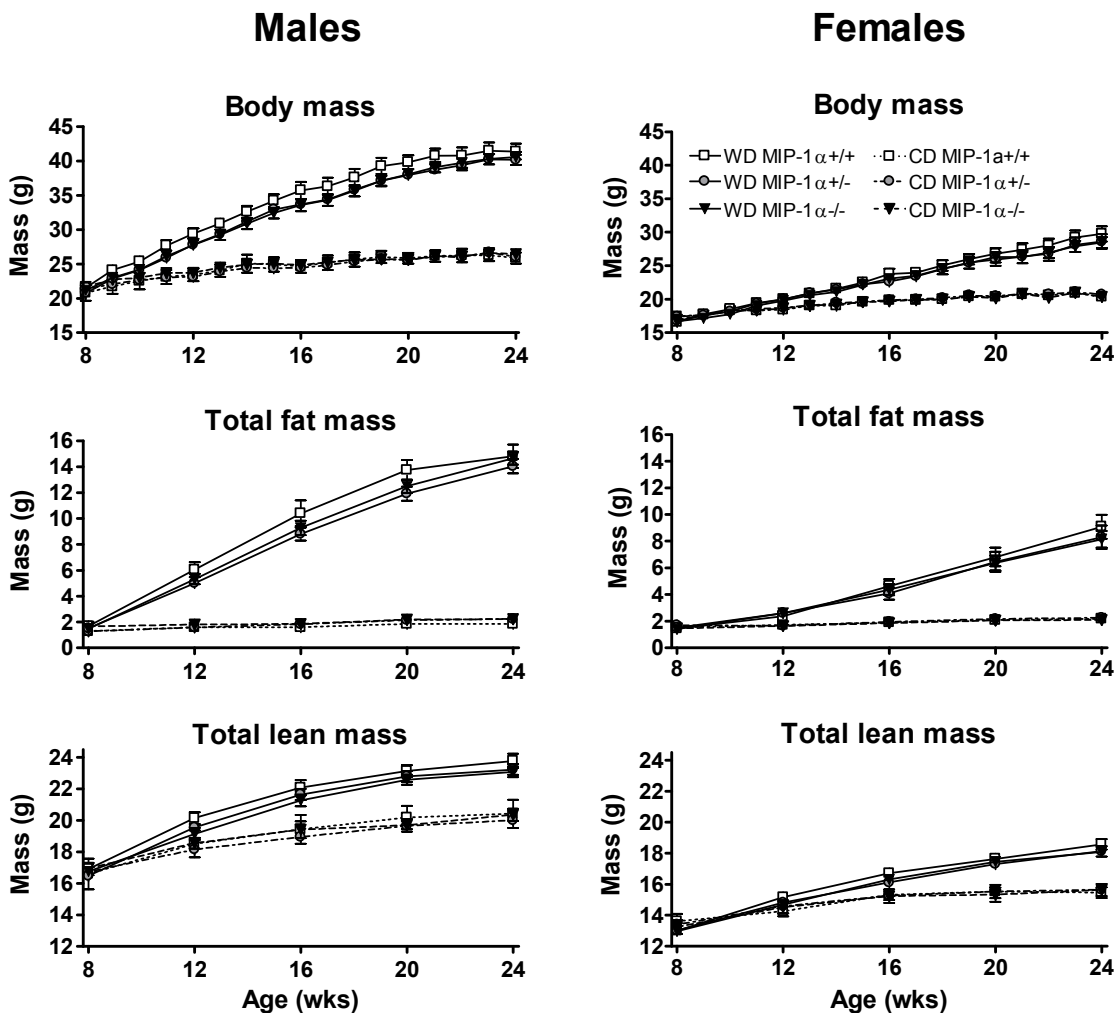

Figure 4.2. Body mass and total fat and lean mass in MIP-1α$^{+/+}$, MIP-1α$^{+/-}$, and MIP-1α$^{-/-}$ mice. Mice were either started on WD (solid lines) at wk 8 or kept on CD (dashed lines). Data shown is for the 16 wk study period: body mass for male (A) and female (B) mice, total fat mass measured by NMR for male (C) and female (D) mice, and total lean mass measured by NMR in male (E) and female (F) mice. □, MIP-1α$^{+/+}$; ●, MIP-1α$^{+/-}$; ▼, MIP-1α$^{-/-}$. Abbreviations: CD, chow diet; WD, Western Diet.

To compare the metabolic phenotype of MIP-1α$^{-/-}$ mice with MIP-1α$^{+/+}$ and MIP-1α$^{+/-}$ mice more comprehensively, we measured energy expenditure of individually housed WD-fed male mice (n=7-9 mice per genotype) following 8 wks of WD feeding. As expected, energy expenditure was elevated during the dark

hours relative to the light hours (p<0.0001, light effect). Consistent with the absence of differences in body mass and fat mass, no significant differences in energy expenditure were detected among the mice with varying MIP-1α expression levels (Figure 4.3). Likewise, daily food consumption was similar among MIP-1α$^{-/-}$, MIP-1α$^{+/-}$, and MIP-1α$^{+/+}$ mice (Figure 4.4).

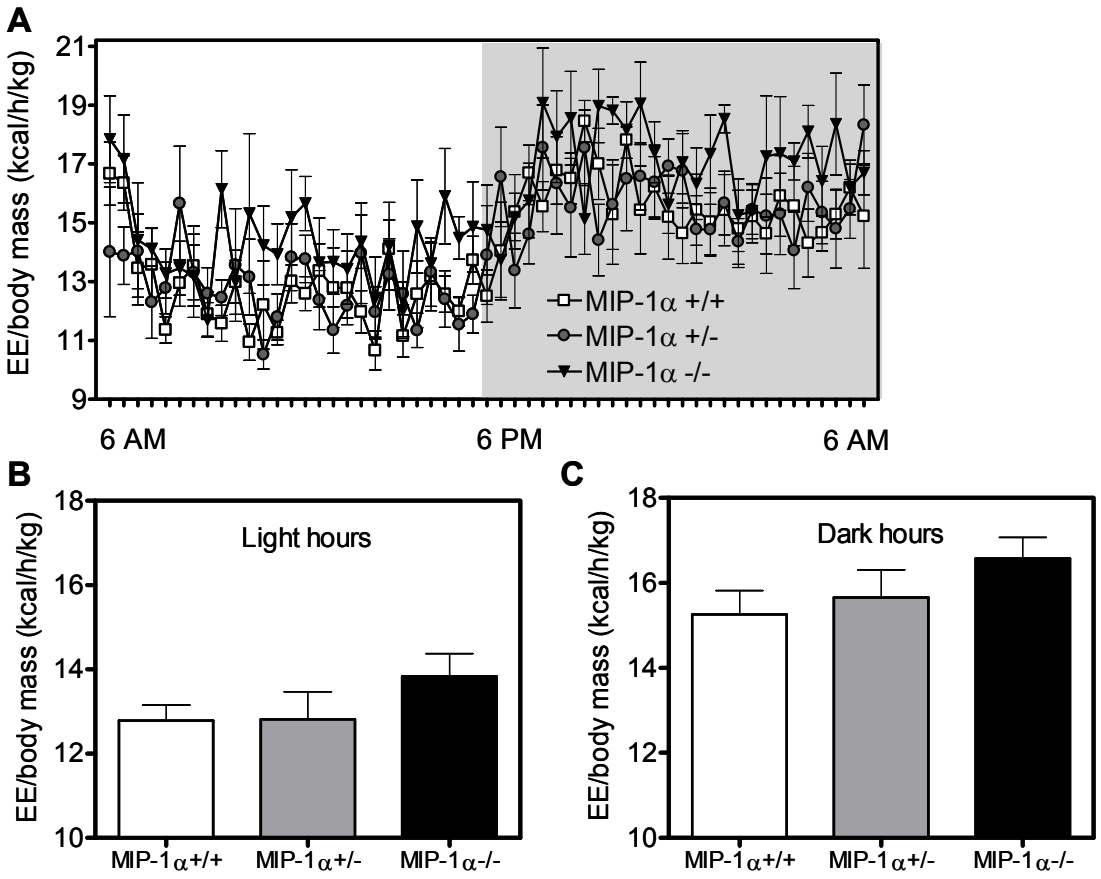

Figure 4.3. Energy expenditure relative to body mass in male MIP-1α$^{+/+}$, MIP-1α$^{+/-}$, and MIP-1α$^{-/-}$ mice. Energy expenditure is plotted to include all time points at which data was collected during a 24 h period (A). Data is plotted as mean ± SEM for each group during the 12 h of light (left panel) or 12 h of dark (right panel) of the 24 h light/dark cycle (B). Mice were weighed at the start of the experiment, and their energy expenditure was analyzed relative to their body mass. Abbreviations: EE, energy expenditure. n=7-9 mice/group.

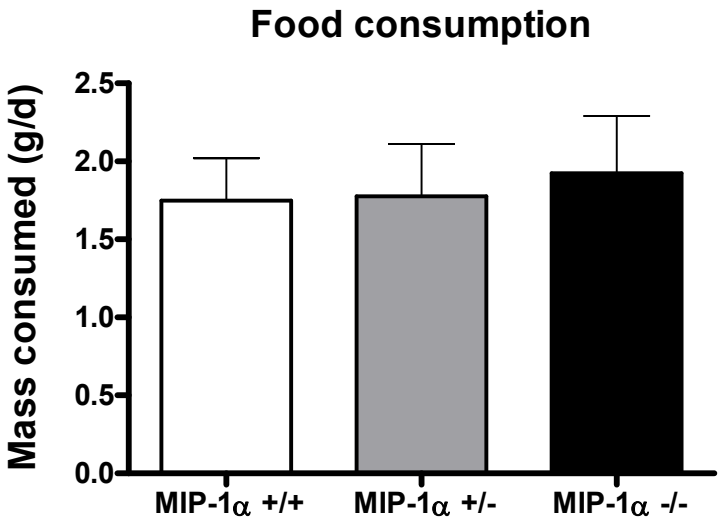

Figure 4.4. Daily food consumption of male mice after 8 wks on Western Diet. Food consumption was measured while mice were individually housed during the energy expenditure experiment. Change in food mass per hour was calculated and converted into grams per day. n=7-9 male mice/group.

Plasma parameters

Mean fasting blood glucose was significantly higher in MIP-1α$^{-/-}$ and MIP-1α$^{+/-}$ male mice, relative to their MIP-1α$^{+/+}$ littermates after 16 wks on WD (p<0.05), but among CD-fed mice, glucose concentrations did not differ (Table 4.3). Fasting plasma insulin concentrations for the WD-fed male and female mice were similar among all genotypes (Table 4.3). Plasma NEFA concentrations in MIP-1α$^{-/-}$ and MIP-1α$^{+/-}$ male mice were significantly lower than plasma NEFAs of MIP-1α$^{+/+}$ mice (p<0.05 relative to MIP-1α$^{+/+}$ mice, Table 4.3). The absence of MIP-1α did not alter plasma cholesterol or TGs in males or females on either diet (Table 4.3).

Gene expression in the WAT

Gene expression of macrophage markers F4/80 and CD68 were significantly elevated by WD feeding in both males and females ($p \leq 0.05$). However, gene expression of these macrophage markers was not influenced by MIP-1α genotype (Figure 4.5A-D). Expression of CD3ε, a general T-lymphocyte marker, was significantly increased in WD-fed compared to CD-fed mice, but this was not altered by MIP-1α deficiency (Figure 4.5E-F; $p<0.005$, diet effect). T-regulatory lymphocyte infiltration of obese WAT, as measured by FoxP3 gene expression, was also not influenced by the absence of MIP-1α (Figure 4.5G-H). Regardless of diet, gene expression of MIP-1α was absent in MIP-1α$^{-/-}$ mice and highest in MIP-1α$^{+/+}$ mice, and its expression was increased with WD feeding (Figure 4.5I-J; $p<0.005$ for genotype effect and diet effect, $p<0.05$ for diet x genotype interaction).

The expression pattern of MIP-1β was influenced by the expression level of MIP-1α such that male MIP-1α$^{-/-}$ mice had lower MIP-1β expression than MIP-1α$^{+/+}$ and MIP-1α$^{+/-}$ mice (Figure 4.5K). In fact, both diet and genotype significantly affected MIP-1β expression in male mice ($p<0.05$ for diet effect, genotype effect, and diet x genotype interaction). MIP-1β expression was increased by WD feeding in female mice ($p<0.005$), but the genotype effect was not significant (Figure 4.5L). The CC chemokine RANTES was also elevated with obesity (Figure 4.5M-N; $p<0.0005$), and in male mice, its expression was significantly affected by MIP-1α expression level ($p=0.05$). Gene expression of MCP-1, another CC chemokine, was elevated with obesity but unaffected by the

level of MIP-1α expression (Figure 4.5O-P; $p<0.0005$, diet effect). The pro-inflammatory cytokine TNFα and the insulin-sensitizing adipokine adiponectin as well as the anti-inflammatory markers arginase 1 and IL-10 (which is secreted by ATMs (170)) were expressed to a similar extent in MIP-1α$^{-/-}$, MIP-1α$^{+/-}$, and MIP-1α$^{+/+}$ WD-fed mice (Figure 4.6).

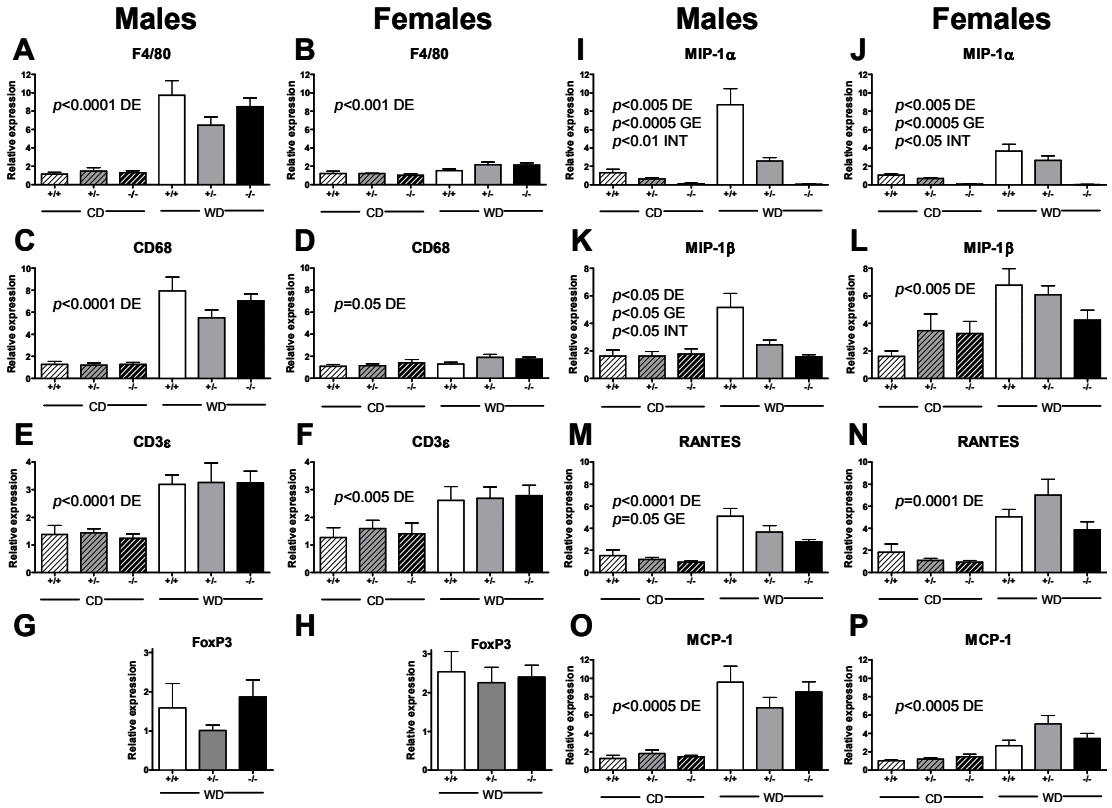

Figure 4.5. WAT gene expression in 24 wk old CD- and WD-fed mice. Relative gene expression is shown for male (A, C, E, G, I, K, M, O) and female (B, D, F, H, J, L, N, P) MIP-1α+/+, MIP-1α+/-, and MIP-1α-/- mice. Mice were either fed CD for 24 wks or switched from CD to WD at 8 wks of age (for a total of 16 wks of WD feeding). RNA was isolated from perigonadal WAT and used to synthesize cDNA, which was used for real time PCR. Data was analyzed by 2-way ANOVA. Abbreviations: CD, chow diet; DE, diet effect; GE, genotype effect; INT, diet x genotype interaction; WD, Western diet; WAT, white adipose tissue.

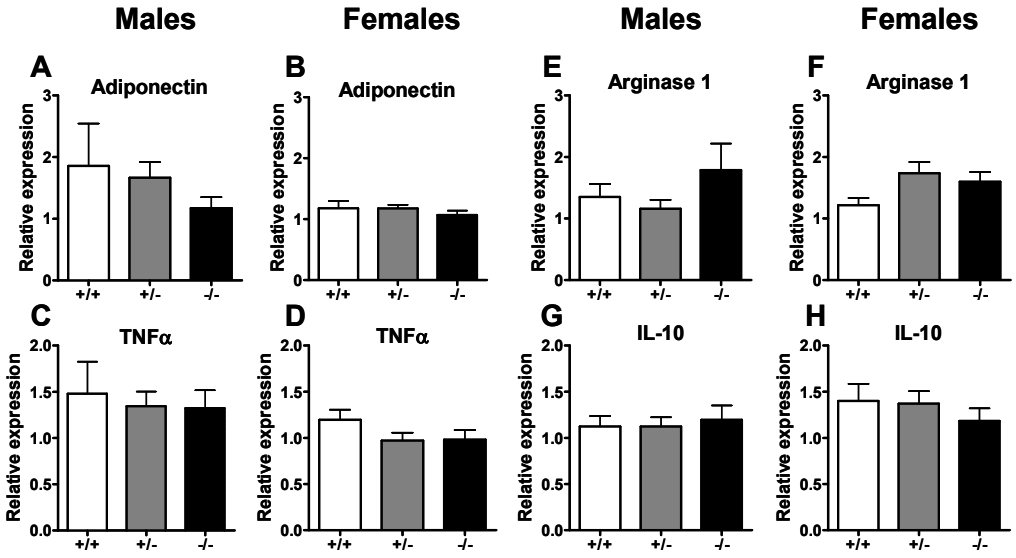

Figure 4.6. WAT gene expression in Western Diet-fed mice. MIP-1α$^{+/+}$, MIP-1α$^{+/-}$, and MIP-1α$^{-/-}$ mice were fed Western Diet for 16 wks. RNA was isolated from perigonadal WAT and used to synthesize cDNA, which was used for real time PCR. Data shows the relative gene expression of adiponectin (A-B), TNFα (C-D), arginase-1 (E-F), and IL-10 (G-H).

In males, after 16 wks on WD, gene expression of F4/80 and CD68 were on average at least 6-fold greater than they were in their lean counterparts. In females, F4/80 and CD68 expression in WAT was significantly elevated relative to CD-fed females, but the differences were only about 2-fold or less. To address the reason for these gender differences, we plotted linear regression curves of total fat mass versus macrophage marker gene expression for males and females (Figure 4.7). The slopes were not statistically different for males as

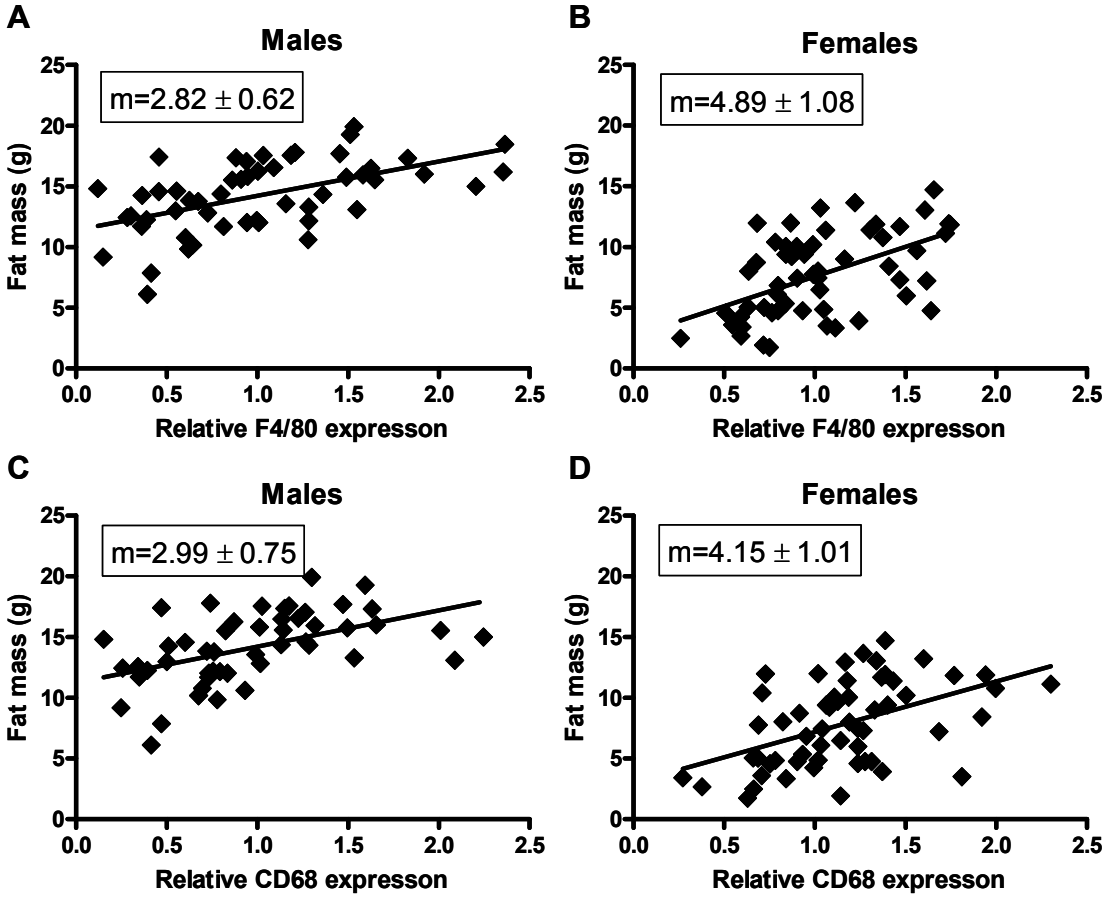

Figure 4.7. Correlation between total fat mass and macrophage markers. Relative gene expression of F4/80 (A-B) and CD68 (C-D) are plotted versus the total fat mass of individual mice after 16 wks on Western Diet. Data from MIP-1α$^{-/-}$, MIP-1α$^{+/-}$, and MIP-1α$^{+/+}$ mice have been analyzed together. The slope (m) of each linear regression line is shown. The slopes in A and B and in C and D do not differ significantly from each other.

compared with females for either F4/80 or CD68 expression, which implies that the males had a greater fold difference in ATM recruitment than the females due to their larger fat mass.

WAT morphology

WAT tissue was sectioned and stained with toluidine blue O to compare the morphology of WAT from MIP-1α$^{-/-}$ mice with that of MIP-1α$^{+/+}$ and MIP-1α$^{+/-}$ mice. Adipocytes tended to be larger and crown-like structures were more frequently observed in male mice; however, the absence of MIP-1α did not appear to influence WAT morphology in either males or females, and crown-like structures were observed in all 6 groups of mice (Figure 4.8).

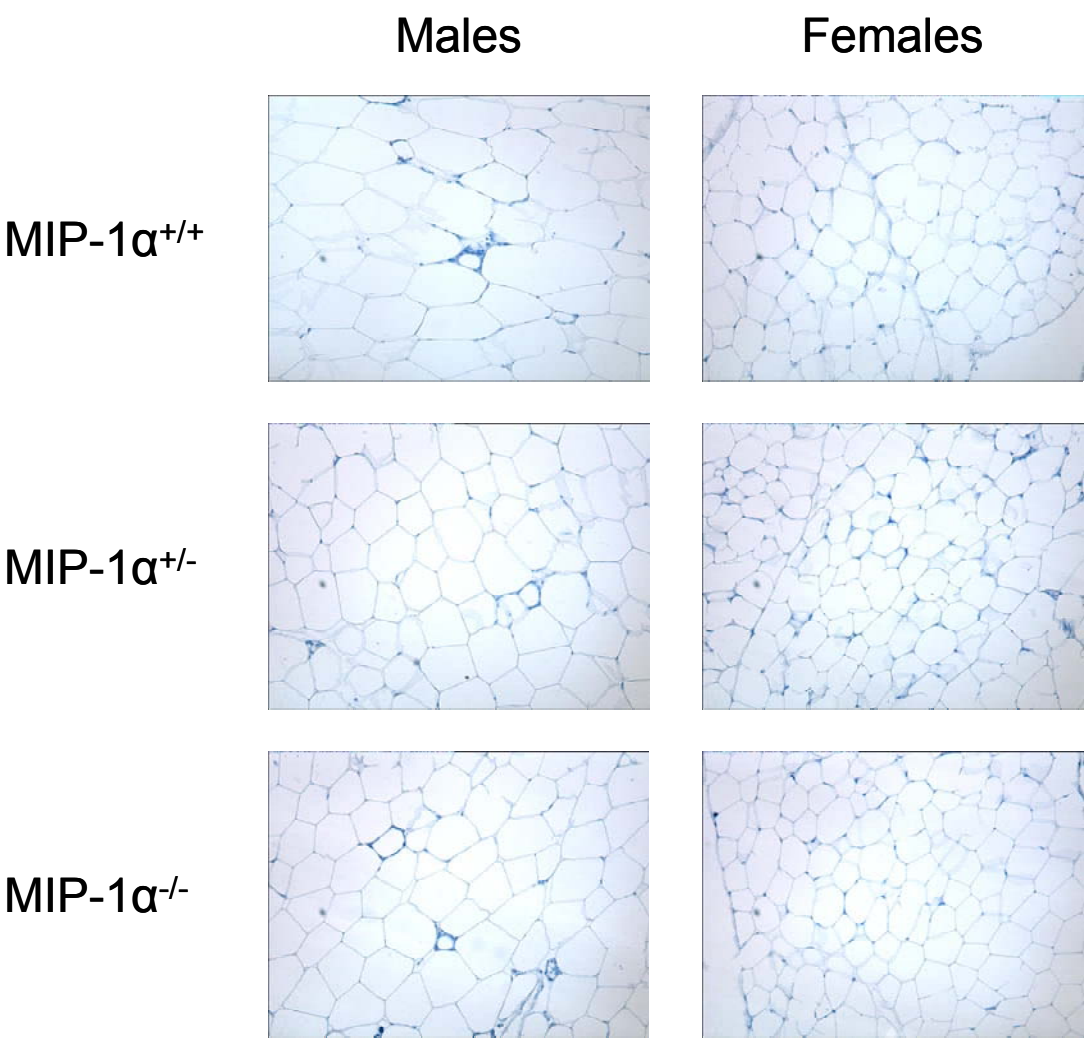

Figure 4.8. Toluidine blue O stained WAT in mice after 16 wks of Western Diet feeding. Perigonadal WAT was harvested from mice, weighed, and a portion was fixed overnight in 10% formalin, transferred to 70% ethanol, and paraffin embedded. Tissue was cut into 7μm sections and stained with toluidine blue O. Representative sections are shown. Images were taken at 100x magnification.

Leukocyte migration

Our main endpoint for this study was macrophage and T-lymphocyte migration to WAT in the WD-fed mice. Because of this, we wanted to determine whether leukocytes from MIP-1α$^{-/-}$ mice are able to migrate similarly to leukocytes from MIP-1α$^{+/+}$ mice. To address this question we injected MIP-1α$^{-/-}$ and MIP-

$1\alpha^{+/+}$ mice intraperitoneally with thioglycollate to induce sterile inflammation. We then collected primary peritoneal cells (the majority of which are macrophages), counted the number of cells obtained per mouse and used these cells for migration experiments. We used a Boyden chamber to measure the migration of cells to 4 different chemokines using the well-established chemoattractant C5a as a positive control. MIP-1α deficiency did not interfere with the recruitment of immune cells to the peritoneal cavity (Figure 4.9). In addition, peritoneal cells from both C57BL/6 (MIP-$1\alpha^{+/+}$) and MIP-$1\alpha^{-/-}$ mice responded robustly to C5a (p<0.0001 vs. all other chemoattractants, Figure 4.10). Cells from MIP-$1\alpha^{-/-}$ mice migrated towards MIP-1α (p<0.0001 vs. all other chemoattractants), but for cells from MIP-$1\alpha^{+/+}$ mice response to MIP-1α was not significant. With both genotypes, few cells migrated towards MCP-1, MCP-3, and MCP-5.

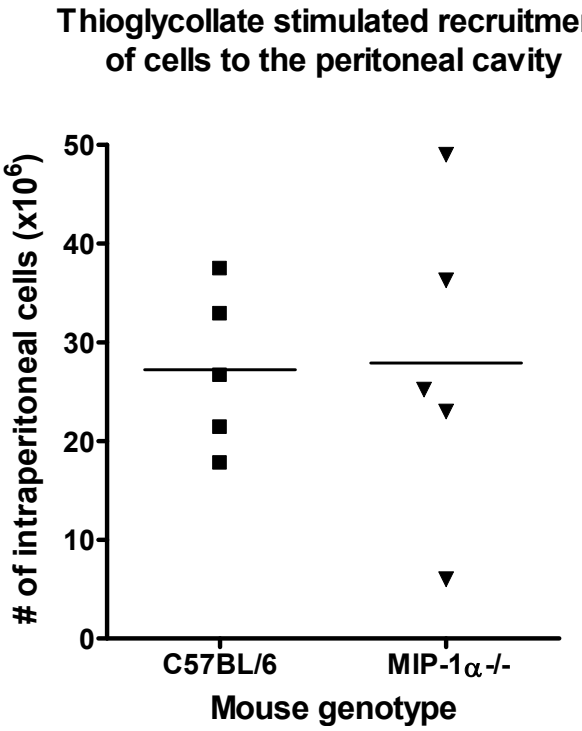

Figure 4.9. Thioglycollate stimulated recruitment of cells to the peritoneal cavity. C57BL/6 (MIP-1α$^{+/+}$) and MIP-1α$^{-/-}$ mice were intraperitoneally injected with 3% thioglycollate to induce sterile inflammation. After 3 days, immune cells that had been recruited to the peritoneal cavity were collected and counted with a hemacytometer. n=5 mice/genotype.

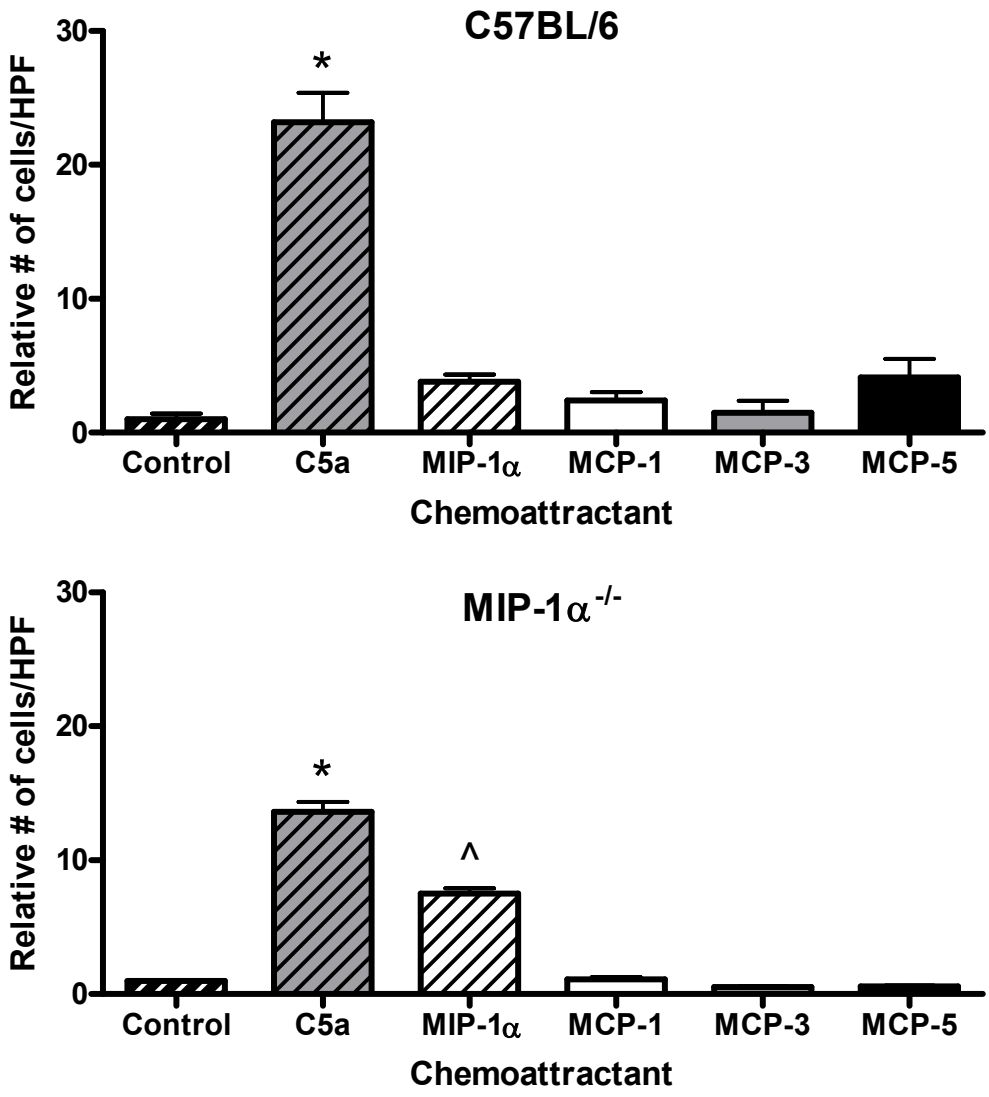

Figure 4.10. Migration of primary peritoneal cells towards 5 different chemoattractants. Cells were harvested from the peritoneal cavity of thioglycollate-injected mice as described in the Methods. Migratory ability of the cells was assessed using a Boyden chamber. Chemoattractants were plated in duplicate or triplicate in the bottom wells of the Boyden chamber, cells from C57BL/6 (MIP-1$\alpha^{+/+}$) or MIP-1$\alpha^{-/-}$ mice were placed in the upper wells, and a membrane was sandwiched between the cells and the chemoattractants. Cells that migrated through the pores of the membrane during a 2 hour incubation period were fixed on the membrane, stained with Crystal Violet, and counted. Graph shows the mean ± SE for 4 replicates, and cells were counted in 5 high powered fields (HPF) per well. *p<0.0001 vs. all chemokines besides C5a, ^p<0.0001 vs. all chemokines other than MIP-1α.

Liver phenotype

Because the liver plays a critical role in lipid metabolism and hepatic steatosis is often present in obese mice, we measured hepatic TG concentrations and visualized hepatic neutral lipid accumulation with oil red O staining of liver sections. MIP-1α deficiency did not influence the TG content of the liver, although males had significantly more hepatic TGs than females after 16 wks on WD (Figure 4.11B; $p<0.0001$ for gender effect), which was also reflected by oil red O staining (Figure 4.11A). As shown in Figure 4.12, absence of MIP-1α did not impact liver gene expression of F4/80, CD68, or pro-inflammatory serum amyloid A1 (Saa1), TNFα, and MCP-1. Expression of Saa1 and MCP-1 were significantly lower in females than in males ($p<0.0001$).

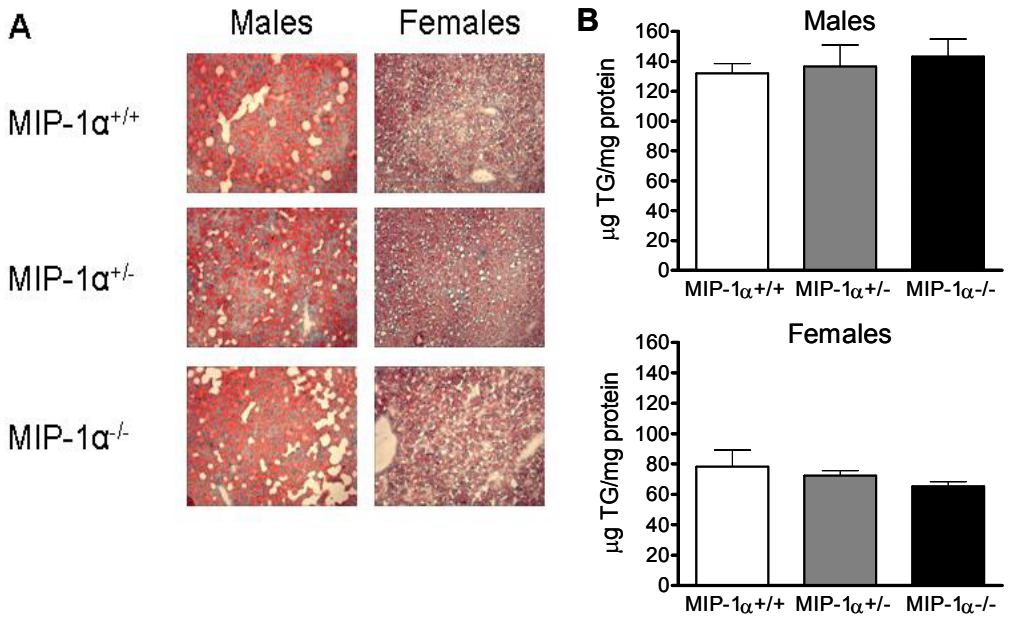

Figure 4.11. Hepatic triglyceride content in Western Diet-fed male and female MIP-1α$^{+/+}$, MIP-1α$^{+/-}$, and MIP-1α$^{-/-}$ mice. Representative oil red O stained liver sections (A) and quantitative analysis of hepatic TGs in mice after 16 wks of Western Diet feeding (B) are shown. Hepatic TGs were measured as described in the Methods. Abbreviations: TGs, triglycerides.

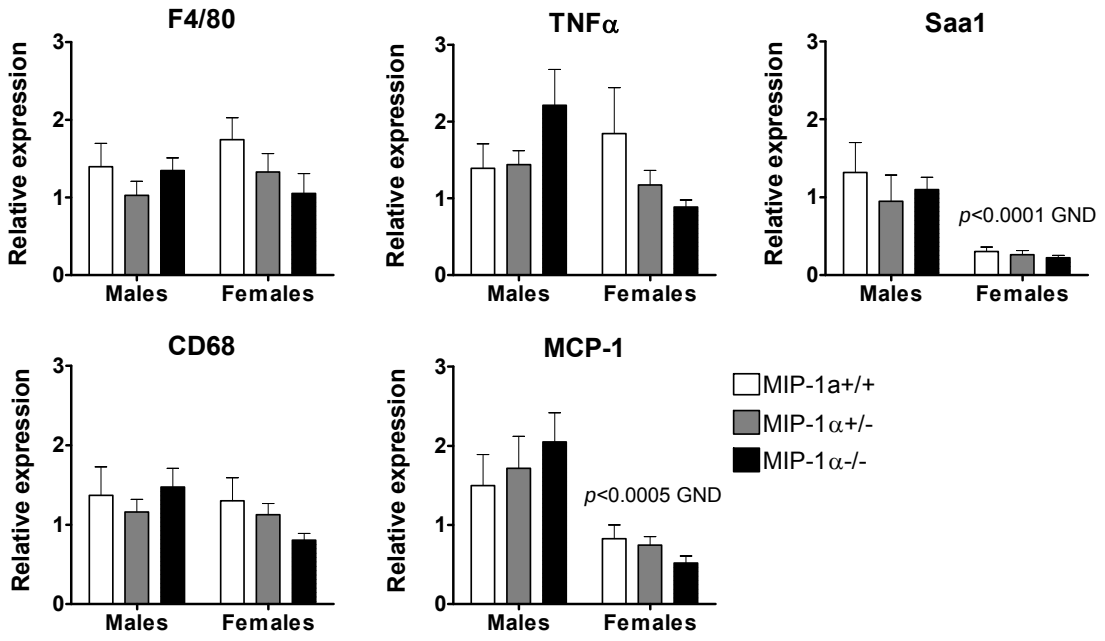

Figure 4.12. Hepatic gene expression in male and female mice after 16 wks on Western Diet. RNA was isolated from liver and used to synthesize cDNA, which was used for real time PCR. Data from males and females were analyzed by 2-way ANOVA using the same real time PCR threshold. Abbreviation: GND=gender effect.

Table 4.1 Tissue masses in mice at 24 weeks of age

Genotype	Perigonadal WAT Mass (g)		Liver Mass (g)	
	CD	WD	CD	WD
Males				
MIP-1α$^{+/+}$	0.32 ± 0.02	2.18 ± 0.10	1.13 ± 0.09	2.83 ± 0.25
MIP-1α$^{+/-}$	0.34 ± 0.02	2.02 ± 0.06	1.12 ± 0.02	2.68 ± 0.14
MIP-1α$^{-/-}$	0.33 ± 0.02	1.98 ± 0.05	1.15 ± 0.03	3.07 ± 0.13
Females				
MIP-1α$^{+/+}$	0.27 ± 0.05	1.17 ± 0.14	0.85 ± 0.03	1.46 ± 0.08
MIP-1α$^{+/-}$	0.26 ± 0.03	0.98 ± 0.12	0.93 ± 0.03	1.41 ± 0.08
MIP-1α$^{-/-}$	0.23 ± 0.02	0.98 ± 0.09	0.92 ± 0.05	1.45 ± 0.06

Data shown is mean ± SEM. Abbreviations: CD, chow diet; WD, Western Diet.

Table 4.2 Tissue masses of 24 wk old mice

Genotype	Perirenal WAT (mg)		Spleen (mg)		Kidneys (mg)	
	CD	WD	CD	WD	CD	WD
Males						
MIP-1α$^{+/+}$	68 ± 9	930 ± 76	72 ± 11	103 ± 6	341 ± 19	379 ± 13
MIP-1α$^{+/-}$	92 ± 12	866 ± 39	63 ± 20	103 ± 4	324 ± 12	376 ± 9
MIP-1α$^{-/-}$	72 ± 16	955 ± 41	71 ± 4	111 ± 6	339 ± 13	369 ± 9
Females						
MIP-1α$^{+/+}$	99 ± 19	622 ± 74	63 ± 2	117 ± 7	247 ± 11	285 ± 8
MIP-1α$^{+/-}$	66 ± 5*	587 ± 80	73 ± 5	111 ± 5	260 ± 8	273 ± 7
MIP-1α$^{-/-}$	96 ± 13	566 ± 54	68 ± 5	118 ± 5	246 ± 9	262 ± 10

Data shown is mean ± SEM. *p<0.05 for one-way ANOVA, but Tukey's Multiple Comparison Test revealed no significant differences between MIP-1α$^{+/+}$, MIP-1α$^{+/-}$, and MIP-1α$^{-/-}$ female mice. Abbreviations: CD, chow diet; WD, Western Diet.

Table 4.3 Plasma parameters in mice at 24 weeks of age

Genotype	n	Glucose (mmol/l)	Insulin (ng/ml)	TC (mmol/l)	TG (mmol/l)	NEFA (mEq/l)
Chow Diet						
Males						
MIP-1α$^{+/+}$	4^	5.66 ± 0.44	ND	1.86 ± 0.18	0.55 ± 0.02	1.19 ± 0.19
MIP-1α$^{+/-}$	16	5.77 ± 0.22	ND	1.68 ± 0.05	0.54 ± 0.01	0.79 ± 0.10
MIP-1α$^{-/-}$	7	5.44 ± 0.33	ND	1.71 ± 0.05	0.57 ± 0.03	1.05 ± 0.11
Females						
MIP-1α$^{+/+}$	6	5.22 ± 0.44	ND	1.24 ± 0.08	0.50 ± 0.02	0.74 ± 0.06
MIP-1α$^{+/-}$	15^	5.05 ± 0.28	ND	1.30 ± 0.03	0.52 ± 0.01	0.77 ± 0.05
MIP-1α$^{-/-}$	6	5.05 ± 0.17	ND	1.30 ± 0.08	0.55 ± 0.02	0.80 ± 0.07
Western Diet						
Males						
MIP-1α$^{+/+}$	14-15	6.83 ± 0.28	4.24 ± 0.82	4.82 ± 0.28	0.50 ± 0.02	0.73 ± 0.06
MIP-1α$^{+/-}$	29-32	7.70 ± 0.22*	3.29 ± 0.32	4.71 ± 0.13	0.54 ± 0.01	0.49 ± 0.03**
MIP-1α$^{-/-}$	22-24	7.66 ± 0.17*	3.42 ± 0.36	5.13 ± 0.16	0.53 ± 0.02	0.55 ± 0.04*
Females						
MIP-1α$^{+/+}$	18-20	6.55 ± 0.22	1.06 ± 0.10	2.86 ± 0.13	0.44 ± 0.02	0.45 ± 0.04
MIP-1α$^{+/-}$	22-23	6.77 ± 0.22	0.81 ± 0.08	2.77 ± 0.10	0.41 ± 0.02	0.42 ± 0.02
MIP-1α$^{-/-}$	22-24	6.77 ± 0.22	0.91 ± 0.10	2.84 ± 0.10	0.43 ± 0.02	0.49 ± 0.03

Mice were 8 wks old when started on WD. Data shown is mean ± SEM and was analyzed using 1-way ANOVA with Tukey's Multiple Comparison Test. *p<0.05 and **p<0.001 vs. WD-fed MIP-1a$^{+/+}$ males. ^Blood glucose measurements were only obtained for 3 (male MIP-1α$^{+/+}$) or 14 (female MIP-1α$^{+/-}$) mice. Variation in "n" is due to the removal of outliers (see Methods). Abbreviations: TC, total cholesterol; TG, triglyceride; NEFA, non-esterified fatty acid; ND, not determined.

Discussion

The elevation of MIP-1α in WAT of obese humans and mice is well-established. Based on its known ability to chemoattract monocytes, macrophages, and T-lymphocytes, we hypothesized that MIP-1α has an important role in the recruitment of these cells into WAT during diet induced weight gain. Therefore, we predicted that MIP-1α$^{-/-}$ mice would have less accumulation of macrophages and T-lymphocytes in their WAT. However, F4/80, CD68, and CD3ε were expressed to the same degree in diet induced obese MIP-1α$^{-/-}$ mice compared with obese MIP-1α$^{+/+}$ mice. Furthermore, *in vitro* migration experiments demonstrated that leukocytes from MIP-1α$^{-/-}$ mice retain their ability to migrate in response to inflammatory stimuli. These data suggest that MIP-1α does not contribute to the recruitment of monocytes and T-lymphocytes to WAT during DIO.

Gene expression of MIP-1β and RANTES in the perigonadal WAT was significantly affected by MIP-1α genotype. It is possible that MIP-1α regulates the expression of MIP-1β as previous *in vitro* reports have established some precedence for one chemokine influencing the secretion of another chemokine in neutrophils (122, 123). In particular, MIP-1α can induce secretion of TNFα (122), which can in turn stimulate chemokine secretion, and MIP-2/CXCL2 can induce MIP-1α secretion (123). Due to the proximity of the MIP-1α gene to the MIP-1β and RANTES genes (0.01cM from MIP-1β gene and 0.2 cM from RANTES gene on chromosome 11), distal promoter or enhancer elements of the MIP-1β and RANTES genes might have been disrupted when a portion of the MIP-1α gene

was deleted to generate MIP-1α$^{-/-}$ mice (29). An alternative explanation is that MIP-1β and RANTES might be expressed at lower levels in the original 129 background strain and that, even after 10 backcrosses, the genomic sequences close to MIP-1α are still of the 129 origin.

Unlike MIP-1β and RANTES, expression of the chemokine MCP-1 was elevated in all WD-fed mice and unaffected by MIP-1α expression level. The role of MCP-1 in recruitment of monocytes to WAT has been somewhat controversial (61, 65, 66, 74, 168), but there is evidence to demonstrate the likelihood that MCP-1 is involved in this process. In our study, WAT relative gene expression of both F4/80 and CD68 significantly and positively correlated with MCP-1 expression level in the WAT (Figure 4.13; r^2=0.79 and r^2=0.77, respectively; *P*<0.0001 for the slope's deviation from zero). Thus, our data support the idea the MCP-1 is distinct from other CC chemokines in its involvement in monocyte recruitment to WAT during obesity.

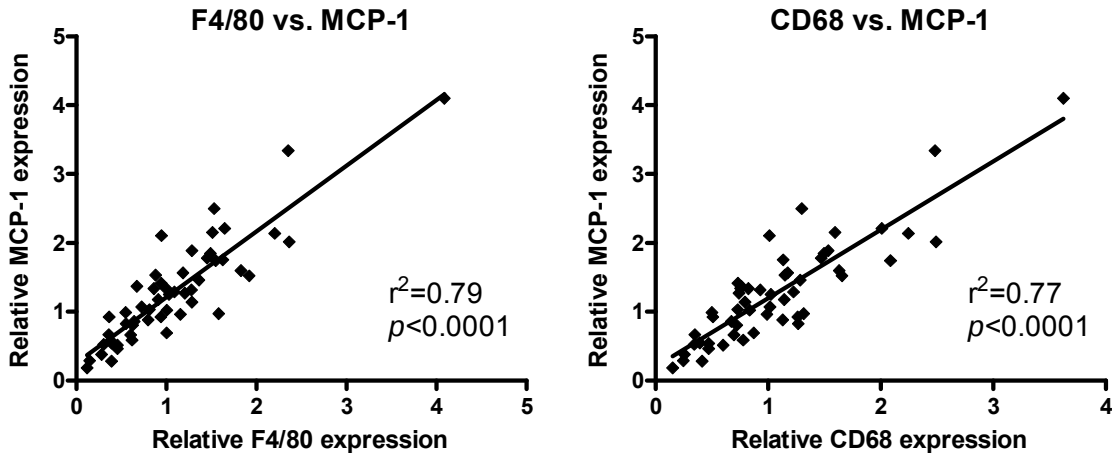

Figure 4.13. Correlation between MCP-1 expression and macrophage markers. Relative gene expression of F4/80 and CD68 are plotted versus MCP-1 relative gene expression for individual mice after 16 wks on Western Diet. Data from male MIP-1α$^{-/-}$, MIP-1α$^{+/-}$, and MIP-1α$^{+/+}$ mice have been analyzed together. Linear regression line is shown. *p* values indicate the significance of each slope's deviation from zero.

We predicted that MIP-1α$^{-/-}$ mice would have lower fasting glucose and plasma insulin concentrations based on the improved insulin and glucose tolerance observed in other genetic models of chemokine deficiency, specifically in MCP-1$^{-/-}$, CCR2$^{-/-}$, and CXCL14$^{-/-}$ mice (66, 104, 158), and the fact that expression of MIP-1α in WAT is positively correlated with fasting plasma insulin concentrations in humans (55, 102, 160). However, after 16 wks on WD, male MIP-1α$^{-/-}$ and MIP-1α$^{+/-}$ mice had higher fasting blood glucose levels than male MIP-1α$^{+/+}$ mice, and blood glucose concentrations did not differ among female mice. The cause of elevated blood glucose, but not plasma insulin, in male MIP-1α$^{-/-}$ and MIP-1α$^{+/-}$ mice is not known. It is possible that MIP-1α$^{-/-}$ and MIP-1α$^{+/-}$ mice have minor pancreatic dysfunction when challenged with WD. In that case, elevated circulating glucose could subsequently increase the percentage of

NEFAs that are re-esterified in the WAT, driving down the plasma NEFAs, as was observed in male MIP-1α$^{-/-}$ and MIP-1α$^{+/-}$ mice. Since glucokinase and islet-specific glucose-6-phosphatase catalytic subunit-related protein (IGRP) regulate glucose-stimulated insulin secretion by the pancreas, expression of these genes may be affected by MIP-1α deficiency. Alternatively, the lipolytic rate may be decreased in male MIP-1α$^{-/-}$ and MIP-1α$^{+/-}$ mice, in which case not only NEFAs but also plasma glycerol concentrations would be decreased. Future experiments will be necessary to determine the source of these differences in plasma insulin and NEFAs.

We have recently used another model of MIP-1α deficiency to investigate its role in atherosclerosis. In this model, we lethally irradiated low density lipoprotein receptor deficient (LDLR$^{-/-}$) mice and then transplanted them with bone marrow from MIP-1α$^{+/+}$ or MIP-1α$^{-/-}$ mice. This yielded mice with MIP-1α deficiency only in their bone marrow derived cells (BMDCs, MIP-1α$^{-/-}$→LDLR$^{-/-}$) and mice with expression of MIP-1α in all of their cells (MIP-1α$^{+/+}$→LDLR$^{-/-}$). Similar to the WAT phenotype we observed in MIP-1α$^{-/-}$ mice, diet induced obese MIP-1α$^{-/-}$→LDLR$^{-/-}$ mice did not differ from MIP-1α$^{+/+}$→LDLR$^{-/-}$ mice in their expression of macrophage and T-lymphocyte markers (unpublished data). Thus, two different models of MIP-1α deficiency in diet induced obese mice indicate that MIP-1α is not required for monocyte and T-lymphocyte accumulation in WAT.

Upregulation of MIP-1α is likely a consequence of the changes that occur in obese WAT such as excess exposure to lipids and inflammatory factors. Both

murine and human macrophages express MIP-1α *in vitro* upon stimulation with very low density lipoprotein and pro-inflammatory stimuli (132, 170). In addition, administration of free fatty acids upregulates MIP-1α release by 3T3-L1 adipocytes via NFκB, a transcription factor which regulates inflammatory genes (63). Therefore, we believe that initial changes in the WAT during the onset of obesity secondarily induce MIP-1α production by the adipocytes or immune cells. In agreement with this, MIP-1α protein is elevated in WAT of mice after 20 wks of high fat diet feeding, but not after 1 wk (63). In contrast, other chemokines, including MCP-1, MCP-2, MCP-3, and MRP-2, are produced in WAT in response to 1 wk of high fat diet feeding (63). In addition, high fat diet induces early infiltration of T-lymphocytes into WAT in mice (105). Taken within the context of the literature, our data indicate that elevated MIP-1α in WAT is a consequence of obesity, but its contribution to inflammation within the WAT of obese mice remains undetermined.

In conclusion, our data demonstrate that simultaneously lowering the expression of 3 different CC chemokines—MIP-1α, MIP-1β, and RANTES—does not impact macrophage or T-lymphocyte accumulation in WAT of diet induced obese mice. This indicates that although these pro-inflammatory chemokines are present in obese WAT, they do not contribute to macrophage recruitment to WAT, and their involvement in WAT inflammation is different than the role of MCP-1.

CHAPTER V

METABOLIC PHENOTYPE OF HYPERLIPIDEMIC MACROPHAGE INFLAMMATORY PROTEIN-1α DEFICIENT MICE

Introduction

Macrophage inflammatory protein-1α (MIP-1α), a member of the CC chemokine family, is elevated in the WAT of obese mice and humans. Since MIP-1α is a chemoattractant of monocytes and T-lymphocytes, we previously hypothesized that it was important for the recruitment of leukocytes to WAT during obesity. As demonstrated in Chapter IV, our data do not support this hypothesis. Therefore, the consequence of the increased presence of MIP-1α in WAT of obese mice and humans remains unknown.

Hyperlipidemia previously has been associated with elevated leukocyte MIP-1α secretion in human and mouse studies. Unstimulated human blood monocytes from hyperlipidemic patients secrete more MIP-1α than those of normolipidemic humans (53), and our laboratory has demonstrated that administration of VLDL increases MIP-1α gene expression by murine macrophages (132). In addition, WD-fed $LDLR^{-/-}$ hyperlipidemic mice have a significant 11.4-fold increase in hepatic MIP-1α gene expression relative to $LDLR^{-/-}$ mice on a chow diet, but in WD-fed $LDLR^{+/+}$ mice this effect is mild and non-significant (163). These data suggest that monocytes and macrophages

secrete more MIP-1α under hyperlipidemic conditions in comparison to normolipidemic conditions.

Previous unpublished observations from our laboratory identified an unexpected phenotype in hyperlipidemic mice with bone marrow derived cell (BMDC) MIP-1α deficiency. Briefly, LDLR$^{-/-}$ mice were lethally irradiated before being transplanted with bone marrow from MIP-1α$^{+/+}$ or MIP-1α$^{-/-}$ mice (see Figure 5.1 for experimental design). This resulted in mice with MIP-1α deficiency only in their BMDCs (MIP-1α$^{-/-}$→LDLR$^{-/-}$) and mice with expression of MIP-1α in all of their cells (MIP-1α$^{+/+}$→LDLR$^{-/-}$). Surprisingly, we discovered that after 12 wks of WD feeding the male MIP-1α$^{-/-}$→LDLR$^{-/-}$ mice had 56% less total fat than the MIP-1α$^{+/+}$→LDLR$^{-/-}$ mice with only slightly less lean mass, indicating that the lower fat mass accounted for most of the decrease in overall body mass (P<0.05, Figure 5.2). MIP-1α$^{-/-}$→LDLR$^{-/-}$ mice also had smaller atherosclerotic lesions (P<0.05 for females after 6 wks on WD and for males after 12 wks on WD, Figure 5.3).

MIP-1α$^{-/-}$;LDLR$^{+/+}$ mice have a similar degree of adiposity as MIP-1α$^{+/+}$;LDLR$^{+/+}$ mice (Chapter IV) and are not a suitable model for atherosclerosis studies, therefore we crossed MIP-1α$^{-/-}$ mice with LDLR$^{-/-}$ mice and bred their progeny to generate LDLR$^{-/-}$ mice that had produced no MIP-1α (MIP-1α$^{-/-}$;LDLR$^{-/-}$), were heterozygous for MIP-1α (MIP-1α$^{+/-}$;LDLR$^{-/-}$), or had normal production of MIP-1α (MIP-1α$^{+/+}$;LDLR$^{-/-}$). We used these mice to determine whether hyperlipidemia was responsible for the smaller WAT mass and lesions observed in the MIP-1α$^{-/-}$→LDLR$^{-/-}$ mice. We hypothesized that WD-fed MIP-1α$^{-/-}$;LDLR$^{-/-}$

mice would have less total fat mass and smaller atherosclerotic lesions than MIP-1α$^{+/+}$;LDLR$^{-/-}$ mice.

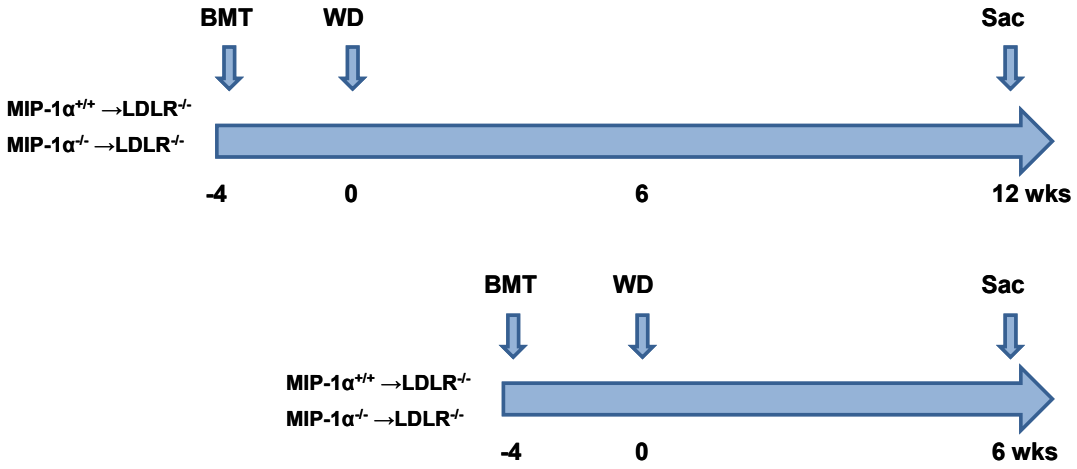

Figure 5.1. Experimental design of bone marrow transplantation study. "BMT" indicates time of bone marrow transplantation. "WD" indicates transition from chow diet to Western Diet, and mice were fed WD for either 12 or 6 wks. Mice were euthenized at the end of study, designated "Sac".

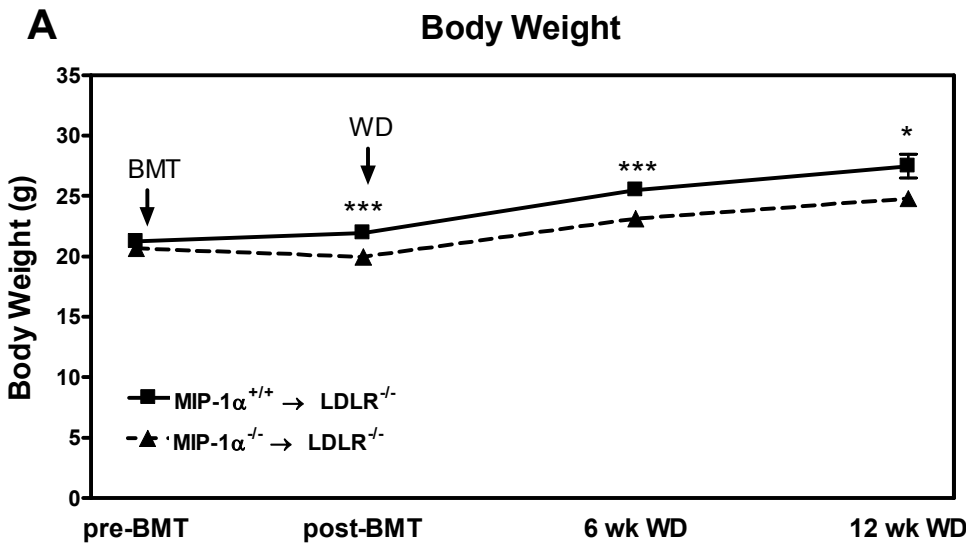
A
Body Weight
Body Weight (g)
35
30
25
20
15
10
5
0
BMT
WD
***
***
*
MIP-1α+/+ → LDLR-/-
MIP-1α-/- → LDLR-/-
pre-BMT
post-BMT
6 wk WD
12 wk WD

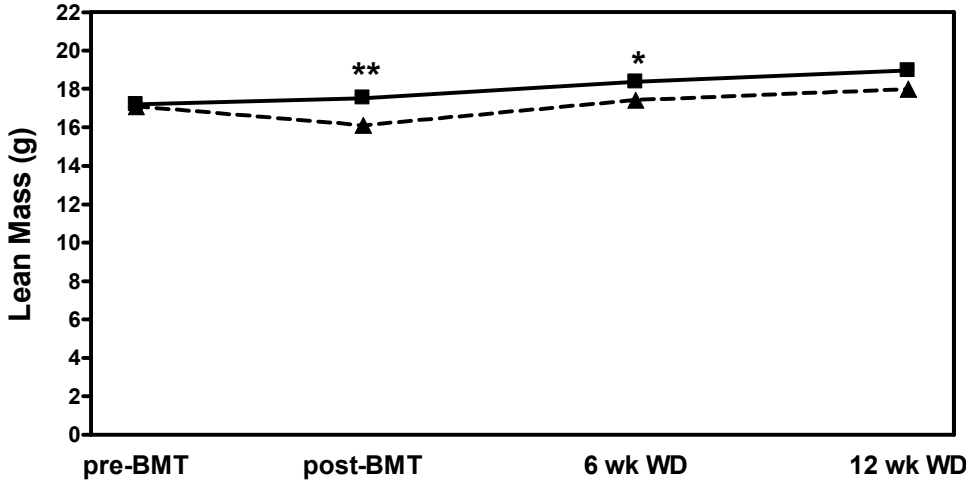
B
Total Body Lean Mass
Lean Mass (g)
22
20
18
16
14
12
10
8
6
4
2
0
**
*
pre-BMT
post-BMT
6 wk WD
12 wk WD

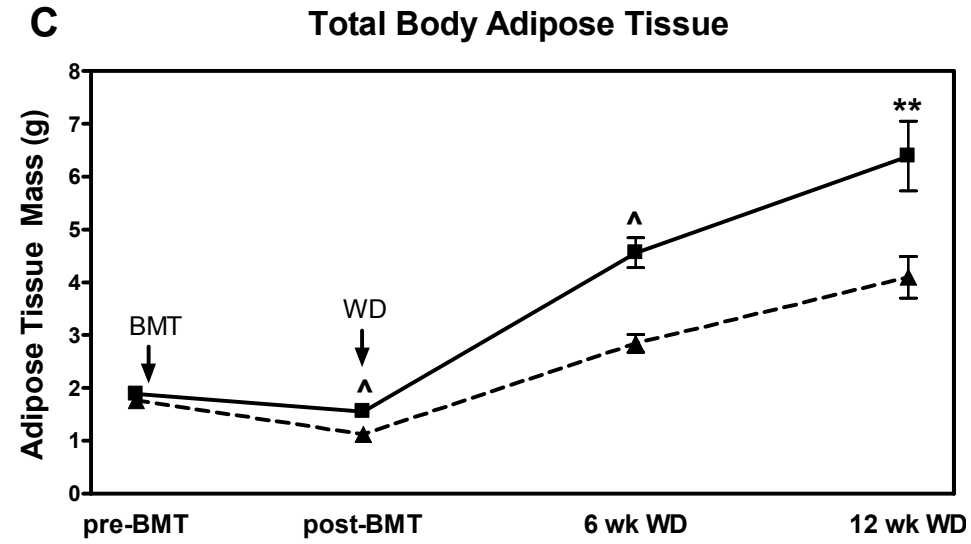
C
Total Body Adipose Tissue
Adipose Tissue Mass (g)
8
7
6
5
4
3
2
1
0
BMT
WD
^
^
**
pre-BMT
post-BMT
6 wk WD
12 wk WD

Figure 5.2. Time course of body weight, lean, and fat mass in male mice. LDLR$^{-/-}$ mice were transplanted with MIP-1α$^{+/+}$ or MIP-1α$^{-/-}$ bone marrow. At 4 weeks post-BMT, mice were placed on WD for either 6 or 12 weeks. Body weight as well as total body lean and fat mass were measured by NMR pre-BMT, 4 weeks post-BMT and at 6 and 12 weeks post-WD. There were no differences between the two transplantations groups at pre-BMT, 4 weeks post-BMT, and 6 weeks post-WD, thus, these values are presented for both cohorts of mice together. The 12 week post-WD data represent only the mice sacrificed at that time point. *p<0.05, **p<0.01, ***p<0.0005, ^p<0.0001

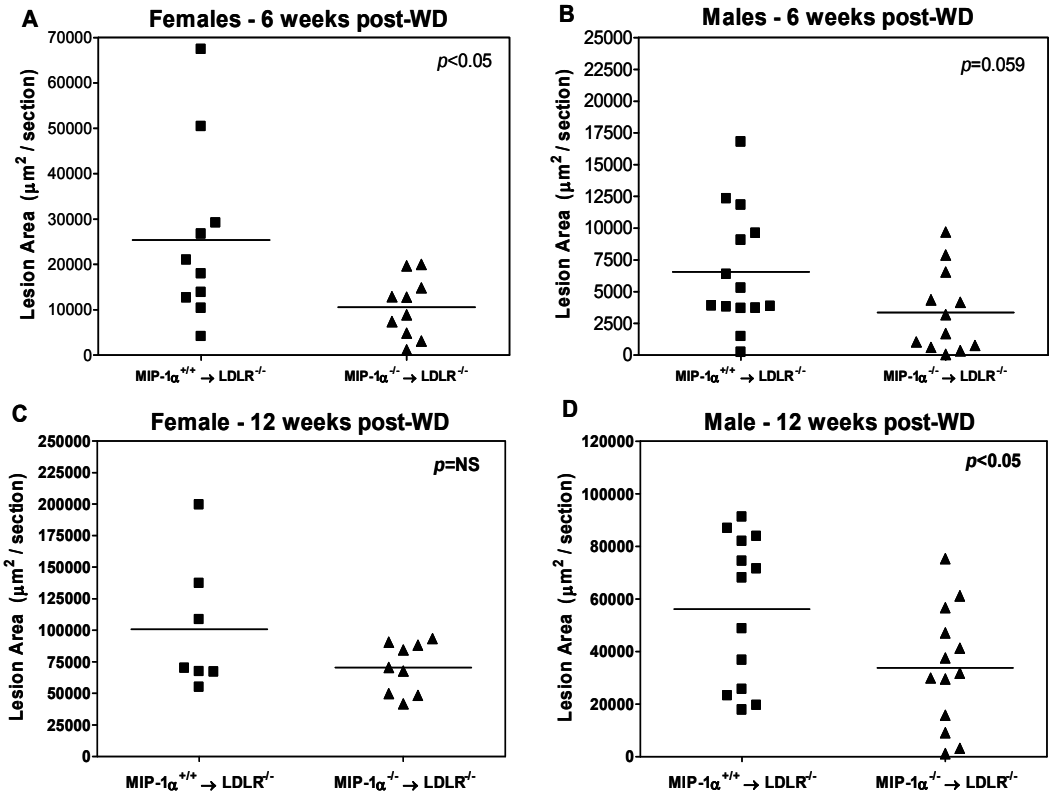

Figure 5.3. Recipients of MIP-1α$^{-/-}$ bone marrow have reduced lesion area. LDLR$^{-/-}$ mice were transplanted with MIP-1α$^{+/+}$ or MIP-1α$^{-/-}$ bone marrow. At 4 weeks post-BMT, mice were placed on WD for 6 or 12 weeks. Aortic root lesion area was quantified according to the Methods section. Panels A and B show lesion area from female and male mice after 6 weeks of WD feeding, respectively. Data are presented as mean ± SEM from 7-14 mice per group. Panels C and D show the lesion area from female and male mice after 12 weeks of WD feeding, respectively. Data are mean ± SEM from 7-13 mice per group.

Results

Experimental design

Male and female MIP-1α$^{+/+}$;LDLR$^{-/-}$, MIP-1α$^{+/-}$;LDLR$^{-/-}$, and MIP-1α$^{-/-}$; LDLR$^{-/-}$ mice were started on WD at 8 wks of age. Mice were weighed weekly, body composition was measured every few weeks, and mice were bled at baseline and after 12 wks on WD (Figure 5.4).

Plasma lipids, insulin, and glucose

FPLC was used to separate plasma cholesterol and TGs by density. Plasma TC was significantly increased in male and female mice after 12 wks of WD (P<0.01 AUC for baseline vs. AUC for 12 wks on WD, Figure 5.5), with a dramatic increase in the IDL/LDL fraction. Plasma TC, TGs, and NEFAs were significantly higher in male than in female mice (p<0.0001 for TC and TGs and p<0.05 for NEFAs, gender effect). After 12 weeks on WD, male MIP-1α$^{-/-}$;LDLR$^{-/-}$ mice had significantly lower plasma NEFAs relative to MIP-1α$^{+/+}$;LDLR$^{-/-}$ mice (p<0.05, Table 5.1). Plasma TGs were lower in male MIP-1α$^{-/-}$;LDLR$^{-/-}$ mice, as shown by plasma TG FPLC and enzymatic assay (Figure 5.6 and Table 5.1), but this difference was not significant. No other differences among plasma lipids were observed in mice after 12 wks of WD feeding. Plasma glucose, insulin, and leptin concentrations were significantly higher in male than in female mice (p<0.0001, gender effect; Table 5.1). These parameters were unaffected by

MIP-1α expression, although plasma insulin concentrations in male MIP-1α$^{+/-}$ LDLR$^{-/-}$ mice were elevated non-significantly (p=0.076).

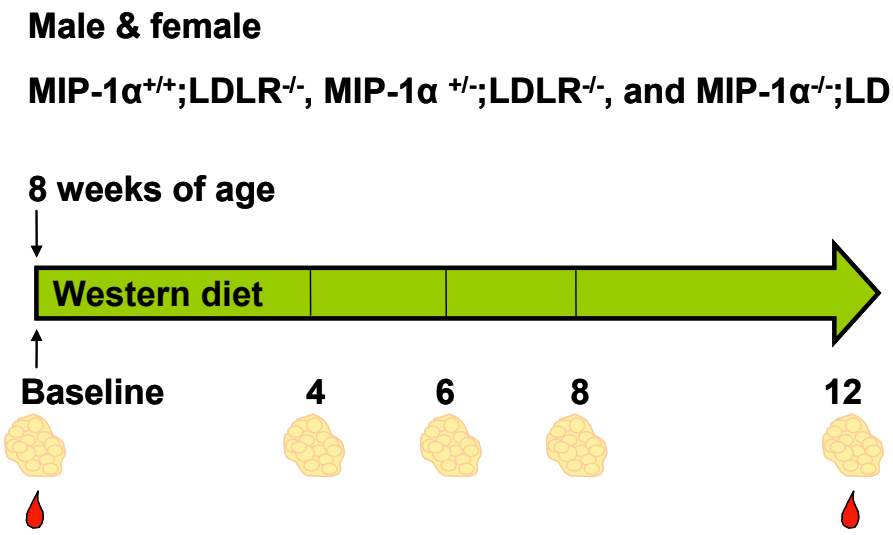

Figure 5.4. Experimental design (Chapter V). Numbers indicate wks on WD. Body composition was measured at each week shown, and plasma parameters were determined at baseline and 12 wks post-WD. Mice were weighed weekly.

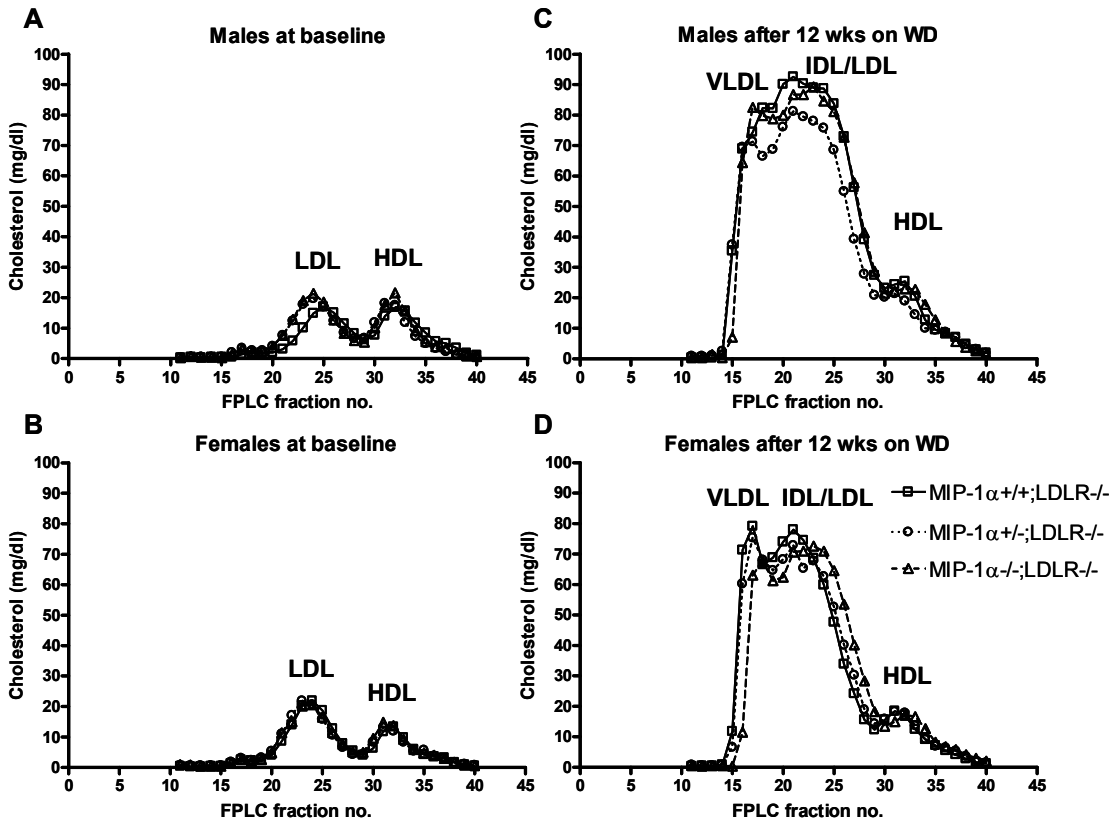

Figure 5.5. FPLC analysis of lipoprotein profiles (cholesterol). Plasma lipids were fractionated and cholesterol quantified as described in the Methods section. MIP-1α$^{+/+}$;LDLR$^{-/-}$ mice are represented by squares, MIP-1α$^{+/-}$;LDLR$^{-/-}$ mice are represented by circles, and MIP-1α$^{-/-}$;LDLR$^{-/-}$ mice are represented by triangles. A, males at baseline (just before start of WD feeding); B, females at baseline; C, males at 12 weeks post-WD; D, females at 12 weeks post-WD.

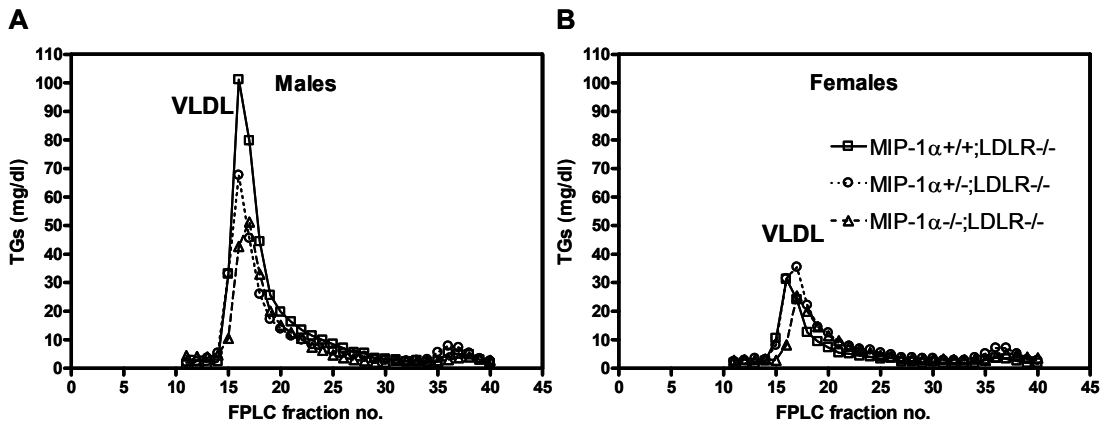

Figure 5.6. FPLC analysis of lipoprotein profiles (triglycerides). Plasma lipids were fractionated and triglycerides quantified as described in the Methods section. MIP-1α$^{+/+}$;LDLR$^{-/-}$ mice are represented by squares, MIP-1α$^{+/-}$;LDLR$^{-/-}$ mice are represented by circles, and MIP-1α$^{-/-}$;LDLR$^{-/-}$ mice are represented by triangles. A, males at 12 weeks post-WD; B, females at 12 weeks post-WD.

Body composition

When the mice were 8 wks old, we took baseline body composition measurements. Among male mice, MIP-1α genotype did not influence baseline body mass or total lean and fat mass (Table 5.2 and Figure 5.7). Female MIP-1α$^{-/-}$;LDLR$^{-/-}$ mice weighed significantly more (p<0.005 vs. MIP-1α$^{+/-}$;LDLR$^{-/-}$ and MIP-1α$^{+/+}$;LDLR$^{-/-}$ mice, 1-way ANOVA) and had significantly more lean mass (p<0.01 vs. MIP-1α$^{+/+}$;LDLR$^{-/-}$ mice) at 8 wks of age, although their total fat masses were not different (Table 5.2 and Figure 5.7). After 12 wks on WD, body weight, lean mass, and fat mass were not significantly different among the groups for either males or females (Table 5.3). Similarly, the presence or absence of MIP-1α did not influence the mass of their various tissues, with the exception of female MIP-1α$^{-/-}$;LDLR$^{-/-}$ mice, which had a significantly greater

mean liver mass than MIP-1α$^{+/+}$;LDLR$^{-/-}$ mice (p<0.05, Tukey's Multiple Comparison post hoc test).

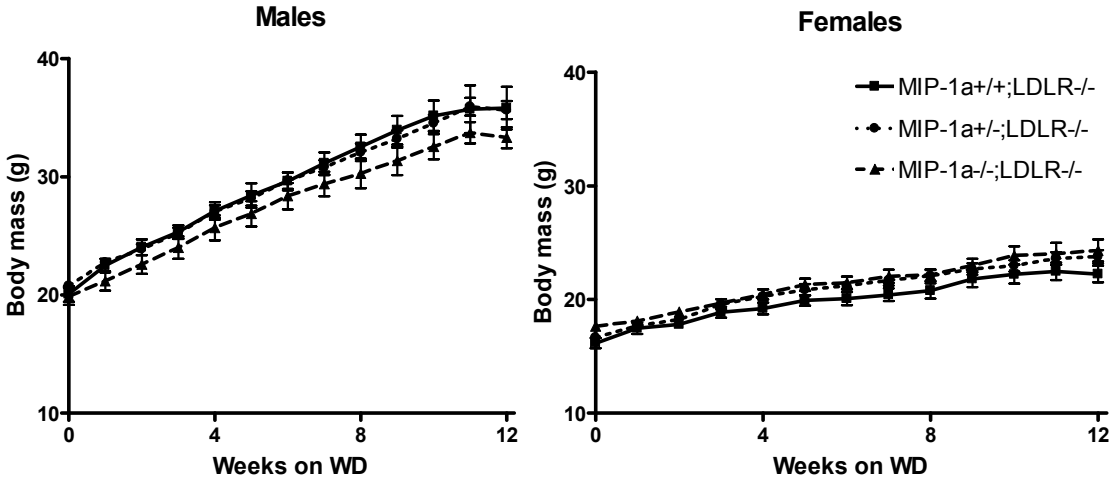

Figure 5.7. Body mass during WD feeding. Mice were started on WD at 8 wks of age. Data shown is for the 12 wk study period: body mass for males (left) and females (right).

Atherosclerosis

Atherosclerotic lesion area was quantified at the aortic root and no differences based on MIP-1α genotype were detected (Figure 5.8). In addition, the male mice had similar lesion area to the female mice despite their nearly 2-fold higher plasma TC concentrations.

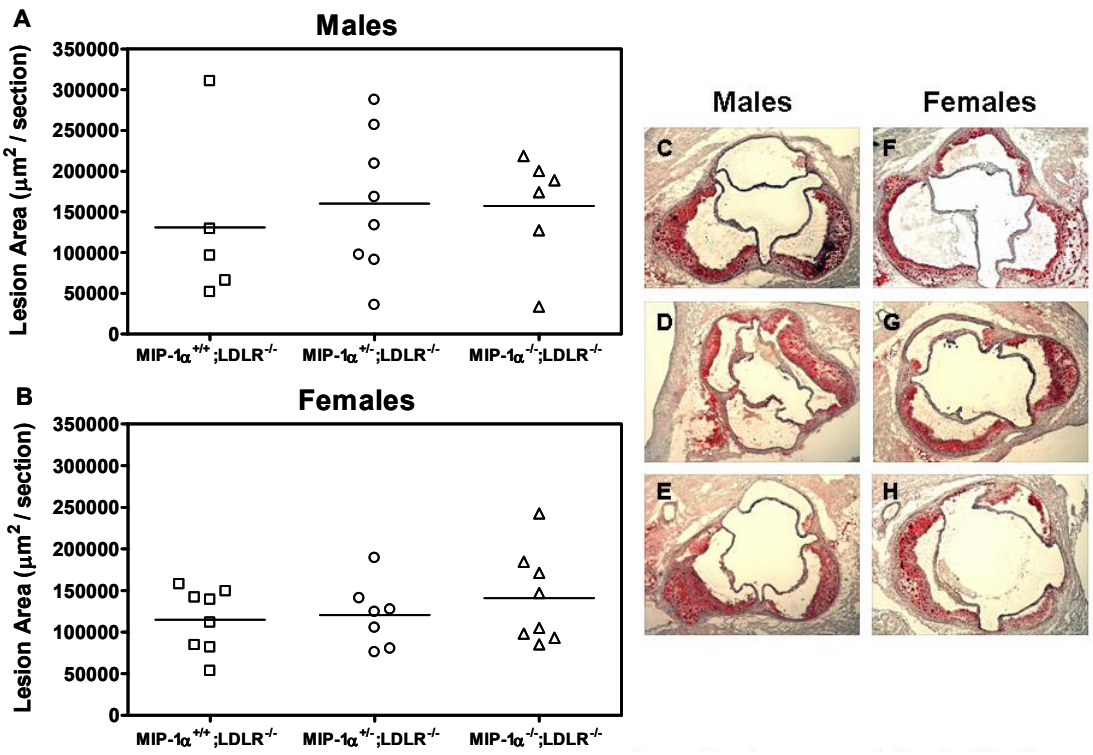

Figure 5.8: Aortic root lesion quantification. Aortic root lesions were stained with oil red O and quantified (A) as described in the Methods. (B) Representative oil red O stained sections from MIP-1α$^{+/+}$;LDLR$^{-/-}$ (C & F), MIP-1α$^{+/-}$;LDLR$^{-/-}$ (D & G), and MIP-1α$^{-/-}$;LDLR$^{-/-}$ (E & H) mice.

WAT gene expression and morphology

Expression of several genes involved in the immune response was quantified in perigonadal WAT (Figure 5.9). Similar to what we previously observed in MIP-1α$^{-/-}$;LDLR$^{+/+}$ mice, expression of macrophage and T-lymphocyte markers, F4/80 and CD3ε, were not significantly altered by MIP-1α deficiency (Figure 5.9A-B). The inflammatory cytokine TNF-α as well as IL-10 and Mgl2—markers of alternative activation—were expressed to a similar extent in all three genotypes (Figure 5.9C-D, F). However, expression of macrophage galactose N-acetyl-galactosamine specific lectin 1 (Mgl1), another marker of

alternatively activated (M2) macrophages, was decreased in male and female MIP-1α$^{+/-}$;LDLR$^{-/-}$ mice (p<0.001 genotype effect, Figure 5.9E). MIP-1α was reduced in the MIP-1α$^{+/-}$;LDLR$^{-/-}$ mice compared to the MIP-1α$^{+/+}$;LDLR$^{-/-}$ mice and was not detected in MIP-1α$^{-/-}$;LDLR$^{-/-}$ mice (p<0.0001 genotype effect, Figure 5.9G). MIP-1β was reduced in the male MIP-1α$^{-/-}$;LDLR$^{-/-}$ and MIP-1α$^{+/-}$;LDLR$^{-/-}$ mice compared to MIP-1α$^{+/+}$;LDLR$^{-/-}$ mice (p<0.05 genotype effect, Figure 5.9H). MIP-1α deficiency did not significantly impact expression of the chemokines MCP-1 and RANTES (Figure 5.9I-J). Compared with males, females had lower expression of several of the genes examined: F4/80 (p<0.0001) , TNFα (p<0.0001), IL-10 (p<0.01), Mgl1 (p<0.001), MIP-1α (p<0.0001 gender effect, p<0.0001 interaction between genotype and gender effects), MIP-1β (p<0.005 gender effect, p<0.05 interaction between genotype and gender effects), RANTES (p<0.005), and MCP-1 (p<0.0001, Figure 5.9).

WAT was stained with toluidine blue O to visualize tissue morphology, but we did not observe any obvious differences among genotypes (Figure 5.10).

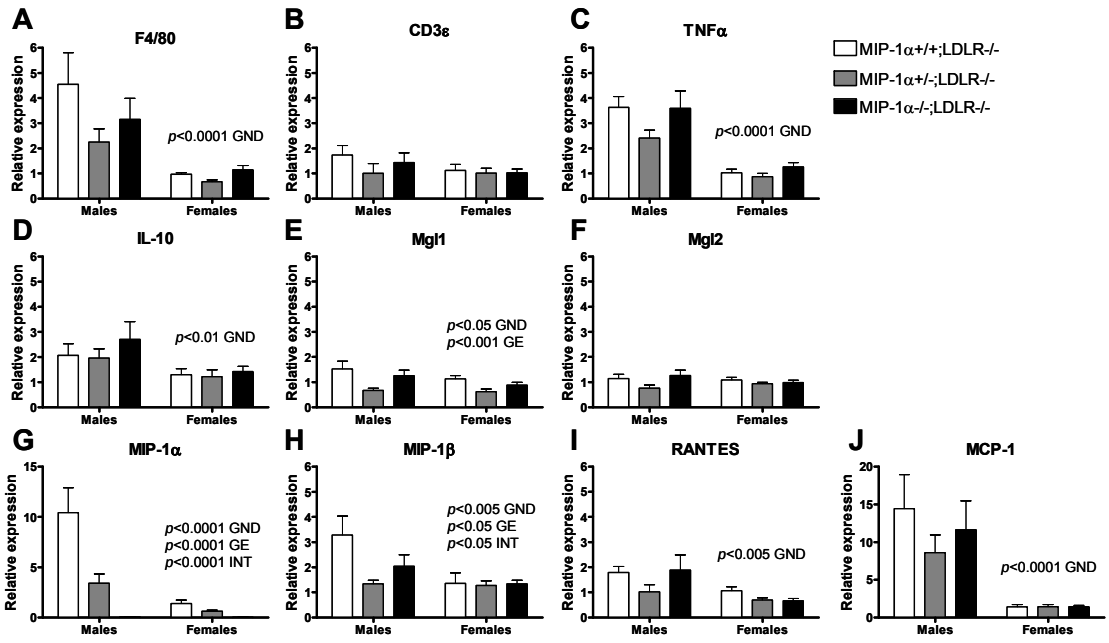

Figure 5.9. WAT gene expression after 12 wks on WD. RNA was isolated from perigonadal WAT and used to synthesize cDNA, which was used for real time PCR. Data were analyzed by 2-way ANOVA. Abbreviations: GND=gender effect, GE=genotype effect, INT=interaction between gender and genotype effects

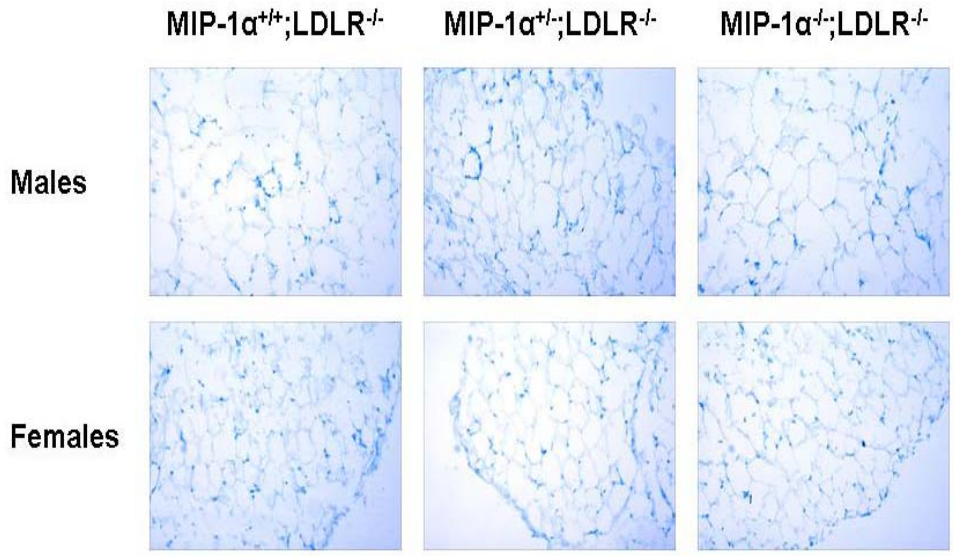

Figure 5.10. Toluidine blue O stained WAT in mice after 12 wks on Western Diet. Perigonadal WAT was harvested from mice, weighed, and a portion was fixed overnight in 10% formalin, transferred to 70% ethanol, and paraffin embedded. Tissue was cut into 7μm sections and stained with toluidine blue O. Representative sections are shown. Images were taken at 100x magnification.

Liver lipids and gene expression

Hepatic TG accumulation was significantly greater in male than in female mice ($p<0.05$) but was not influenced by MIP-1α expression level (Figure 5.11). Quantification of hepatic gene expression for inflammatory markers, TNFα and MCP-1; two of MIP-1α's receptors, CCR1 and CCR5; and factors involved in lipid metabolism, sterol regulatory element binding protein-1c and stearoyl-CoA desaturase-1; revealed no differences based on genotype, but expression of CCR5 was higher in females than in males ($p<0.005$, Figure 5.12).

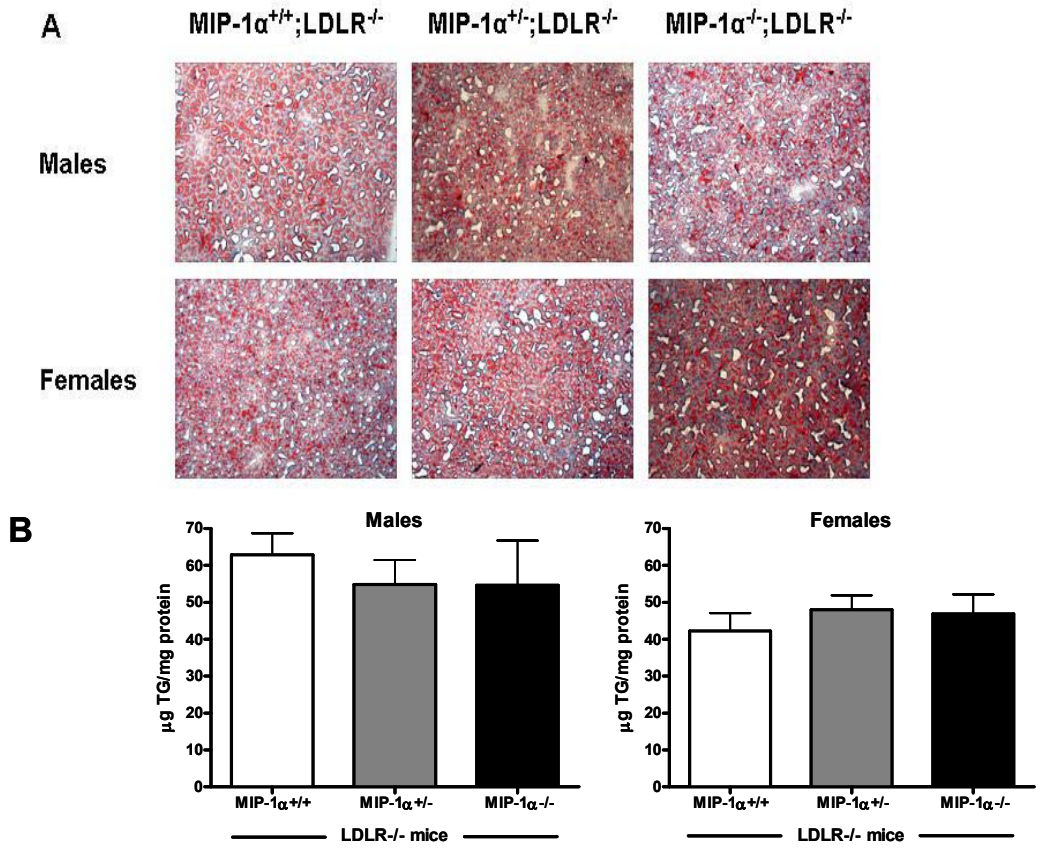

Figure 5.11. Hepatic triglyceride content in Western Diet-fed mice. Representative oil red O stained liver sections (A) and quantitative analysis of hepatic TGs in mice after 16 wks of Western Diet feeding (B) are shown. Hepatic TGs were measured as described in the Methods. Abbreviations: TGs, triglycerides.

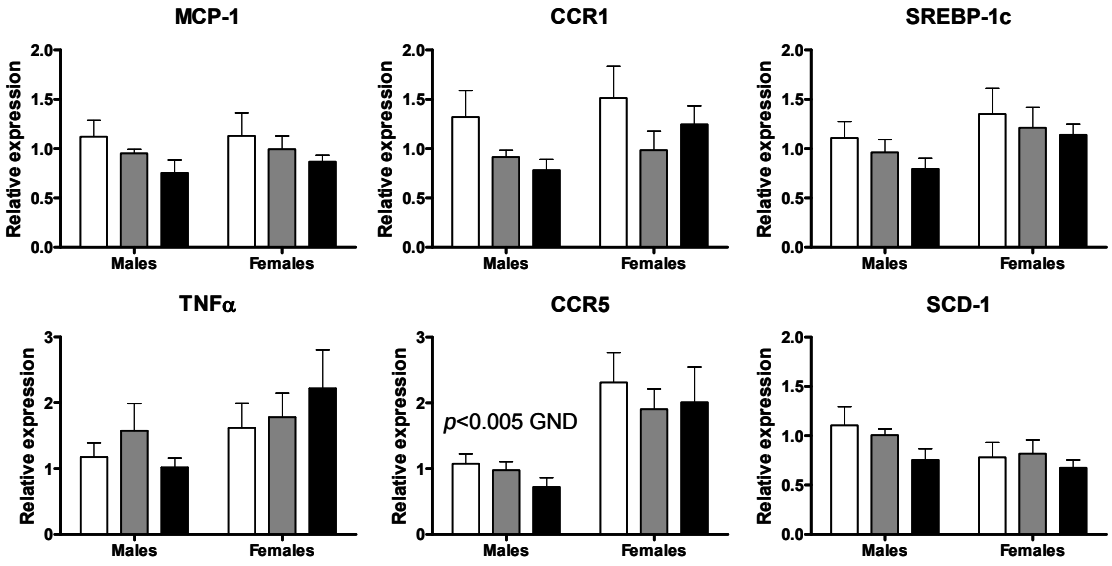

Figure 5.12. Hepatic gene expression in male and female mice after 12 wks on Western Diet. RNA was isolated from liver and used to synthesize cDNA, which was used for real time PCR. Data from males and females were analyzed by 2-way ANOVA using the same real time PCR threshold. Abbreviation: GND=gender effect.

Table 5.1 Plasma Parameters after 12 Weeks of Western Diet Feeding

Genotype	n	TC (mg/dl)	TG (mg/dl)	NEFA (mEq/l)	Glucose (mg/dl)	Insulin (ng/ml)	Leptin (ng/ml)
Male							
MIP-1a$^{+/+}$;LDLR$^{-/-}$	5	1238 ± 62	375 ± 51	3.05 ± 0.17	123 ± 6	1.35 ± 0.18	50.3 ± 10.6
MIP-1a$^{+/-}$;LDLR$^{-/-}$	7-17	1139 ± 52	332 ± 26	3.13 ± 0.12	115 ± 4	2.27 ± 0.37	45.6 ± 6.1
MIP-1a$^{-/-}$;LDLR$^{-/-}$	7-8	1076 ± 94	280 ± 31	2.50 ± 0.19*	118 ± 5	1.29 ± 0.26	46.1 ± 9.4
Female							
MIP-1a$^{+/+}$;LDLR$^{-/-}$	8	659 ± 34	146 ± 17	2.36 ± 0.16	94 ± 9	0.49 ± 0.06	6.8 ± 1.4
MIP-1a$^{+/-}$;LDLR$^{-/-}$	8-10	741 ± 46	179 ± 18	2.79 ± 0.24	104 ± 3	0.60 ± 0.10	10.4 ± 1.9
MIP-1a$^{-/-}$;LDLR$^{-/-}$	8-11	790 ± 39	199 ± 27	2.43 ± 0.24	97 ± 4	0.50 ± 0.05	14.5 ± 4.7

*p<0.05 vs. MIP-1α$^{+/-}$;LDLR$^{-/-}$ (1-way ANOVA), p<0.05 vs. MIP-1α$^{+/-}$;LDLR$^{-/-}$ (Tukey's Multiple Comparison post hoc test)

Table 5.2 Body composition at 8 wks of age

Genotype	n	Body Weight (g)	Total WAT Mass (g)	Lean Tissue Mass (g)
Male				
MIP-1a$^{+/+}$;LDLR$^{-/-}$	5	20.1 ± 0.7	1.49 ± 0.06	15.6 ± 0.6
MIP-1a$^{+/-}$;LDLR$^{-/-}$	17	20.8 ± 0.3	1.43 ± 0.05	15.9 ± 0.2
MIP-1a$^{-/-}$;LDLR$^{-/-}$	7-8	19.9 ± 0.7	1.63 ± 0.13	15.2 ± 0.5
Female				
MIP-1a$^{+/+}$;LDLR$^{-/-}$	7-8	16.2 ± 0.4	1.44 ± 0.06	12.3 ± 0.3
MIP-1a$^{+/-}$;LDLR$^{-/-}$	10	16.7 ± 0.2	1.38 ± 0.08	12.9 ± 0.2
MIP-1a$^{-/-}$;LDLR$^{-/-}$	11	17.7 ± 0.2*§	1.39 ± 0.09	13.6 ± 0.2§

*p<0.05 vs. MIP-1a$^{+/-}$;LDLR$^{-/-}$, $^{\S}p$<0.01 vs. MIP-1a$^{+/+}$;LDLR$^{-/-}$

Table 5.3 Body and Tissue Masses after 12 Weeks of Western Diet Feeding

Genotype	n	Body Weight (g)	Total WAT Mass (g)	Lean Tissue Mass (g)	Perigonadal WAT Mass (g)	Liver Mass (g)
Male						
MIP-1a$^{+/+}$;LDLR$^{-/-}$	5	35.8 ± 1.8	11.3 ± 1.4	21.3 ± 0.5	1.65 ± 0.23	1.86 ± 0.17
MIP-1a$^{+/-}$;LDLR$^{-/-}$	17	35.6 ± 0.8	10.9 ± 0.5	21.6 ± 0.3	1.59 ± 0.08	1.88 ± 0.08
MIP-1a$^{-/-}$;LDLR$^{-/-}$	7-8	33.3 ± 0.9	10.0 ± 0.7	20.4 ± 0.3	1.33 ± 0.09	1.80 ± 0.10
Female						
MIP-1a$^{+/+}$;LDLR$^{-/-}$	7-8	22.2 ± 0.7	3.0 ± 0.5	16.4 ± 0.4	0.34 ± 0.12	1.11 ± 0.06
MIP-1a$^{+/-}$;LDLR$^{-/-}$	10	23.8 ± 0.6	4.0 ± 0.4	17.1 ± 0.3	0.45 ± 0.06	1.26 ± 0.07
MIP-1a$^{-/-}$;LDLR$^{-/-}$	11	24.3 ± 1.0	4.6 ± 0.7	17.1 ± 0.5	0.54 ± 0.10	1.43 ± 0.11*

*p=0.05 vs. MIP-1α$^{+/+}$;LDLR$^{-/-}$ (1-way ANOVA), p<0.05 vs. MIP-1α$^{+/+}$;LDLR$^{-/-}$ (Tukey's Multiple Comparison post hoc test)

Discussion

Using WD feeding to induce hyperlipidemia in MIP-1α$^{-/-}$;LDLR$^{-/-}$ mice, we addressed the potential interaction between hyperlipidemia and MIP-1α. Based on the literature, we expected that monocytes/macrophages exposed to high plasma VLDL (as they are in WD-fed LDLR$^{-/-}$ mice) would produce greater amounts of MIP-1α than monocytes/macrophages from normolipidemic mice. In addition, when compared with 17 other cytokines/chemokines, MIP-1α alone is significantly elevated in the plasma of hyperlipidemic LDLR$^{-/-}$ or apolipoprotein E deficient mice (173). Thus, we expected MIP-1α deficiency to have a greater impact on metabolic parameters in hyperlipidemic mice than in normolipidemic mice.

As shown in the results, MIP-1α$^{-/-}$;LDLR$^{-/-}$ and MIP-1α$^{+/+}$;LDLR$^{-/-}$ mice had similar body compositions with no differences in total fat mass or atherosclerotic lesion area. Plasma cholesterol strongly correlates with atherosclerotic lesion area in mice, but in a gender specific manner as demonstrated in our studies. In comparison with the bone marrow transplanted mice discussed in this chapter's introduction, plasma TC concentrations in non-irradiated male LDLR$^{-/-}$ mice were twice as high (587 ± 34 and 634 ± 34 mg/dl in MIP-1α$^{-/-}$→LDLR$^{-/-}$ and MIP-1α$^{+/+}$→LDLR$^{-/-}$ males, respectively, vs. 1238 ± 62, 1139 ± 52, and 1076 ± 94 mg/dl in MIP-1α$^{+/+}$;LDLR$^{-/-}$, MIP-1α$^{+/-}$;LDLR$^{-/-}$, and MIP-1α$^{-/-}$;LDLR$^{-/-}$ mice, respectively), and their lesion area was likewise 2-fold higher. Thus, male LDLR$^{-/-}$ mice did not develop lesions matching the lesion size of the females unless their plasma cholesterol concentrations were much higher than those of the

females. Furthermore, irradiation and bone marrow transplantation greatly attenuated the rise in plasma TC only in the male mice, but the reason for this is unknown.

The higher liver mass in MIP-1α$^{-/-}$;LDLR$^{-/-}$ as compared to MIP-1α$^{+/+}$; LDLR$^{-/-}$ female mice does not appear to indicate liver-specific differences. The increased liver mass corresponded to a general increase in body and lean mass throughout the study among the female mice that was significant at baseline but not significant after 12 wks on WD. The similarity in hepatic lipid content and expression level of inflammatory genes among all of the female mice demonstrates that the increased liver mass did not represent a change in hepatic steatosis or inflammation.

WAT expression of MIP-1α was reduced in a stepwise manner according to the mice's genotypes, but the expression of other genes examined was not significantly influenced by MIP-1α expression level, with the exception of Mgl1 and MIP-1β. The reason for Mgl1 being decreased in the MIP-1α$^{+/-}$;LDLR$^{-/-}$ mice is unknown, but the decreased expression of MIP-1β is consistent with what we observed in MIP-1α$^{+/-}$;LDLR$^{+/+}$ and MIP-1α$^{-/-}$; LDLR$^{+/+}$ mice (Figure 4.5K).

In conclusion, our data demonstrate that despite occurrence of hyperlipidemia in MIP-1α$^{-/-}$;LDLR$^{-/-}$ mice after 12 wks on WD, they were similar to MIP-1α$^{+/+}$;LDLR$^{-/-}$ in nearly all of the metabolic parameters tested. The literature gives evidence of a correlation between MIP-1α and hyperlipidemia, but we have shown that hyperlipidemia alone did not potentiate the effect of MIP-1α deficiency on weight gain, atherosclerosis, or inflammation. Both adipocytes and stromal

vascular cells in WAT are sensitive to total body irradiation, and irradiated mice have smaller adipocytes, reduced WAT mass, and lower adipogenic differentiation potential of their adipocyte precursors (118). Therefore, since the combination of MIP-1α deficiency and hyperlipidemia was not sufficient to protect mice from diet induced weight gain, we propose two potential reasons for the dramatic decrease in WAT mass observed in the bone marrow transplanted mice. First, either MIP-1α is involved in adipocyte maturation or another aspect of adipose tissue expansion and the sudden absence of MIP-1α—rather than its absence throughout development—prevents compensation for its role, or, second, that lethal irradiation and MIP-1α deficiency synergistically lower the capacity of adipocytes for TG storage in $LDLR^{-/-}$ mice.

CHAPTER VI

DISCUSSION

Summary

In Chapter III we demonstrated that removal of LepR from all BMDCs did not influence atherosclerotic lesion formation. This suggested that non-hematopoietic cells, rather than macrophages, are potential mediators of leptin's effects on aortic root lesion formation. In Chapter IV, we demonstrated that although expression of MIP-1α increases as a consequence of weight gain this chemokine is not critical for the recruitment of monocytes and T-lymphocytes to WAT in mice with DIO. Furthermore, the presence of hyperlipidemia (Chapter V) was not sufficient to attenuate fat mass gain or atherosclerosis in MIP-1α$^{-/-}$ mice during WD feeding. In the following paragraphs we will discuss how perivascular WAT could influence atherosclerotic lesion formation as a local source of leptin and chemokines. We will also summarize what is currently known about the timeline of events occurring in WAT inflammation during obesity and demonstrate how we think MIP-1α is involved. In chapter VII we will discuss our overall conclusions and potential future directions of this doctoral work.

Role of perivascular WAT

As mentioned in the Discussion of Chapter III, our experiments to evaluate the role of leptin in atherosclerotic lesion formation focused on lesions at the

aortic root. However, other regions of the aorta are encompassed by more perivascular WAT than the aortic root, and leptin coming directly from the perivascular WAT might affect the development of lesions in a way that a general elevation in plasma leptin does not. Because perivascular WAT mass increases with high fat diet feeding (52), we proposed in our discussion at that time that secretion of leptin from the perivascular WAT has a local effect on the artery wall in the abdominal and thoracic regions of the aorta. Since the publication of our research (142), perivascular WAT has been further characterized as described below.

In comparison to subcutaneous and perirenal adipocytes, perivascular adipocytes are smaller and more irregularly shaped (17). *In vitro* differentiated perivascular adipocytes have lower expression of adipogenic regulatory genes, decreased secretion of leptin and adiponectin, and elevated secretion of MCP-1, IL-8, and IL-6 relative to adipocytes from other depots (17). This indicates that they are not as mature/differentiated as other adipocytes and are likely more inflammatory. In chow-fed mice, leptin gene expression was much lower in perivascular WAT than it was in subcutaneous, epididymal, or perirenal WAT, and MIP-1α expression was similar in all of the depots (17) (Figure 6.1A). A striking change occurred when mice were fed a high fat diet for 2 wks. In perivascular WAT, expression of leptin rose nearly to 1000-fold its expression in chow-fed mice, and MIP-1α expression increased to 600-fold its expression in chow-fed mice (Figure 6.1B) (17). Thus, when mice ate a high fat diet, perivascular WAT quickly became the depot with the greatest expression of MIP-

1α. In addition, because expression of leptin in the perivascular WAT of chow diet-fed mice was much lower than it was in other fat depots, the dramatic increase in leptin expression induced by high fat diet feeding caused leptin expression in perivascular WAT to become comparable to that of the other depots in high fat diet-fed mice.

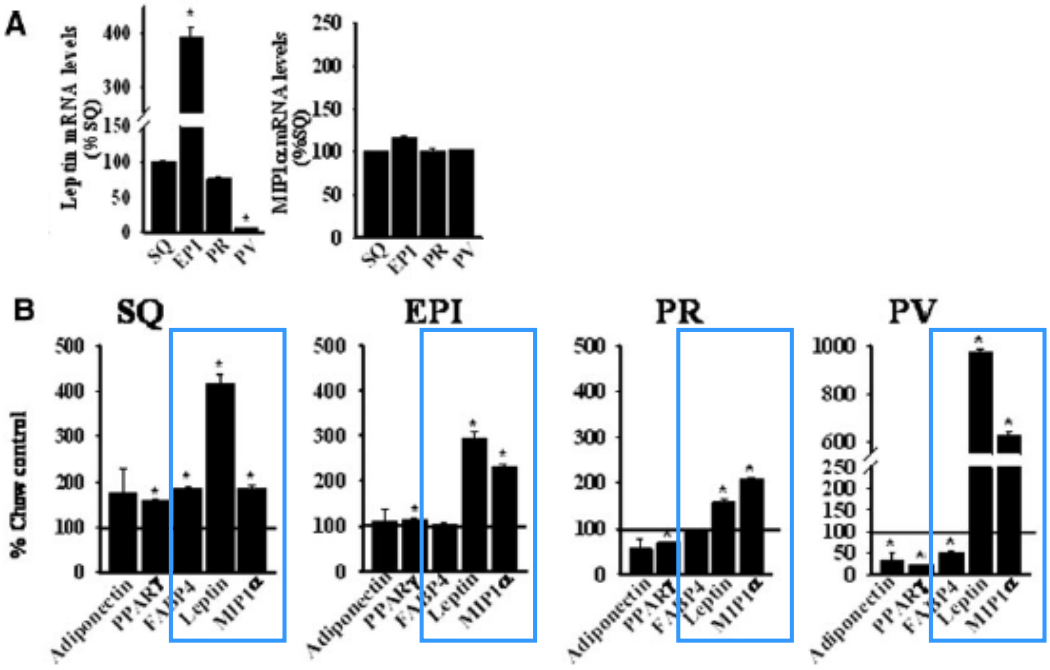

Figure 6.1. Real-time PCR determination of adiponectin, PPAR, FABP4, leptin, and MIP1α mRNA expression in subcutaneous (SQ), epididymal (EPI), perirenal (PR), and perivascular (PV) adipose tissues of C57BL/6 mice fed a chow (A) or a high fat diet (B) for 2 weeks. mRNA levels in A are expressed relative to subcutaneous adipose tissue data, whereas in B, levels are expressed relative to the corresponding depot in chow-fed mice. Values represent the mean SEM of 3 to 5 mice per group. *p<0.05 vs SQ data (A) or vs corresponding chow-fed data (B). Adapted from Chatterjee et al. *Circ Res.* 2009 Feb 27;104(4):541-9. Epub 2009 Jan 2.

Expression of leptin and MIP-1α in perivascular WAT is more sensitive to high fat diet induced regulation than in subcutaneous, epididymal, and perirenal WAT—at least at the timepoint examined. Based on this, we believe that perivascular WAT has emerged as an important contributor to local inflammation in the artery wall. In fact, in addition to the pro-inflammatory roles of leptin described in Chapter III, we have demonstrated *in vitro* that leptin is a chemoattractant for THP-1 monocytes (47). We expect future studies detailing how perivascular WAT-derived leptin and chemokines contribute to atherosclerotic lesion development to enhance our comprehension of the interaction between obesity and CVD (Figure 6.2).

Because MIP-1α expression is so highly upregulated in perivascular WAT, perhaps studying the effect of MIP-1α deficiency in this fat depot in high fat diet fed mice could serve as a helpful model system for uncovering the general role of MIP-1α in WAT. Initially, perivascular WAT could be isolated from high fat diet fed mice and examined by flow cytometry or immunostaining to detect the presence of specific leukocyte populations. Findings within the perivascular WAT would hopefully generate new hypotheses to test in regard to why MIP-1α is elevated in visceral and subcutaneous fat depots.

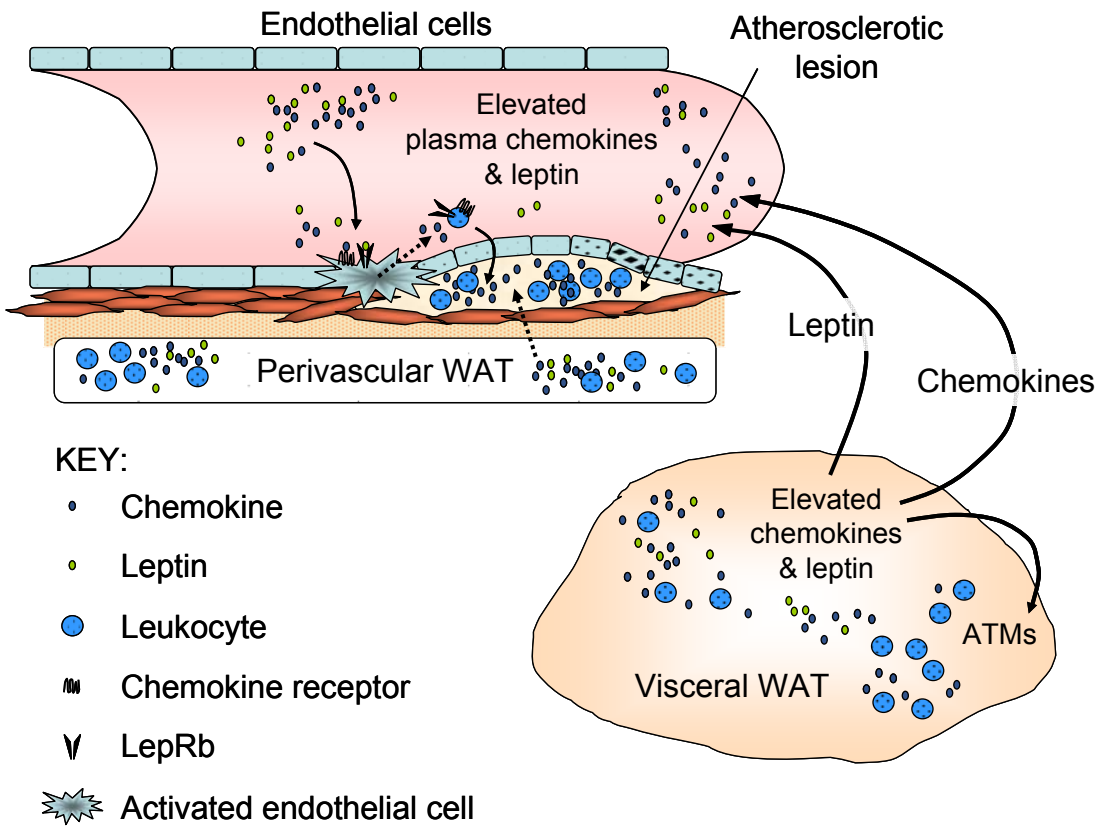

Figure 6.2. Contribution of perivascular and visceral WAT to the elevation in local and circulating concentrations of leptin and chemokines during obesity. Chemokine and leptin receptors are present on many different cell types including monocytes, macrophages, endothelial cells, smooth muscle cells, and T-lymphocytes. While visceral WAT can influence the artery wall in an endocrine manner by secreting leptin and chemokines into the circulation, perivascular WAT is adjacent to the arterial wall adventia and can have a local effect.

The role of chemokines during the progression of obesity

The role of MIP-1α in human WAT

As described in the Introduction (Chapter I), expression of MIP-1α and its receptors is elevated in obese humans. In addition, several studies have found an association between insulin resistance and increased MIP-1α expression in

human WAT. Even though we demonstrated that WD-fed MIP-1α$^{-/-}$ mice did not differ from MIP-1α$^{+/+}$ mice in the degree of WAT inflammation or plasma insulin concentration (Chapter IV), it remains possible that MIP-1α is an important contributor to obesity and insulin resistance in humans. In fact, although many studies have indicated that the chemokine MCP-1 is important in monocyte mobilization from the bone marrow and recruitment to WAT during obesity (43), the results from MCP-1 deficient (MCP-1$^{-/-}$) mice have been inconsistent (as described below). Continued research in humans as well as a thorough understanding of the timeline of events that occurs during obesity-related WAT inflammation will address the reason for elevation of MIP-1α and other chemokines in WAT of obese individuals.

The role of an alternate chemokine, MCP-1, in leukocyte recruitment to WAT

To date, MCP-1 and its receptor CCR2 are the best-studied of the chemokine ligands and receptors for their role in macrophage accumulation in WAT and obesity-induced insulin resistance. MCP-1 is upregulated at the mRNA and protein levels in mesenteric, epididymal, subcutaneous, and perirenal WAT of diet induced obese mice (168). F4/80 and CD68 expression is also increased in these WAT depots (168). In addition, *in vitro* migration experiments show increased macrophage migration to mesenteric WAT-conditioned media, and an antibody for MCP-1 blocks this migration (168).

Two different groups have engineered transgenic mice using the human adipocyte fatty acid binding protein (aP2) gene promoter to overexpress MCP-1

in WAT (65, 66). WAT of the MCP-1 overexpressing mice contains more macrophages than WAT from wild type mice, and MCP-1 transgenic mice are insulin resistant and glucose intolerant, suggesting that MCP-1 may promote macrophage infiltration and insulin resistance during obesity. In addition, attenuation of MCP-1 activity with a dominant negative approach, improved insulin sensitivity and glucose tolerance in both $LepR^{db/db}$ and diet induced obese mice (66). On the other hand, experiments with MCP-$1^{-/-}$ mice have yielded inconsistent results. Kanda et al. found that diet induced obese MCP-$1^{-/-}$ mice had fewer ATMs and were more insulin sensitive and glucose tolerant although they demonstrated no differences in body weight relative to wild type controls (66). In contrast, Inouye et al. observed significantly increased body weight in diet induced obese MCP-$1^{-/-}$ mice and possibly a slight increase in macrophage accumulation in WAT combined with decreased insulin sensitivity (61). Kirk et al. found similar results to Inouye et al. except that they observed no differences in insulin or glucose tolerance (73). In regard to the receptor CCR2, Lumeng et al. have demonstrated that CCR2 deficiency partially attenuates the recruitment of inflammatory monocytes into WAT, suggesting that inflammatory monocytes are recruited in CCR2-dependent and -independent ways (89).

As the field of obesity-related WAT inflammation advances, it is becoming more apparent that the inflammatory process in WAT is highly dynamic. Numerous cell types are involved and different chemokines are elevated at distinct times and in particular fat depots. Thus, we believe that some of the variability observed in the studies related to MCP-1 and unexpected results in our

MIP-1α studies are due to the timepoints chosen and the adaptability of the immune system. In the following section we will assimilate what is already known about the cell types and chemokines that contribute to WAT inflammation in mice and indicate some future experiments that are needed.

The progression of inflammation in WAT during weight gain

Many groups have contributed to our current understanding of the inflammatory process in WAT during high fat diet feeding and weight gain. Figure 6.3 illustrates how cell populations and chemokine expression and production shift during high fat diet feeding. Following is a synopsis of the literature on this topic.

After only one day of high fat diet feeding WAT secretion of MCP-1 immediately increases in mice (63). By day three of the high fat diet, neutrophils have infiltrated the WAT, and secretion of MCP-1, -2, and -3 are all elevated (38, 63). Neutrophils are retained in the WAT through day 7, at which point secretion of MRP-2 is also elevated (38, 63). Interestingly, MCP-1 and MIP-1α have been implicated in neutrophil recruitment (125). The early upregulation by MCP-1 immediately before infiltration of neutrophils suggests that it may be involved; however, it is not likely that MIP-1α is important for this initial recruitment of neutrophils since MIP-1α is not upregulated as early as MCP-1.

The next leukocytes on the scene are the $CD3^+CD8^+CD4^-$ T-lymphocytes, which are present by the second week of the diet (105). $CD8^+$ T-lymphocytes remain in the WAT throughout the development of obesity and peak by 11-16

wks of high fat diet feeding (105). Not as much is known about the role of $CD19^+$ B-lymphocytes in this process, but their presence in WAT nearly doubles after 3 wks on diet, and they are also increased after 6 wks (36). The earliest timepoint at which the number of $F4/80^+$ macrophages increases above that of lean mice is after 6 wks of high fat diet feeding (105). Macrophages continue to accumulate in the WAT and peak at 16-26 wks after the initiation of the high fat diet (105, 140). The number of $CD3^+CD8^-CD4^+$ T-lymphocytes begins to decrease by week 6 and remains decreased (105). By 11 wks on the diet, fewer $Foxp3^+$ T_{reg} lymphocytes remain in the WAT, and their presence continues to be low (105).

An elevation in chemokines is one of the first events observed in WAT of mice fed a high fat diet, and many chemokines are upregulated in the WAT during the progression of obesity, some of which are indicated in Figure 6.3. MIP-1α expression is elevated by week 12 and continues to be elevated through 26 wks of high fat diet feeding (Figure 4.5 and (63, 105, 166)). Activated $CD8^+$ T-lymphocytes are one of the main cellular sources of MIP-1α (27, 71). Nishimura et al. has demonstrated that in mice with pre-established obesity, administration of CD8 blocking antibody partially attenuates MIP-1α expression in the WAT (105). Based on this, $CD8^+$ T-lymphocytes are probably one—but not the only—cellular source of MIP-1α during WAT inflammation.

MIP-1α is also a chemoattract for $CD8^+$ T-lymphocytes. However, as Figure 6.3 demonstrates, MIP-1α upregulation occurs after $CD8^+$ T-lymphocyte recruitment to WAT, and the complete absence of MIP-1α does not interfere with WAT inflammation (Chapter IV). Therefore, although Nishimura et al. have

demonstrated that $CD8^+$ T-lymphocytes have a critical role in WAT inflammation and the subsequent development of systemic insulin resistance (105), we have demonstrated that MIP-1α is not essential for this. As indicated by the multitude of references used to build the timeline in Figure 6.3, many groups are interested in understanding the contribution of chemokines to WAT inflammation. Several studies have suggested that MIP-1α is important for recruitment of leukocytes to the WAT, but our work is the first to actually test this hypothesis. Now that we have demonstrated that MIP-1α is not necessary for monocyte or T-lymphocyte recruitment to WAT in obesity, future studies can focus on whether MIP-1α plays a role in human obesity.

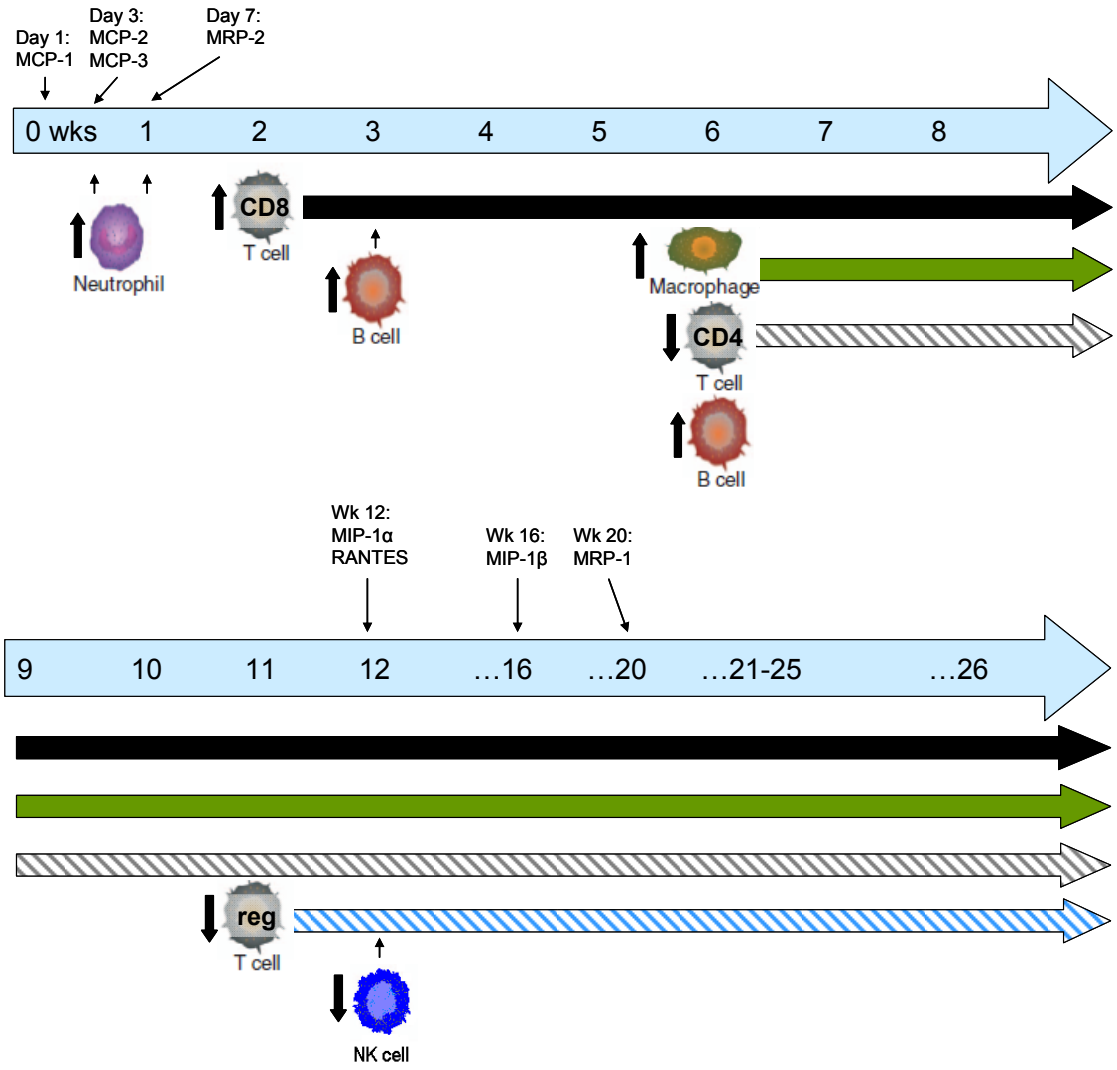

Figure 6.3. Up- or downregulation of specific chemokines and leukocytes in WAT of high fat diet fed mice. Diagram indicates only the initial upregulation of each chemokine during high fat diet feeding and is based on the following references: Jiao et al. *Diabetes* 2009, Nishimura et al. *Nature Medicine* 2009, and Chapter IV. Numbers on blue arrows represent the number of wks on high fat diet. The initial reported increase or decrease in each cell type is shown; the horizontal arrows indicate that high fat diet fed mice continue to have more macrophages and CD8+ T-lymphocytes and fewer CD4+ T-lymphocytes and Treg lymphocytes throughout high fat diet feeding. Additional sources used: Duffaut et al. *BBRC* 2009, Feurer et al. *Nature Medicine* 2009, Winer et al. *Nature Medicine* 2009, Rausch et al. *I J Obesity* 2007, Weisberg et al. *JCI* 2003, Xu et al. *JCI* 2003, Strissel et al. *Diabetes* 2007, Coenen et al. *Diabetes* 2007, Caspar-Bauguil et al. *FEBS Letters* 2005.

CHAPTER VII

CONCLUSION AND FUTURE DIRECTIONS

Contribution of our research to understanding the roles of chemokines in WAT inflammation

Leukocytes have an essential role in atherosclerosis and obesity, which are both chronic inflammatory diseases. Macrophages and T-lymphocytes are recruited to the artery wall and to WAT in response to pathological changes which occur within each tissue. Chemokines and chemokine receptors are known to be important for lesion formation in atherosclerosis, but their role as initiators and propagators of WAT inflammation is not as clear. Prior to the studies presented in Chapters IV and V, many groups observed elevated expression and production of MIP-1α in atherosclerotic lesions and in WAT of obese mice and humans, and MIP-1α levels were known to be associated with insulin resistance and hyperlipidemia. However, the particular role of MIP-1α in the metabolic phenotype of lean, obese, or hyperlipidemic mice had not been tested. We have extensively investigated the role of MIP-1α in metabolism in lean and obese mice and have shown that even when mice are challenged with WD, MIP-1α deficiency does not protect mice from atherosclerotic lesion development, WAT inflammation, elevated fasting plasma insulin, and hepatic steatosis. Our data demonstrate that MIP-1α is not necessary for leukocyte

recruitment to the artery wall or WAT, suggesting that its elevation in these tissues might serve a different purpose than what we originally expected.

Furthermore, we demonstrated in multiple mouse models that the WD-induced elevation in WAT expression of MIP-1β is attenuated in MIP-1α$^{+/-}$ and MIP-1α$^{-/-}$ male mice. Therefore, we have demonstrated that a simultaneous reduction in MIP-1α and MIP-1β does not influence accumulation of macrophages or CD3^{+} T-lymphocytes in the WAT of diet induced obese mice.

Future Directions

A role in WAT inflammation that goes beyond chemotaxis

It is important to note that the role of chemokines and their receptors in atherosclerosis is not limited to chemotaxis. They are involved in mobilization of cells from the bone marrow, cell adhesion, cell survival during differentiation, cell retention within the lesion, and lipid scavenging. Therefore, while pursuing a better understanding of how chemokines participate in WAT inflammation as fat mass is increasing, experiments that test for the influence of chemokines on WAT properties besides accumulation of immune cells will be helpful. Bone marrow transplantation of MIP-1α$^{-/-}$ BMDCs into lethally irradiated LDLR$^{-/-}$ mice dramatically attenuated fat mass gain without having an obvious effect on adipocyte size (Figure 5.2C and unpublished data). Moreover, hepatic TGs were not elevated in MIP-1α$^{-/-}$→LDLR$^{-/-}$ mice (unpublished data), ruling out the possibility that decreased lipid storage in the WAT was increasing ectopic lipid

storage in the liver. A Cre/lox model could be used to remove MIP-1α expression from adult mice just before they are started on WD. By measuring body composition in these mice at various times before and during WD feeding, we could test whether the sudden removal of MIP-1α is able to recapitulate the phenotype observed in MIP-1α$^{-/-}$→LDLR$^{-/-}$ mice. If it is, this would validate the findings from the bone marrow transplantation experiment and demonstrate that MIP-1α has a role in WAT expansion even without the stress of lethal irradiation. If removal of MIP-1α from adult mice is not able to reduce their sensitivity to diet induced weight gain, then this would indicate that lethal irradiation and/or bone marrow reconstitution are critical factors in the results of our bone marrow transplantation experiments.

As mentioned above, chemokines help to mobilize hematopoietic cells from the bone marrow. During inflammatory conditions, such as high fat diet feeding, CCR2 and its receptors MCP-1 and MCP-3 are known to be involved in this mobilization process (149). To see if MIP-1α also regulates BMDC mobilization we could place MIP-1α$^{-/-}$ and MIP-1α$^{+/+}$ mice on WD and quantify specific populations of hematopoietic cells (using flow cytometry) in the bone marrow and blood. As an important control we could measure CCR2, MCP-1, and MCP-3 in BMDCs to see whether MIP-1α deficiency alters expression of these proteins. In addition, we could lethally irradiate MIP-1α$^{-/-}$ and MIP-1α$^{+/+}$ mice and reconstitute them with MIP-1α$^{-/-}$ or MIP-1α$^{+/+}$ bone marrow. Using flow cytometry we could then quantify the various populations of hematopoietic cells

in the bone marrow and blood to test whether MIP-1α deficiency impedes reconstitution after lethal irradiation.

Inflammation in the artery wall versus WAT

Although chemokines are abundantly expressed in WAT of obese mice and humans, many questions regarding their roles remain unanswered. As research in this field continues it will be important to distinguish between the contributions of specific chemokines to the inflammation in the artery wall versus in the WAT. Leukocyte infiltration of the artery wall has frequently served as a model of what might occur in WAT during the onset of obesity. However, important differences between these two tissues are apparent. For example, within the WAT, leukocytes circulate through small blood vessels and capillaries before extravasating into the tissue. In contrast, athersclerosis occurs in the aorta (in mice) and in coronary arteries (in humans) in which blood is circulating with more force and in greater volume. In addition, during obesity, WAT is actively growing to accommodate more lipid storage whereas the increased lipid storage in atherosclerosis is ectopic and pathogenic. Furthermore, the populations of adipocytes proximal to the artery wall versus adipocytes in omental or subcutaneous WAT, for example, have distinct inflammatory properties, as demonstrated by Chatterjee et al. (17). All of these differences could account for distinct roles of chemokines in each disease. For instance, perhaps hypoxia plays a bigger role in recruitment of leukocytes into growing WAT whereas chemokines may be especially important for their participation in

leukocyte activation and adhesion to the endothelium in the arteries that are vulnerable to atherosclerosis. Designing experiments based on the particular context in which leukocyte infiltration is occurring should provide insight into the role of not only MIP-1α but also of other chemokines. Determining how inflammation in obesity and atherosclerosis progresses and how it can be resolved will be helpful for treating people suffering from either of these highly prevalent conditions.

REFERENCES

1. A Report of the NIH Obesity Research Task Force Strategic Plan for NIH OBESITY RESEARCH: U.S. Department of Health and Human Services, 2004.

2. Statistics Related to Overweight and Obesity: U.S. Department of Health and Human Services, 2007.

3. **Ardigo D, Assimes TL, Fortmann SP, Go AS, Hlatky M, Hytopoulos E, Iribarren C, Tsao PS, Tabibiazar R, and Quertermous T.** Circulating chemokines accurately identify individuals with clinically significant atherosclerotic heart disease. *Physiol Genomics* 31: 402-409, 2007.

4. **Beltowski J.** Leptin and atherosclerosis. *Atherosclerosis* 189: 47-60, 2006.

5. **Beltowski J, Wojcicka G, and Jamroz A.** Leptin decreases plasma paraoxonase 1 (PON1) activity and induces oxidative stress: the possible novel mechanism for proatherogenic effect of chronic hyperleptinemia. *Atherosclerosis* 170: 21-29, 2003.

6. **Bischoff SC, Krieger M, Brunner T, Rot A, von Tscharner V, Baggiolini M, and Dahinden CA.** RANTES and related chemokines activate human basophil granulocytes through different G protein-coupled receptors. *Eur J Immunol* 23: 761-767, 1993.

7. **Bluher S, Shah S, and Mantzoros CS.** Leptin Deficiency: Clinical Implications and Opportunities for Therapeutic Interventions. *J Investig Med*, 2009.

8. **Bodary PF, Gu S, Shen Y, Hasty AH, Buckler JM, and Eitzman DT.** Recombinant leptin promotes atherosclerosis and thrombosis in apolipoprotein E-deficient mice. *Arterioscler Thromb Vasc Biol* 25: e119-122, 2005.

9. **Bodary PF, Shen Y, Ohman M, Bahrou KL, Vargas FB, Cudney SS, Wickenheiser KJ, Myers MG, Jr., and Eitzman DT.** Leptin regulates neointima formation after arterial injury through mechanisms independent of blood pressure and the leptin receptor/STAT3 signaling pathways involved in energy balance. *Arterioscler Thromb Vasc Biol* 27: 70-76, 2007.

10. **Boden G and Shulman GI.** Free fatty acids in obesity and type 2 diabetes: defining their role in the development of insulin resistance and beta-cell dysfunction. *Eur J Clin Invest* 32 Suppl 3: 14-23, 2002.

11. **Bouloumie A, Marumo T, Lafontan M, and Busse R.** Leptin induces oxidative stress in human endothelial cells. *FASEB J* 13: 1231-1238, 1999.

12. **Braunersreuther V, Zernecke A, Arnaud C, Liehn EA, Steffens S, Shagdarsuren E, Bidzhekov K, Burger F, Pelli G, Luckow B, Mach F, and Weber C.** Ccr5 but not Ccr1 deficiency reduces development of diet-induced atherosclerosis in mice. *Arterioscler Thromb Vasc Biol* 27: 373-379, 2007.

13. **Breland UM, Halvorsen B, Hol J, Oie E, Paulsson-Berne G, Yndestad A, Smith C, Otterdal K, Hedin U, Waehre T, Sandberg WJ, Froland SS, Haraldsen G, Gullestad L, Damas JK, Hansson GK, and Aukrust P.** A potential role of the CXC chemokine GROalpha in atherosclerosis and plaque destabilization: downregulatory effects of statins. *Arterioscler Thromb Vasc Biol* 28: 1005-1011, 2008.

14. **Bruun JM, Lihn AS, Pedersen SB, and Richelsen B.** Monocyte chemoattractant protein-1 release is higher in visceral than subcutaneous human adipose tissue (AT): implication of macrophages resident in the AT. *J Clin Endocrinol Metab* 90: 2282-2289, 2005.

15. **Cabrero A, Cubero M, Llaverias G, Alegret M, Sanchez R, Laguna JC, and Vazquez-Carrera M.** Leptin down-regulates peroxisome proliferator-activated receptor gamma (PPAR-gamma) mRNA levels in primary human monocyte-derived macrophages. *Mol Cell Biochem* 275: 173-179, 2005.

16. **Campfield LA, Smith FJ, Guisez Y, Devos R, and Burn P.** Recombinant mouse OB protein: evidence for a peripheral signal linking adiposity and central neural networks. *Science* 269: 546-549, 1995.

17. **Chatterjee TK, Stoll LL, Denning GM, Harrelson A, Blomkalns AL, Idelman G, Rothenberg FG, Neltner B, Romig-Martin SA, Dickson EW, Rudich S, and Weintraub NL.** Proinflammatory phenotype of perivascular adipocytes: influence of high-fat feeding. *Circ Res* 104: 541-549, 2009.

18. **Chehab FF.** Obesity and lipodystrophy--where do the circles intersect? *Endocrinology* 149: 925-934, 2008.

19. **Chen A, Mumick S, Zhang C, Lamb J, Dai H, Weingarth D, Mudgett J, Chen H, Macneil DJ, Reitman ML, and Qian S.** Diet induction of monocyte chemoattractant protein-1 and its impact on obesity. *Obes Res* 13: 1311-1320, 2005.

20. **Chen Y and Heiman ML.** Chronic leptin administration promotes lipid utilization until fat mass is greatly reduced and preserves lean mass of normal female rats. *Regul Pept* 92: 113-119, 2000.

21. **Chiba T, Shinozaki S, Nakazawa T, Kawakami A, Ai M, Kaneko E, Kitagawa M, Kondo K, Chait A, and Shimokado K.** Leptin deficiency suppresses progression of atherosclerosis in apoE-deficient mice. *Atherosclerosis*, 2007.

22. **Cinti S, Mitchell G, Barbatelli G, Murano I, Ceresi E, Faloia E, Wang S, Fortier M, Greenberg AS, and Obin MS.** Adipocyte death defines macrophage localization and function in adipose tissue of obese mice and humans. *J Lipid Res* 46: 2347-2355, 2005.

23. **Coenen KR and Hasty AH.** Obesity potentiates development of fatty liver and insulin resistance, but not atherosclerosis, in high-fat diet-fed agouti LDLR-deficient mice. *Am J Physiol Endocrinol Metab* 293: E492-499, 2007.

24. **Coleman DL.** Effects of parabiosis of obese with diabetes and normal mice. *Diabetologia* 9: 294-298, 1973.

25. **Coleman DL and Hummel KP.** Effects of parabiosis of normal with genetically diabetic mice. *flc386* 217: 1298-1304, 1969.

26. **Combadiere C, Potteaux S, Rodero M, Simon T, Pezard A, Esposito B, Merval R, Proudfoot A, Tedgui A, and Mallat Z.** Combined inhibition of CCL2, CX3CR1, and CCR5 abrogates Ly6C(hi) and Ly6C(lo) monocytosis and almost abolishes atherosclerosis in hypercholesterolemic mice. *Circulation* 117: 1649-1657, 2008.

27. **Conlon K, Lloyd A, Chattopadhyay U, Lukacs N, Kunkel S, Schall T, Taub D, Morimoto C, Osborne J, Oppenheim J, and et al.** CD8+ and CD45RA+ human peripheral blood lymphocytes are potent sources of macrophage inflammatory protein 1 alpha, interleukin-8 and RANTES. *Eur J Immunol* 25: 751-756, 1995.

28. **Considine RV, Sinha MK, Heiman ML, Kriauciunas A, Stephens TW, Nyce MR, Ohannesian JP, Marco CC, McKee LJ, Bauer TL, and et al.** Serum immunoreactive-leptin concentrations in normal-weight and obese humans. *N Engl J Med* 334: 292-295, 1996.

29. **Cook DN, Beck MA, Coffman TM, Kirby SL, Sheridan JF, Pragnell IB, and Smithies O.** Requirement of MIP-1 alpha for an inflammatory response to viral infection. *Science* 269: 1583-1585, 1995.

30. **Cross AK, Richardson V, Ali SA, Palmer I, Taub DD, and Rees RC.** Migration responses of human monocytic cell lines to alpha- and beta-chemokines. *Cytokine* 9: 521-528, 1997.

31. **Dahlman I, Kaaman M, Olsson T, Tan GD, Bickerton AS, Wahlen K, Andersson J, Nordstrom EA, Blomqvist L, Sjogren A, Forsgren M, Attersand A, and Arner P.** A unique role of monocyte chemoattractant protein 1 among chemokines in adipose tissue of obese subjects. *J Clin Endocrinol Metab* 90: 5834-5840, 2005.

32. **de Jager SC, Kraaijeveld AO, Grauss RW, de Jager W, Liem SS, van der Hoeven BL, Prakken BJ, Putter H, van Berkel TJ, Atsma DE, Schalij MJ, Jukema JW, and Biessen EA.** CCL3 (MIP-1 alpha) levels are elevated during acute coronary syndromes and show strong prognostic power for future ischemic events. *J Mol Cell Cardiol* 45: 446-452, 2008.

33. **de Oliveira RT, Mamoni RL, Souza JR, Fernandes JL, Rios FJ, Gidlund M, Coelho OR, and Blotta MH.** Differential expression of cytokines, chemokines and chemokine receptors in patients with coronary artery disease. *Int J Cardiol* 136: 17-26, 2009.

34. **De Rosa V, Procaccini C, Cali G, Pirozzi G, Fontana S, Zappacosta S, La Cava A, and Matarese G.** A key role of leptin in the control of regulatory T cell proliferation. *Immunity* 26: 241-255, 2007.

35. **De Taeye BM, Novitskaya T, McGuinness OP, Gleaves L, Medda M, Covington JW, and Vaughan DE.** Macrophage TNF-alpha contributes to insulin resistance and hepatic steatosis in diet-induced obesity. *Am J Physiol Endocrinol Metab* 293: E713-725, 2007.

36. **Duffaut C, Galitzky J, Lafontan M, and Bouloumie A.** Unexpected trafficking of immune cells within the adipose tissue during the onset of obesity. *Biochem Biophys Res Commun* 384: 482-485, 2009.

37. **Eckel RH.** Obesity and heart disease: a statement for healthcare professionals from the Nutrition Committee, American Heart Association. *Circulation* 96: 3248-3250, 1997.

38. **Elgazar-Carmon V, Rudich A, Hadad N, and Levy R.** Neutrophils transiently infiltrate intra-abdominal fat early in the course of high-fat feeding. *J Lipid Res* 49: 1894-1903, 2008.

39. **Feuerer M, Herrero L, Cipolletta D, Naaz A, Wong J, Nayer A, Lee J, Goldfine AB, Benoist C, Shoelson S, and Mathis D.** Lean, but not obese, fat is enriched for a unique population of regulatory T cells that affect metabolic parameters. *Nat Med* 15: 930-939, 2009.

40. **Fonseca V.** Effect of thiazolidinediones on body weight in patients with diabetes mellitus. *Am J Med* 115 Suppl 8A: 42S-48S, 2003.

41. **Fujioka Y and Ishikawa Y.** Remnant lipoproteins as strong key particles to atherogenesis. *J Atheroscler Thromb* 16: 145-154, 2009.

42. **Gainsford T, Willson TA, Metcalf D, Handman E, McFarlane C, Ng A, Nicola NA, Alexander WS, and Hilton DJ.** Leptin can induce proliferation, differentiation, and functional activation of hemopoietic cells. *Proc Natl Acad Sci U S A* 93: 14564-14568, 1996.

43. **Gautier EL, Jakubzick C, and Randolph GJ.** Regulation of the migration and survival of monocyte subsets by chemokine receptors and its relevance to atherosclerosis. *Arterioscler Thromb Vasc Biol* 29: 1412-1418, 2009.

44. **Gerhardt CC, Romero IA, Cancello R, Camoin L, and Strosberg AD.** Chemokines control fat accumulation and leptin secretion by cultured human adipocytes. *Mol Cell Endocrinol* 175: 81-92, 2001.

45. **Goossens GH.** The role of adipose tissue dysfunction in the pathogenesis of obesity-related insulin resistance. *Physiol Behav* 94: 206-218, 2008.

46. **Gordon S and Taylor PR.** Monocyte and macrophage heterogeneity. *Nat Rev Immunol* 5: 953-964, 2005.

47. **Gruen ML, Hao M, Piston D, and Hasty AH.** Leptin requires canonical migratory signaling pathways for induction of monocyte and macrophage chemotaxis. *Am J Physiol Cell Physiol*, 2007.

48. **Gruen ML, Saraswathi V, Nuotio-Antar AM, Plummer MR, Coenen KR, and Hasty AH.** Plasma insulin levels predict atherosclerotic lesion burden in obese hyperlipidemic mice. *Atherosclerosis* 186: 54-64, 2006.

49. **Guri AJ, Hontecillas R, Ferrer G, Casagran O, Wankhade U, Noble AM, Eizirik DL, Ortis F, Cnop M, Liu D, Si H, and Bassaganya-Riera J.** Loss of PPARgamma in immune cells impairs the ability of abscisic acid to improve insulin sensitivity by suppressing monocyte chemoattractant protein-1 expression and macrophage infiltration into white adipose tissue. *J Nutr Biochem*, 2007.

50. **Halaas JL, Gajiwala KS, Maffei M, Cohen SL, Chait BT, Rabinowitz D, Lallone RL, Burley SK, and Friedman JM.** Weight-reducing effects of the plasma protein encoded by the obese gene. *Science* 269: 543-546, 1995.

51. **Hasty AH, Gruen ML, Terry ES, Surmi BK, Atkinson RD, Gao L, and Morrow JD.** Effects of vitamin E on oxidative stress and atherosclerosis in an obese hyperlipidemic mouse model. *J Nutr Biochem* 18: 127-133, 2007.

52. **Henrichot E, Juge-Aubry CE, Pernin A, Pache JC, Velebit V, Dayer JM, Meda P, Chizzolini C, and Meier CA.** Production of chemokines by

perivascular adipose tissue: a role in the pathogenesis of atherosclerosis? *Arterioscler Thromb Vasc Biol* 25: 2594-2599, 2005.

53. **Holven KB, Myhre AM, Aukrust P, Hagve TA, Ose L, and Nenseter MS.** Patients with familial hypercholesterolaemia show enhanced spontaneous chemokine release from peripheral blood mononuclear cells ex vivo. Dependency of xanthomas/xanthelasms, smoking and gender. *Eur Heart J* 24: 1756-1762, 2003.

54. **Hosogai N, Fukuhara A, Oshima K, Miyata Y, Tanaka S, Segawa K, Furukawa S, Tochino Y, Komuro R, Matsuda M, and Shimomura I.** Adipose tissue hypoxia in obesity and its impact on adipocytokine dysregulation. *Diabetes* 56: 901-911, 2007.

55. **Huber J, Kiefer FW, Zeyda M, Ludvik B, Silberhumer GR, Prager G, Zlabinger GJ, and Stulnig TM.** CC chemokine and CC chemokine receptor profiles in visceral and subcutaneous adipose tissue are altered in human obesity. *J Clin Endocrinol Metab* 93: 3215-3221, 2008.

56. **Huber J, Kiefer FW, Zeyda M, Ludvik B, Silberhumer GR, Prager G, Zlabinger GJ, and Stulnig TM.** CC chemokine and CC chemokine receptor profiles in visceral and subcutaneous adipose tissue are altered in human obesity. *J Clin Endocrinol Metab*, 2008.

57. **Huber J. KF, Zeyda M., Prager G., Stulnig T. M.** *American Diabetes Association Conference*, Chicago, IL, 2007.

58. **Hubert HB, Feinleib M, McNamara PM, and Castelli WP.** Obesity as an independent risk factor for cardiovascular disease: a 26-year follow-up of participants in the Framingham Heart Study. *Circulation* 67: 968-977, 1983.

59. **Hummel KP, Dickie MM, and Coleman DL.** Diabetes, a new mutation in the mouse. *Science* 153: 1127-1128, 1966.

60. **Ingalls AM, Dickie MM, and Snell GD.** Obese, a new mutation in the house mouse. *J Hered* 41: 317-318, 1950.

61. **Inouye KE, Shi H, Howard JK, Daly CH, Lord GM, Rollins BJ, and Flier JS.** Absence of CC chemokine ligand 2 does not limit obesity-associated infiltration of macrophages into adipose tissue. *Diabetes* 56: 2242-2250, 2007.

62. **Ishibashi S, Brown MS, Goldstein JL, Gerard RD, Hammer RE, and Herz J.** Hypercholesterolemia in low density lipoprotein receptor knockout mice and its reversal by adenovirus-mediated gene delivery. *J Clin Invest* 92: 883-893, 1993.

63. **Jiao P, Chen Q, Shah S, Du J, Tao B, Tzameli I, Yan W, and Xu H.** Obesity-related upregulation of monocyte chemotactic factors in adipocytes: involvement of nuclear factor-kappaB and c-Jun NH2-terminal kinase pathways. *Diabetes* 58: 104-115, 2009.

64. **Kalra SP.** Central leptin gene therapy ameliorates diabetes type 1 and 2 through two independent hypothalamic relays; a benefit beyond weight and appetite regulation. *Peptides* 30: 1957-1963, 2009.

65. **Kamei N, Tobe K, Suzuki R, Ohsugi M, Watanabe T, Kubota N, Ohtsuka-Kowatari N, Kumagai K, Sakamoto K, Kobayashi M, Yamauchi T, Ueki K, Oishi Y, Nishimura S, Manabe I, Hashimoto H, Ohnishi Y, Ogata H, Tokuyama K, Tsunoda M, Ide T, Murakami K, Nagai R, and Kadowaki T.** Overexpression of monocyte chemoattractant protein-1 in adipose tissues causes macrophage recruitment and insulin resistance. *J Biol Chem* 281: 26602-26614, 2006.

66. **Kanda H, Tateya S, Tamori Y, Kotani K, Hiasa K, Kitazawa R, Kitazawa S, Miyachi H, Maeda S, Egashira K, and Kasuga M.** MCP-1 contributes to macrophage infiltration into adipose tissue, insulin resistance, and hepatic steatosis in obesity. *J Clin Invest* 116: 1494-1505, 2006.

67. **Kang L, Sebastian BM, Pritchard MT, Pratt BT, Previs SF, and Nagy LE.** Chronic ethanol-induced insulin resistance is associated with macrophage infiltration into adipose tissue and altered expression of adipocytokines. *Alcohol Clin Exp Res* 31: 1581-1588, 2007.

68. **Kannel WB, Wilson PW, Nam BH, and D'Agostino RB.** Risk stratification of obesity as a coronary risk factor. *Am J Cardiol* 90: 697-701, 2002.

69. **Khan T, Muise ES, Iyengar P, Wang ZV, Chandalia M, Abate N, Zhang BB, Bonaldo P, Chua S, and Scherer PE.** Metabolic dysregulation and adipose tissue fibrosis: role of collagen VI. *Mol Cell Biol* 29: 1575-1591, 2009.

70. **Kiefer FW, Zeyda M, Todoric J, Huber J, Geyeregger R, Weichhart T, Aszmann O, Ludvik B, Silberhumer GR, Prager G, and Stulnig TM.** Osteopontin expression in human and murine obesity: extensive local upregulation in adipose tissue but minimal systemic alterations. *Endocrinology*, 2007.

71. **Kim TK, St John LS, Wieder ED, Khalili J, Ma Q, and Komanduri KV.** Human Late Memory CD8+ T Cells Have a Distinct Cytokine Signature Characterized by CC Chemokine Production without IL-2 Production. *J Immunol*, 2009.

72. **Kintscher U, Hartge M, Hess K, Foryst-Ludwig A, Clemenz M, Wabitsch M, Fischer-Posovszky P, Barth TF, Dragun D, Skurk T, Hauner H, Bluher M, Unger T, Wolf AM, Knippschild U, Hombach V, and Marx N.** T-lymphocyte Infiltration in Visceral Adipose Tissue. A Primary Event in Adipose Tissue Inflammation and the Development of Obesity-Mediated Insulin Resistance. *Arterioscler Thromb Vasc Biol*, 2008.

73. **Kirk EA, Sagawa ZK, McDonald TO, O'Brien KD, and Heinecke JW.** Macrophage chemoattractant protein-1 deficiency fails to restrain macrophage infiltration into adipose tissue. *Diabetes* 57: 1254-1261, 2008.

74. **Kirk EA, Sagawa ZK, McDonald TO, O'Brien KD, and Heinecke JW.** Monocyte chemoattractant protein deficiency fails to restrain macrophage infiltration into adipose tissue [corrected]. *Diabetes* 57: 1254-1261, 2008.

75. **Klein S, Burke LE, Bray GA, Blair S, Allison DB, Pi-Sunyer X, Hong Y, and Eckel RH.** Clinical implications of obesity with specific focus on cardiovascular disease: a statement for professionals from the American Heart Association Council on Nutrition, Physical Activity, and Metabolism: endorsed by the American College of Cardiology Foundation. *Circulation* 110: 2952-2967, 2004.

76. **Knudson JD, Dincer UD, Zhang C, Swafford AN, Jr., Koshida R, Picchi A, Focardi M, Dick GM, and Tune JD.** Leptin receptors are expressed in coronary arteries, and hyperleptinemia causes significant coronary endothelial dysfunction. *Am J Physiol Heart Circ Physiol* 289: H48-56, 2005.

77. **Kobusiak-Prokopowicz M, Orzeszko J, Mazur G, Mysiak A, Orda A, Poreba R, and Mazurek W.** Chemokines and left ventricular function in patients with acute myocardial infarction. *Eur J Intern Med* 18: 288-294, 2007.

78. **Koenen TB, Tack CJ, Kroese JM, Hermus AR, Sweep FC, van der Laak J, Stalenhoef AF, de Graaf J, van Tits LJ, and Stienstra R.** Pioglitazone treatment enlarges subcutaneous adipocytes in insulin-resistant patients. *J Clin Endocrinol Metab* 94: 4453-4457, 2009.

79. **Konturek SJ, Konturek JW, Pawlik T, and Brzozowski T.** Brain-gut axis and its role in the control of food intake. *J Physiol Pharmacol* 55: 137-154, 2004.

80. **Kraaijeveld AO, de Jager SC, de Jager WJ, Prakken BJ, McColl SR, Haspels I, Putter H, van Berkel TJ, Nagelkerken L, Jukema JW, and Biessen EA.** CC chemokine ligand-5 (CCL5/RANTES) and CC chemokine ligand-18 (CCL18/PARC) are specific markers of refractory unstable angina pectoris and are transiently raised during severe ischemic symptoms. *Circulation* 116: 1931-1941, 2007.

81. **Kuziel WA, Dawson TC, Quinones M, Garavito E, Chenaux G, Ahuja SS, Reddick RL, and Maeda N.** CCR5 deficiency is not protective in the early stages of atherogenesis in apoE knockout mice. *Atherosclerosis* 167: 25-32, 2003.

82. **Lara-Castro C and Garvey WT.** Intracellular lipid accumulation in liver and muscle and the insulin resistance syndrome. *Endocrinol Metab Clin North Am* 37: 841-856, 2008.

83. **Lee FY, Li Y, Yang EK, Yang SQ, Lin HZ, Trush MA, Dannenberg AJ, and Diehl AM.** Phenotypic abnormalities in macrophages from leptin-deficient, obese mice. *flc386* 276: C386-394., 1999.

84. **Lee YH, Nair S, Rousseau E, Allison DB, Page GP, Tataranni PA, Bogardus C, and Permana PA.** Microarray profiling of isolated abdominal subcutaneous adipocytes from obese vs non-obese Pima Indians: increased expression of inflammation-related genes. *Diabetologia* 48: 1776-1783, 2005.

85. **Libby P.** Inflammation in atherosclerosis. *Nature* 420: 868-874, 2002.

86. **Lloyd-Jones D, Adams R, Carnethon M, De Simone G, Ferguson TB, Flegal K, Ford E, Furie K, Go A, Greenlund K, Haase N, Hailpern S, Ho M, Howard V, Kissela B, Kittner S, Lackland D, Lisabeth L, Marelli A, McDermott M, Meigs J, Mozaffarian D, Nichol G, O'Donnell C, Roger V, Rosamond W, Sacco R, Sorlie P, Stafford R, Steinberger J, Thom T, Wasserthiel-Smoller S, Wong N, Wylie-Rosett J, and Hong Y.** Heart disease and stroke statistics--2009 update: a report from the American Heart Association Statistics Committee and Stroke Statistics Subcommittee. *Circulation* 119: e21-181, 2009.

87. **Lloyd CM, Phillips AR, Cooper GJ, and Dunbar PR.** Three-colour fluorescence immunohistochemistry reveals the diversity of cells staining for macrophage markers in murine spleen and liver. *J Immunol Methods* 334: 70-81, 2008.

88. **Loffreda S, Yang SQ, Lin HZ, Karp CL, Brengman ML, Wang DJ, Klein AS, Bulkley GB, Bao C, Noble PW, Lane MD, and Diehl AM.** Leptin regulates proinflammatory immune responses. *Faseb J* 12: 57-65, 1998.

89. **Lumeng CN, DelProposto JB, Westcott DJ, and Saltiel AR.** Phenotypic switching of adipose tissue macrophages with obesity is generated by spatiotemporal differences in macrophage subtypes. *Diabetes* 57: 3239-3246, 2008.

90. **Maffei M, Halaas J, Ravussin E, Pratley RE, Lee GH, Zhang Y, Fei H, Kim S, Lallone R, Ranganathan S, and al. e.** Leptin levels in human and

rodent: measurement of plasma leptin and ob RNA in obese and weight-reduced subjects. *Nat Med* 1: 1155-1161, 1995.

91. **Magni P, Liuzzi A, Ruscica M, Dozio E, Ferrario S, Bussi I, Minocci A, Castagna A, Motta M, and Savia G.** Free and bound plasma leptin in normal weight and obese men and women: relationship with body composition, resting energy expenditure, insulin-sensitivity, lipid profile and macronutrient preference. *Clin Endocrinol (Oxf)* 62: 189-196, 2005.

92. **Mantovani A, Sica A, Sozzani S, Allavena P, Vecchi A, and Locati M.** The chemokine system in diverse forms of macrophage activation and polarization. *Trends Immunol* 25: 677-686, 2004.

93. **Marais AD, Firth JC, and Blom DJ.** Homozygous familial hypercholesterolemia and its management. *Semin Vasc Med* 4: 43-50, 2004.

94. **Mark AL, Correia ML, Rahmouni K, and Haynes WG.** Selective leptin resistance: a new concept in leptin physiology with cardiovascular implications. *J Hypertens* 20: 1245-1250, 2002.

95. **Martin-Romero C and Sanchez-Margalet V.** Human leptin activates PI3K and MAPK pathways in human peripheral blood mononuclear cells: possible role of Sam68. *Cell Immunol* 212: 83-91., 2001.

96. **Maurer M and von Stebut E.** Macrophage inflammatory protein-1. *Int J Biochem Cell Biol* 36: 1882-1886, 2004.

97. **McGill HC, Jr., McMahan CA, Herderick EE, Zieske AW, Malcom GT, Tracy RE, and Strong JP.** Obesity accelerates the progression of coronary atherosclerosis in young men. *Circulation* 105: 2712-2718, 2002.

98. **Menten P, Wuyts A, and Van Damme J.** Macrophage inflammatory protein-1. *Cytokine Growth Factor Rev* 13: 455-481, 2002.

99. **Mokdad AH, Bowman BA, Ford ES, Vinicor F, Marks JS, and Koplan JP.** The continuing epidemics of obesity and diabetes in the United States. *Jama* 286: 1195-1200, 2001.

100. **Murano I, Barbatelli G, Parisani V, Latini C, Muzzonigro G, Castellucci M, and Cinti S.** Dead adipocytes, detected as crown-like structures (CLS), are prevalent in visceral fat depots of genetically obese mice. *J Lipid Res* 49: 1562-1568, 2008.

101. **Murano I, Barbatelli G, Parisani V, Latini C, Muzzonigro G, Castellucci M, and Cinti S.** Dead adipocytes, detected as crown-like structures (CLS), are prevalent in visceral fat depots of genetically obese mice. *J Lipid Res*, 2008.

102. **Murdolo G, Hammarstedt A, Sandqvist M, Schmelz M, Herder C, Smith U, and Jansson PA.** Monocyte chemoattractant protein-1 in subcutaneous abdominal adipose tissue: characterization of interstitial concentration and regulation of gene expression by insulin. *J Clin Endocrinol Metab* 92: 2688-2695, 2007.

103. **Myers MG, Cowley MA, and Munzberg H.** Mechanisms of leptin action and leptin resistance. *Annu Rev Physiol* 70: 537-556, 2008.

104. **Nara N, Nakayama Y, Okamoto S, Tamura H, Kiyono M, Muraoka M, Tanaka K, Taya C, Shitara H, Ishii R, Yonekawa H, Minokoshi Y, and Hara T.** Disruption of CXC motif chemokine ligand-14 in mice ameliorates obesity-induced insulin resistance. *J Biol Chem* 282: 30794-30803, 2007.

105. **Nishimura S, Manabe I, Nagasaki M, Eto K, Yamashita H, Ohsugi M, Otsu M, Hara K, Ueki K, Sugiura S, Yoshimura K, Kadowaki T, and Nagai R.** CD8+ effector T cells contribute to macrophage recruitment and adipose tissue inflammation in obesity. *Nat Med* 15: 914-920, 2009.

106. **O'Rourke L, Yeaman SJ, and Shepherd PR.** Insulin and leptin acutely regulate cholesterol ester metabolism in macrophages by novel signaling pathways. *Diabetes* 50: 955-961, 2001.

107. **Oda A, Taniguchi T, and Yokoyama M.** Leptin stimulates rat aortic smooth muscle cell proliferation and migration. *Kobe J Med Sci* 47: 141-150, 2001.

108. **Okamoto Y, Higashiyama H, Rong JX, McVey MJ, Kinoshita M, Asano S, and Hansen MK.** Comparison of mitochondrial and macrophage content between subcutaneous and visceral fat in db/db mice. *Exp Mol Pathol* 83: 73-83, 2007.

109. **Organization WH.** Obesity and overweight.

110. **Osuga J, Ishibashi S, Oka T, Yagyu H, Tozawa R, Fujimoto A, Shionoiri F, Yahagi N, Kraemer FB, Tsutsumi O, and Yamada N.** Targeted disruption of hormone-sensitive lipase results in male sterility and adipocyte hypertrophy, but not in obesity. *Proc Natl Acad Sci U S A* 97: 787-792, 2000.

111. **Paigen B, Morrow A, Holmes PA, Mitchell D, and Williams RA.** Quantitative assessment of atherosclerotic lesions in mice. *Atherosclerosis* 68: 231-240, 1987.

112. **Pang C, Gao Z, Yin J, Zhang J, Jia W, and Ye J.** Macrophage Infiltration into Adipose Tissue May Promote Angiogenesis for Adipose Tissue Remodeling in Obesity. *Am J Physiol Endocrinol Metab*, 2008.

113. **Parissis JT, Adamopoulos S, Venetsanou KF, Mentzikof DG, Karas SM, and Kremastinos DT.** Serum profiles of C-C chemokines in acute myocardial infarction: possible implication in postinfarction left ventricular remodeling. *J Interferon Cytokine Res* 22: 223-229, 2002.

114. **Park HY, Kwon HM, Lim HJ, Hong BK, Lee JY, Park BE, Jang Y, Cho SY, and Kim HS.** Potential role of leptin in angiogenesis: leptin induces endothelial cell proliferation and expression of matrix metalloproteinases in vivo and in vitro. *Exp Mol Med* 33: 95-102, 2001.

115. **Paximadis M, Mohanlal N, Gray GE, Kuhn L, and Tiemessen CT.** Identification of new variants within the two functional genes CCL3 and CCL3L encoding the CCL3 (MIP-1alpha) chemokine: implications for HIV-1 infection. *Int J Immunogenet* 36: 21-32, 2009.

116. **Pelleymounter MA, Cullen MJ, Baker MB, Hecht R, Winters D, Boone T, and Collins F.** Effects of the obese gene product on body weight regulation in ob/ob mice. *Science* 269: 540-543, 1995.

117. **Piedrahita JA, Zhang SH, Hagaman JR, Oliver PM, and Maeda N.** Generation of mice carrying a mutant apolipoprotein E gene inactivated by gene targeting in embryonic stem cells. *Proc Natl Acad Sci U S A* 89: 4471-4475, 1992.

118. **Poglio S, Galvani S, Bour S, Andre M, Prunet-Marcassus B, Penicaud L, Casteilla L, and Cousin B.** Adipose tissue sensitivity to radiation exposure. *Am J Pathol* 174: 44-53, 2009.

119. **Potteaux S, Combadiere C, Esposito B, Casanova S, Merval R, Ardouin P, Gao JL, Murphy PM, Tedgui A, and Mallat Z.** Chemokine receptor CCR1 disruption in bone marrow cells enhances atherosclerotic lesion development and inflammation in mice. *Mol Med* 11: 16-20, 2005.

120. **Potteaux S, Combadiere C, Esposito B, Lecureuil C, Ait-Oufella H, Merval R, Ardouin P, Tedgui A, and Mallat Z.** Role of bone marrow-derived CC-chemokine receptor 5 in the development of atherosclerosis of low-density lipoprotein receptor knockout mice. *Arterioscler Thromb Vasc Biol* 26: 1858-1863, 2006.

121. **Quinones MP, Martinez HG, Jimenez F, Estrada CA, Dudley M, Willmon O, Kulkarni H, Reddick RL, Fernandes G, Kuziel WA, Ahuja SK, and Ahuja SS.** CC chemokine receptor 5 influences late-stage atherosclerosis. *Atherosclerosis* 195: e92-103, 2007.

122. **Ramos CD, Canetti C, Souto JT, Silva JS, Hogaboam CM, Ferreira SH, and Cunha FQ.** MIP-1alpha[CCL3] acting on the CCR1 receptor mediates

neutrophil migration in immune inflammation via sequential release of TNF-alpha and LTB4. *J Leukoc Biol* 78: 167-177, 2005.

123. **Ramos CD, Fernandes KS, Canetti C, Teixeira MM, Silva JS, and Cunha FQ.** Neutrophil recruitment in immunized mice depends on MIP-2 inducing the sequential release of MIP-1alpha, TNF-alpha and LTB(4). *Eur J Immunol* 36: 2025-2034, 2006.

124. **Rausch ME, Weisberg S, Vardhana P, and Tortoriello DV.** Obesity in C57BL/6J mice is characterized by adipose tissue hypoxia and cytotoxic T-cell infiltration. *Int J Obes (Lond)* 32: 451-463, 2008.

125. **Reichel CA, Rehberg M, Lerchenberger M, Berberich N, Bihari P, Khandoga AG, Zahler S, and Krombach F.** Ccl2 and Ccl3 mediate neutrophil recruitment via induction of protein synthesis and generation of lipid mediators. *Arterioscler Thromb Vasc Biol* 29: 1787-1793, 2009.

126. **Reilly MP, Iqbal N, Schutta M, Wolfe ML, Scally M, Localio AR, Rader DJ, and Kimmel SE.** Plasma leptin levels are associated with coronary atherosclerosis in type 2 diabetes. *J Clin Endocrinol Metab* 89: 3872-3878, 2004.

127. **Rimm EB, Stampfer MJ, Giovannucci E, Ascherio A, Spiegelman D, Colditz GA, and Willett WC.** Body size and fat distribution as predictors of coronary heart disease among middle-aged and older US men. *Am J Epidemiol* 141: 1117-1127, 1995.

128. **Rot A, Krieger M, Brunner T, Bischoff SC, Schall TJ, and Dahinden CA.** RANTES and macrophage inflammatory protein 1 alpha induce the migration and activation of normal human eosinophil granulocytes. *J Exp Med* 176: 1489-1495, 1992.

129. **Sanchez-Margalet V, Martin-Romero C, Santos-Alvarez J, Goberna R, Najib S, and Gonzalez-Yanes C.** Role of leptin as an immunomodulator of blood mononuclear cells: mechanisms of action. *Clin Exp Immunol* 133: 11-19, 2003.

130. **Santos-Alvarez J, Goberna R, and Sanchez-Margalet V.** Human leptin stimulates proliferation and activation of human circulating monocytes. *Cell Immunol* 194: 6-11, 1999.

131. **Saraswathi V, Gao L, Morrow JD, Chait A, Niswender KD, and Hasty AH.** Fish oil increases cholesterol storage in white adipose tissue with concomitant decreases in inflammation, hepatic steatosis, and atherosclerosis in mice. *J Nutr* 137: 1776-1782, 2007.

132. **Saraswathi V and Hasty AH.** The role of lipolysis in mediating the proinflammatory effects of very low density lipoproteins in mouse peritoneal macrophages. *J Lipid Res* 47: 1406-1415, 2006.

133. **Satriano J.** Arginine pathways and the inflammatory response: interregulation of nitric oxide and polyamines: review article. *Amino Acids* 26: 321-329, 2004.

134. **Schall TJ, Bacon K, Camp RD, Kaspari JW, and Goeddel DV.** Human macrophage inflammatory protein alpha (MIP-1 alpha) and MIP-1 beta chemokines attract distinct populations of lymphocytes. *J Exp Med* 177: 1821-1826, 1993.

135. **Schenk S, Saberi M, and Olefsky JM.** Insulin sensitivity: modulation by nutrients and inflammation. *J Clin Invest* 118: 2992-3002, 2008.

136. **Sears DD, Hsiao G, Hsiao A, Yu JG, Courtney CH, Ofrecio JM, Chapman J, and Subramaniam S.** Mechanisms of human insulin resistance and thiazolidinedione-mediated insulin sensitization. *Proc Natl Acad Sci U S A* 106: 18745-18750, 2009.

137. **Sevastianova K, Sutinen J, Kannisto K, Hamsten A, Ristola M, and Yki-Jarvinen H.** Adipose tissue inflammation and liver fat in patients with highly active antiretroviral therapy-associated lipodystrophy. *Am J Physiol Endocrinol Metab* 295: E85-91, 2008.

138. **Sierra-Honigmann MR, Nath AK, Murakami C, Garcia-Cardena G, Papapetropoulos A, Sessa WC, Madge LA, Schechner JS, Schwabb MB, Polverini PJ, and Flores-Riveros JR.** Biological action of leptin as an angiogenic factor. *Science* 281: 1683-1686, 1998.

139. **Soderberg S, Stegmayr B, Ahlbeck-Glader C, Slunga-Birgander L, Ahren B, and Olsson T.** High leptin levels are associated with stroke. *Cerebrovasc Dis* 15: 63-69, 2003.

140. **Strissel KJ, Stancheva Z, Miyoshi H, Perfield JW, 2nd, DeFuria J, Jick Z, Greenberg AS, and Obin MS.** Adipocyte death, adipose tissue remodeling, and obesity complications. *Diabetes* 56: 2910-2918, 2007.

141. **Suganami T, Nishida J, and Ogawa Y.** A paracrine loop between adipocytes and macrophages aggravates inflammatory changes: role of free fatty acids and tumor necrosis factor alpha. *Arterioscler Thromb Vasc Biol* 25: 2062-2068, 2005.

142. **Surmi BK, Atkinson RD, Gruen ML, Coenen KR, and Hasty AH.** The role of macrophage leptin receptor in aortic root lesion formation. *Am J Physiol Endocrinol Metab* 294: E488-495, 2008.

143. **Surmi BK and Hasty AH.** Macrophage infiltration into adipose tissue: initiation, propagation and remodeling. *Future Lipidol* 3: 545-556, 2008.

144. **Tartaglia LA, Dembski M, Weng X, Deng N, Culpepper J, Devos R, Richards GJ, Campfield LA, Clark FT, Deeds J, Muir C, Sanker S, Moriarty A, Moore KJ, Smutko JS, Mays GG, Wool EA, Monroe CA, and Tepper RI.** Identification and expression cloning of a leptin receptor, OB-R. *Cell* 83: 1263-1271, 1995.

145. **Taub DD, Conlon K, Lloyd AR, Oppenheim JJ, and Kelvin DJ.** Preferential migration of activated CD4+ and CD8+ T cells in response to MIP-1 alpha and MIP-1 beta. *Science* 260: 355-358, 1993.

146. **Taub DD, Sayers TJ, Carter CR, and Ortaldo JR.** Alpha and beta chemokines induce NK cell migration and enhance NK-mediated cytolysis. *J Immunol* 155: 3877-3888, 1995.

147. **Trevaskis JL, Gawronska-Kozak B, Sutton GM, McNeil M, Stephens JM, Smith SR, and Butler AA.** Role of adiponectin and inflammation in insulin resistance of mc3r and mc4r knockout mice. *Obesity (Silver Spring)* 15: 2664-2672, 2007.

148. **Trifilo MJ, Bergmann CC, Kuziel WA, and Lane TE.** CC chemokine ligand 3 (CCL3) regulates CD8(+)-T-cell effector function and migration following viral infection. *J Virol* 77: 4004-4014, 2003.

149. **Tsou CL, Peters W, Si Y, Slaymaker S, Aslanian AM, Weisberg SP, Mack M, and Charo IF.** Critical roles for CCR2 and MCP-3 in monocyte mobilization from bone marrow and recruitment to inflammatory sites. *J Clin Invest* 117: 902-909, 2007.

150. **Uguccioni M, D'Apuzzo M, Loetscher M, Dewald B, and Baggiolini M.** Actions of the chemotactic cytokines MCP-1, MCP-2, MCP-3, RANTES, MIP-1 alpha and MIP-1 beta on human monocytes. *Eur J Immunol* 25: 64-68, 1995.

151. **Van Gaal LF, Mertens IL, and De Block CE.** Mechanisms linking obesity with cardiovascular disease. *Nature* 444: 875-880, 2006.

152. **Vecchione C, Maffei A, Colella S, Aretini A, Poulet R, Frati G, Gentile MT, Fratta L, Trimarco V, Trimarco B, and Lembo G.** Leptin effect on endothelial nitric oxide is mediated through Akt-endothelial nitric oxide synthase phosphorylation pathway. *Diabetes* 51: 168-173, 2002.

153. **Voros G, Maquoi E, Demeulemeester D, Clerx N, Collen D, and Lijnen HR.** Modulation of angiogenesis during adipose tissue development in murine models of obesity. *Endocrinology* 146: 4545-4554, 2005.

154. **Wallace AM, McMahon AD, Packard CJ, Kelly A, Shepherd J, Gaw A, and Sattar N.** Plasma leptin and the risk of cardiovascular disease in the west of Scotland coronary prevention study (WOSCOPS). *Circulation* 104: 3052-3056, 2001.

155. **Wang B, Wood I, and Trayhurn P.** Hypoxia induces leptin gene expression and secretion in human preadipocytes: differential effects of hypoxia on adipokine expression by preadipocytes. *J Endocrinol*, 2008.

156. **Wang B, Wood IS, and Trayhurn P.** Dysregulation of the expression and secretion of inflammation-related adipokines by hypoxia in human adipocytes. *Pflugers Arch* 455: 479-492, 2007.

157. **Weber C, Zernecke A, and Libby P.** The multifaceted contributions of leukocyte subsets to atherosclerosis: lessons from mouse models. *Nat Rev Immunol* 8: 802-815, 2008.

158. **Weisberg SP, Hunter D, Huber R, Lemieux J, Slaymaker S, Vaddi K, Charo I, Leibel RL, and Ferrante AW, Jr.** CCR2 modulates inflammatory and metabolic effects of high-fat feeding. *J Clin Invest* 116: 115-124, 2006.

159. **Weisberg SP, McCann D, Desai M, Rosenbaum M, Leibel RL, and Ferrante AW, Jr.** Obesity is associated with macrophage accumulation in adipose tissue. *J Clin Invest* 112: 1796-1808, 2003.

160. **Westerbacka J, Corner A, Kolak M, Makkonen J, Turpeinen U, Hamsten A, Fisher RM, and Yki-Jarvinen H.** Insulin regulation of MCP-1 in human adipose tissue of obese and lean women. *Am J Physiol Endocrinol Metab* 294: E841-845, 2008.

161. **Willett WC, Manson JE, Stampfer MJ, Colditz GA, Rosner B, Speizer FE, and Hennekens CH.** Weight, weight change, and coronary heart disease in women. Risk within the 'normal' weight range. *Jama* 273: 461-465, 1995.

162. **Winer S, Chan Y, Paltser G, Truong D, Tsui H, Bahrami J, Dorfman R, Wang Y, Zielenski J, Mastronardi F, Maezawa Y, Drucker DJ, Engleman E, Winer D, and Dosch HM.** Normalization of obesity-associated insulin resistance through immunotherapy. *Nat Med* 15: 921-929, 2009.

163. **Wouters K, van Gorp PJ, Bieghs V, Gijbels MJ, Duimel H, Lutjohann D, Kerksiek A, van Kruchten R, Maeda N, Staels B, van Bilsen M, Shiri-Sverdlov R, and Hofker MH.** Dietary cholesterol, rather than liver steatosis,

leads to hepatic inflammation in hyperlipidemic mouse models of nonalcoholic steatohepatitis. *Hepatology* 48: 474-486, 2008.

164. **Wu H, Ghosh S, Perrard XD, Feng L, Garcia GE, Perrard JL, Sweeney JF, Peterson LE, Chan L, Smith CW, and Ballantyne CM.** T-cell accumulation and regulated on activation, normal T cell expressed and secreted upregulation in adipose tissue in obesity. *Circulation* 115: 1029-1038, 2007.

165. **Wu YP and Proia RL.** Deletion of macrophage-inflammatory protein 1 alpha retards neurodegeneration in Sandhoff disease mice. *Proc Natl Acad Sci U S A* 101: 8425-8430, 2004.

166. **Xu H, Barnes GT, Yang Q, Tan G, Yang D, Chou CJ, Sole J, Nichols A, Ross JS, Tartaglia LA, and Chen H.** Chronic inflammation in fat plays a crucial role in the development of obesity-related insulin resistance. *J Clin Invest* 112: 1821-1830, 2003.

167. **Ye J, Gao Z, Yin J, and He Q.** Hypoxia is a potential risk factor for chronic inflammation and adiponectin reduction in adipose tissue of ob/ob and dietary obese mice. *Am J Physiol Endocrinol Metab* 293: E1118-1128, 2007.

168. **Yu R, Kim CS, Kwon BS, and Kawada T.** Mesenteric adipose tissue-derived monocyte chemoattractant protein-1 plays a crucial role in adipose tissue macrophage migration and activation in obese mice. *Obesity (Silver Spring)* 14: 1353-1362, 2006.

169. **Zernecke A, Liehn EA, Gao JL, Kuziel WA, Murphy PM, and Weber C.** Deficiency in CCR5 but not CCR1 protects against neointima formation in atherosclerosis-prone mice: involvement of IL-10. *Blood* 107: 4240-4243, 2006.

170. **Zeyda M, Farmer D, Todoric J, Aszmann O, Speiser M, Gyori G, Zlabinger GJ, and Stulnig TM.** Human adipose tissue macrophages are of an anti-inflammatory phenotype but capable of excessive pro-inflammatory mediator production. *Int J Obes (Lond)* 31: 1420-1428, 2007.

171. **Zhang SH, Reddick RL, Piedrahita JA, and Maeda N.** Spontaneous hypercholesterolemia and arterial lesions in mice lacking apolipoprotein E. *Science* 258: 468-471, 1992.

172. **Zhang Y, Proenca R, Maffei M, Barone M, Leopold L, and Friedman JM.** Positional cloning of the mouse obese gene and its human homologue. *Nature* 372: 425-432, 1994.

173. **Zhao L, Moos MP, Grabner R, Pedrono F, Fan J, Kaiser B, John N, Schmidt S, Spanbroek R, Lotzer K, Huang L, Cui J, Rader DJ, Evans JF, Habenicht AJ, and Funk CD.** The 5-lipoxygenase pathway promotes

pathogenesis of hyperlipidemia-dependent aortic aneurysm. *Nat Med* 10: 966-973, 2004.

174. **Zimmermann R, Lass A, Haemmerle G, and Zechner R.** Fate of fat: the role of adipose triglyceride lipase in lipolysis. *Biochim Biophys Acta* 1791: 494-500, 2009.